

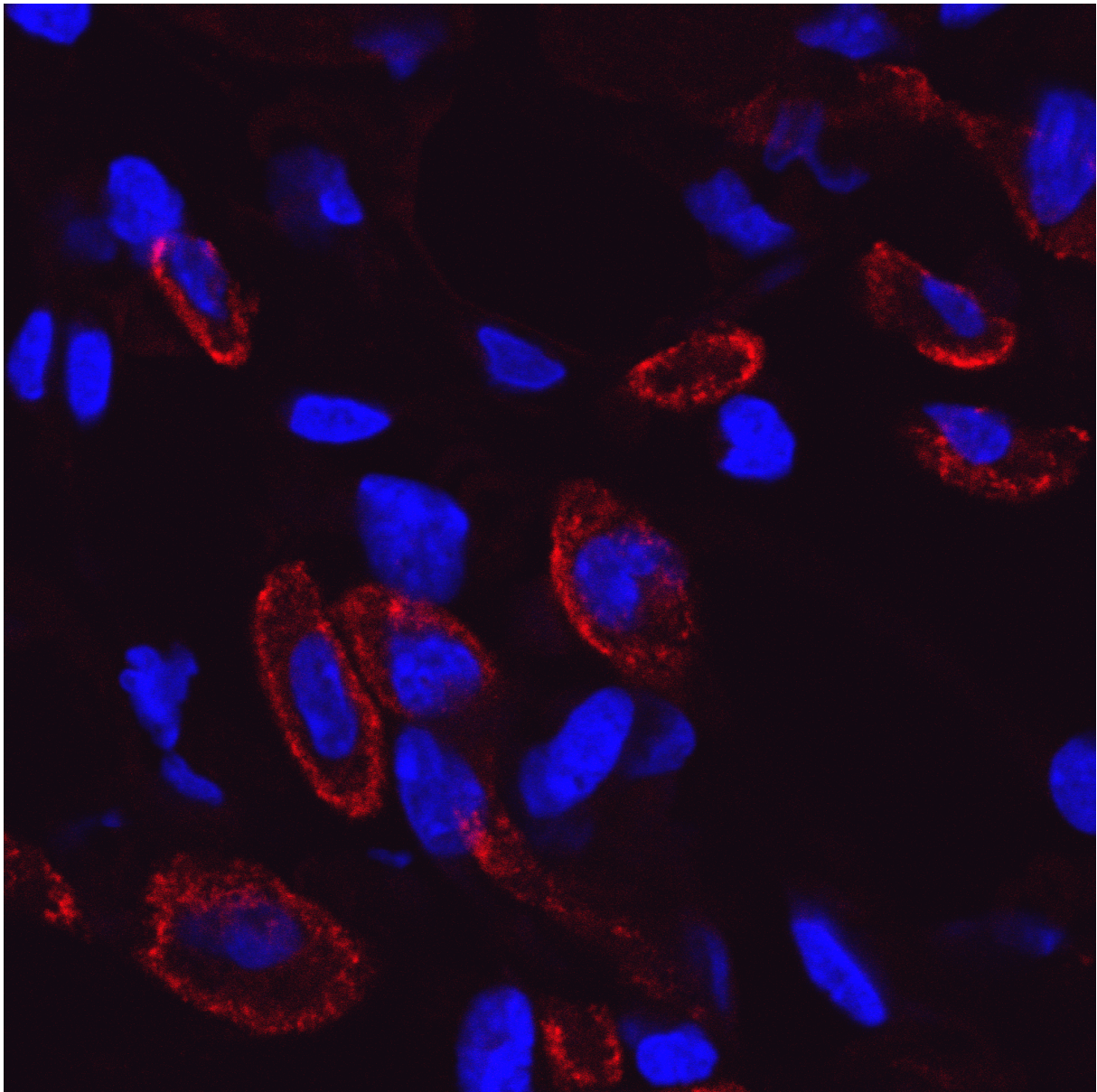
Department of Medical Biology

Role of the mannose receptor in tumor associated macrophages

Studies in a mouse melanoma model

Iselin Rønningen

Master thesis in biomedicine April 2014



“Learn from yesterday, live for today, hope for tomorrow.
The important thing is not to stop questioning”

Albert Einstein

Acknowledgements

This thesis is the finishing work of a master's degree in biomedicine. The study was carried out at the Vascular Biology Research Group, at the Department of Medical Biology, at the University of Tromsø, Norway.

First of all, I would like to express my greatest gratitude to Karen Sørensen, my main supervisor, for giving me the chance to work with this project. From the first lecture I had with you, on my second year as a bachelor student, I was hoping that I would one day be working with you. I am grateful for your knowledge and for introducing me to science. For your support, guidance and for always encouraging me to do better, and doing so with a smile.

I would like thank my supervisor, Jaione Simón-Santamaría, for all your patience, guidance and especially for helping a master student in despair. Your kind and encouraging words has been of great support to me.

Special thanks to Baldur, for your knowledge and for creating the idea behind my project. I also want to thank you for your help, suggestions and troubleshooting.

To my girls, Jaione (again), Ivana, Ana, Cristina and Montse, thank you so much for all your support. You always had time to listen to me, helping me with whatever my problems would be. Thank you for taking me under your wings, and including me in your circle of friends. Thank you Cristina for letting me in to your home so I could get to know the sweetest little boy.

Special thanks to the "Big Boss" Bård Smedsrød for welcoming me and include me in his research group. I would like to give acknowledge to all people at VBRG, thank you for making me feel welcome and for making my last two years very special!.

Dear Mom, thank you for being who you are and for everything you have done for me. I admire your strength and courage. Dad, for always wanting the best for me.

Finally, to the most important creatures in my life. For keeping me company. For all the fresh air and beautiful scenery. You have taught me what quality time means. Little Oskar, for your unconditional love.

Summary

Macrophages are multifunctional cells with important roles in inflammation, immunity, wound healing and for restoring homeostasis in tissues. They are referred to as “janitors” because of their large capacity to remove apoptotic cells and cellular debris. Macrophages have a remarkable plasticity and can change their physiology in response to signals in their environment. In situations of acute inflammation, macrophages are activated and exhibit potent microbicidal and tumoricidal activity, a process called M1 activation. When the inflammation is resolved, the macrophages show a functional shift known as M2 activation in order to stimulate the repair of the damaged tissue, or wound healing.

A solid tumor is in control of its microenvironment and influences its surroundings to serve in its own best interest. Macrophages that are present in tumors, tumor-associated macrophages (TAM) play an important role in cancer-related inflammation. Inflammation has been described as the 7th hallmark of cancer. TAMs are manipulated by their tumor to develop a M2 polarization and therefore have functions required for wound healing. The M2 polarized TAMs will also provide fuel for the tumor and support tumor growth, progression, invasion and metastasis. In addition they induce and maintain tumor angiogenesis and down-regulate the anti-tumor immune response.

M2 macrophages are known to express the mannose receptor (MR). The MR is an endocytic receptor that mediates clathrin-mediated endocytosis of various glycoproteins and non-opsonic phagocytosis of a wide range of microbes. The MR is regarded as a hallmark for the M2 polarized macrophage, and a possible role of this receptor in the M2 polarization of TAMs has been recently suggested.

This study was conducted to investigate the role of the MR in TAMs and tumor development. This was done by examining B16F1 melanoma growth rates and development in mannose receptor knockout (MR-KO) mice and wild-type control mice, followed by histopathological, immunohistochemical, and transcriptomic analyses of tumors harvested from these animals. A key question was whether the MR is necessary for M2 polarization, or just a marker for M2 polarized macrophages.

The histological/immunohistochemical analyses were done in small (1-2 mm), medium sized (3-5 mm) and large (> 8 mm) tumors. We examined % necrosis, blood vessel formation, and leukocyte infiltration in the different tumors, with a special focus on TAMs and TAM activation status. Markers for M1 and M2 macrophages, such as antibodies to inducible nitric oxide synthetase (iNOS), arginase I, MR, and stabilin-1, and the pan macrophage marker in mice, F4/80, were used to try to establish when the switch from M1 to M2 occurs,

as well as the relative amount of M1 and M2 macrophages at various stages in tumor development. First, a pilot study was conducted to test a range of different macrophage markers. Gene expression by quantitative-RT-PCR of some of the same markers was applied on middle-sized tumors.

We found that the first day of visible tumor (“tumor take”) was delayed in MR-KO mice compared to WT mice, but from then on the tumors grew with the same rate in both animal groups. The delay seen in tumor take may be related to the clearance function of MR. There was no marked difference in tumor morphology, and tumor associated necroses and blood vessels between wild-type and MR-KO animals. Already in the smallest tumors examined a large infiltration of TAMs was seen, with a minor portion of these already being M2 polarized. This indicates that the shift from M1 to M2 polarization occurs at an earlier stage than detectable in this study. RT-qPCR results were inconclusive.

Main conclusion: The shift in macrophage polarization occurs very early in the tumor development. Since polarization of macrophages towards M2 happened in both MR-KO and wild-type mice it is likely that the MR is not a driver for polarization. However, it may have a role in early tumor development.

Contents

Chapter 1	1
Introduction	1
1.1 The Macrophage	1
1.2 Macrophage activation	2
1.2.1 Classically activated macrophages (M1)	3
1.2.2 Alternatively activated macrophages (M2)	5
1.3 Macrophage activation and function in inflammation.....	7
1.4 Inflammation and cancer	9
1.4.1 Tumor-associated macrophages	9
1.4.2 Molecular mechanisms in tumor - associated inflammation	10
1.4.3 Role of tumor - associated macrophages in tumor progression	12
1.5 The mannose receptor	15
1.6 Possible functions of the mannose receptor in TAMs.....	17
Chapter 2	18
Aim of the study	18
Chapter 3	19
Material and Methods	19
3.1 Ethic statement	19
3.2 Animals.....	19
3.3 The B16F1 tumor melanoma model	19
3.4 Animal experiments and protocols	20
3.4.1 Culturing of B16F1 melanoma cells.....	20
3.4.2 Preparation of animals for experiments, and injection of tumor cells	21
3.4.3 Monitoring of animals and endpoint criteria	23
3.4.4 Tissue sampling	23
3.5 Testing of gene status of MR-KO mice	24
3.6 Analyses of tumor tissue	29
3.6.1 Histological analyses of tumor tissue	29
3.6.2 Immunohistochemistry	31
3.6.3 Preparation of tissue for immunohistochemistry	32
3.6.4 De-paraffinization and rehydration of tissue sections, and antigen retrieval.....	32

3.6.5	Blocking of unspecific staining	33
3.6.6	Primary antibody.....	34
3.6.7	Secondary antibody labeling and visualization	37
3.6.8	Counterstaining and mounting	39
3.6.9	Evaluation of IHC staining results.....	41
3.7	Gene expression analysis	41
3.7.1	RNA isolation and stabilization.....	42
3.7.2	Isolation of total RNA from tumor biopsies	42
3.7.3	RNA integrity test	44
3.7.4	First strand cDNA synthesis.....	44
3.7.5	Real time PCR	46
3.8	Statistical analyses and software	47
Chapter 4	49
Results	49
4.1	In vivo tumor experiment.....	49
4.1.1	Time from inoculation of tumor cells to visible tumor growth	49
4.1.2	Rate of tumor growth in vivo	50
4.2	Tumor morphology	51
4.2.1	Quantitative analyses of tumor tissue in H&E stained sections.....	56
4.3	Immunohistochemistry	58
4.3.1	IHC screening of macrophage markers in tumors	60
4.2.3	Gene expression analysis – qPCR	78
Chapter 5	81
Discussion	81
Conclusion and further aspects	86
Bibliography	89
Appendix A	96
Materials	96
A.1	Kits	96
A.2	Primers.....	97
A.3	Antibodies.....	97
A.4	Chemicals.....	98
A.4	Reagents	99
Appendix B	100



Contents

Solutions	100
Appendix C	103
Score sheets	103
Score sheet C.1: Assessments of human endpoints, mouse experiments:.....	103
Score sheet C.2: Assessment of IHC staining of B16F1 tumors from mice:	105
Appendix D	106
Protocols	106
Protocol D.1: Fluorescence staining	106
Protocol D.2: Enzyme staining methods	108



List over Figures

1.1	Linear classifications of macrophages	2
1.2	Macrophage classification, color wheel	3
1.3	Immune- and tissue-derived signals that induce polarization in	9
1.4	Plasticity of NF- κ B activation	11
1.5	NF- κ B dependent targets	12
1.6	The complexity of TAMs function in tumor progression	13
1.7	Mannose receptor composition	16
3.1	B16F1 melanoma cells from viability test, experiment 2	22
3.2	Results from testing of gene status in MR-KO mice	28
3.3	Systematic random sampling approach for image collecting	30
4.1	The first day of visible tumor (“tumor take”), experiment 1	49
4.2	The first day of visible tumor (“tumor take”), experiment 2	50
4.3	Growth curve for animals in experiment 2	51
4.4	Morphology of the tumor tissue of the B16F1 melanomas	52
4.5	Tumor morphology of small tumors	53
4.6	Tumor morphology of medium sized tumors	54
4.7	Tumor morphology of large sized tumors	55
4.8	Necrosis (N) in % of tumor area (TA)	56
4.9	Blood vessels (BV) in % of tumor area (TA)	57
4.10	Examples of how scoring intensity was evaluated	62
4.11	F4/80 screening of small melanomas	63
4.12	F4/80 labeling of medium sized melanomas	64
4.13	F4/80 labeling of large sized melanomas	65
4.14	Screening for iNOS expression in medium sized melanomas	67
4.15	Screening for iNOS expression in large sized melanomas	68
4.16	Screening for arginase I expression in medium sized melanomas	70
4.17	Screening for arginase I expression in large sized melanomas	71
4.18	Screening for stabilin-1 expression in medium sized melanomas	73
4.19	Screening for stabilin-1 expression in large sized melanomas	74
4.20	F4/80 and mannose receptor expression in a small sized	76
4.21	F4/80 and mannose receptor expression in medium sized	77
4.22	F4/80 and mannose receptor expression in large sized	79
4.23	Preliminary results for qPCR of target genes	80



List over Tables

1.1	Genes typically expressed in M1 macrophages	4
1.2	Processes that include M2 macrophages, a summary	6
1.3	Genes typically expressed in M2 macrophages	6
3.1	PCR conditions	26
3.2	Master mix A and mix B, used for PCR	26
3.3	Primary antibodies used for testing on B16F1 melanoma	36
3.4	Scoring system for evaluating positive stained cells and staining	41
3.5	Master Mix 1, for genomic DNA elimination reaction	45
3.6	Master Mix 2, for reverse-transcription reaction	45
3.7	Preparations of Master Mix for RT-PCR	47
3.8	The RT-PCR conditions used	47
4.1	Table summarising antibody testing in melanoma tumor biopsies	59
4.2	Staining intensity of F4/80 positive cells	66
4.3	Staining intensity of iNOS positive cells	69
4.4	Staining intensity of arginase I positive cells	72
4.5	Staining intensity of stabilin-1 positive cells	75
4.6	Results from RNA isolation	79
4.7	Results from qPCR	80

Abbreviations

ACTB	Beta actin
AEC	3-amino-9-ethylcarbazole
AMK	Department of Comparative Medicine
B2M	Beta-2 microglobulin
BSA	Bovine serum albumin
BV	Blood vessels
COX-2	Prostaglandin endoperoxide H synthase type 2
CTLDS	C-type lectin-like domains
CysR	Cysteine-rich NH ₂ – terminal domain
DAB	Peroxidase-diaminobenzidine
DAPI	4', 6-diamidino-2-phenylindole
D-GluNAc	D-N-acetylglucosamine
DMEM	Dubelccos modified Eagles medium
dNTPs	Deoxynucleotide Triphosphates
DTT	Dithiothreitol
ECM	Extra cellular matrix
EDTA	Ethylenediaminetetraacetic
EtOH	Ethanol
FCS	Fetal calf serum
FGF	Fibroblast growth factor
FNII	Fibronectin type II domain
GAPDH	Glyceraldehyde-3-phosphate dehydrogenase
GPI	Glycophosphatidylinositol
HMGB1	High-mobility group box1 proteins
HRP	Horseradish peroxidase
HSPs	Heat-shock proteins
H ₂ O ₂	Hydrogen peroxidase
IFN- γ	Interferon-gamma
IHC	Immunohistochemistry
IKK β	I kappa B kinase
IL	Interleukin
iNOS	Inducible nitric oxide synthase
IRF	Interferon regulatory transcription factor
LPS	Lipopolysaccharide
M1	Classically activated macrophages
M2	Alternatively activated macrophages
M-CSF	Macrophage colony stimulating factor
MCP-1	Monocyte chemoattractant protein-1
MHC	Major histocompatibility complex
MMP	Matrix metalloproteinase
MR	Mannose receptor
Mrc1	Mannose receptor, C type 1 gene
MR-KO	Mannose receptor knockout mice
NARA	Norwegian National Animal Research Authority



Abbreviations

ND	Non determined
NF- κ B	Nuclear factor kappa-light-chain-enhancer of - activated B-cells
NK	Natural killer cells
NO	Nitric oxide
NOS2	Nitric oxide synthase 2
PAMPs	Pathogen associated molecular patterns
PBS	Phosphate buffered saline
PBST	Phosphate-buffered saline with Tween20
PCR	Polymerase chain reaction
PDGF	Platelet derived growth factor
PFA	Paraformaldehyde
PIPC	Propeptide of type I and III procollagen
PPRs	Pattern recognition receptors
qPCR	Quantitative real time-PCR
ROS	Reactive oxygen species
RPMI	Roswell Park Memorial Institute
RQI	RNA quality indicator
RT	Reverse transcriptase
SD	Standard deviation
SEM	Standard error of the mean
STAT	Signal transducers and activators of transcription
TA	Tumor area
TAMs	Tumor associated macrophages
TBE	Tris-borate-EDTA buffer
TBS	Tris-buffered saline
TBST	Tris-buffered saline with Tween20
TC	Tumor central
TGF- β	Transforming growth factor – beta
Th1	T helper 1 cell
Th2	T helper 2 cell
Th17	T helper 17 cell
TIMP	Tissue inhibitors of metalloproteinase
TLR	Toll-like receptor
TNF- α	Tumor necrosis factor- alfa
TP	Tumor peripheral
Tregs	Regulatory T cells
UNN	University Hospital North Norway
VEGF	Vascular endothelial growth factor
WT	Wild-type mice
YWHAZ	Phospholipase A

Chapter 1

Introduction

1.1 The Macrophage

The term “macrophage” was proposed in 1884 by the Russian biologist, Elie Metchnikoff, to describe a type of white blood cells with high phagocytic activity. “Macrophage” is Greek and means “big eater”, and reflected exactly what Metchnikoff observed in his microscope: the cells he studied had the ability to avidly ingest and destroy microorganisms and other cellular debris. From his extensive studies in the 1880s of the phenomenon of phagocytosis in various animal systems Metchnikoff proposed the concept of cellular immunity, and in 1908 he and Paul Erlich won the Nobel Prize in medicine for their work as pioneers of cellular and humoral immunology [1, 2].

Later it was found that macrophages originate from bone marrow - derived monocytes. After leaving the bone marrow, monocytes circulate in the blood for 1-2 days in humans, before entering the tissue where they differentiate and become tissue specific macrophages [3]. Macrophages reside in almost every tissue of the body and represent an extremely heterogeneous population of cells, characterized by considerable diversity and plasticity. In response to their microenvironment they will adopt niche-specific functions in the different tissues [4]. An example is the Kupffer cells, or resident liver macrophages, which are located in the liver sinusoids, where they efficiently eliminate blood-borne bacteria and other particulate substances that enter the liver via the portal vein [5]. The Kupffer cells also have functions in modulating iron homeostasis by erythrophagocytosis [6]. Lung alveolar macrophages represent another example of tissue resident macrophages. They are highly phagocytic cells that remove dust particles, foreign material and pathogens from the alveoles, and thus have a critical role in the lung cellular defense against infections [7]. In spleen, resident macrophages ingest tens of billions of dead erythrocytes each day [3], whereas in bone, the osteoclasts represent highly specialized, multinucleated macrophage like cells, with bone resorbing functions [8].

Macrophages are multifunctional cells with important roles in inflammation and immunity [9]. They are essential for regulation of wound healing and for returning the tissue back to homeostasis after injury or infection [9]. As professional phagocytes they function as “janitor cells”, or caretakers [10] constantly removing apoptotic cells and cellular debris. On a daily basis, the phagocytic actions of macrophages occur without inducing inflammatory signals. However, the macrophage is one the body’s most active secretory cells and depending on the signals they receive, they secrete a vast array of mediators, such as cytokines,

chemokines and growth factors that are involved in regulating homeostasis, immune defense, immune surveillance and inflammation [9].

1.2 Macrophage activation

In a normal tissue, resident macrophages and newly recruited macrophages from blood monocytes are subjected to a hierarchy of activation states to ensure that there is a baseline tissue homeostasis. This prevents the constant inflammation that is seen in many chronic diseases [11]. As mentioned the tissue microenvironment is the main determinant of the macrophage activation phenotype. One simple way of classifying macrophages are along a linear scale, where in one end you find classically activated macrophages, also named the M1 phenotype, and in the other end alternatively activated macrophages, or the M2 phenotype (**Figure 1.1**) [10]. Tissue resident macrophages that are uniquely adapted to their location, like Kupffer cells and alveolar macrophages are located in the grey area, and show partial phenotypes from both of the two extremes.



*Figure 1.1: **Linear classification of macrophages:** In one end: classically activated macrophages (M1), and in the other end: alternatively activated macrophages (M2). The grey area in between illustrates a wide array of other phenotypes that macrophages can adopt [10]. The figure is reproduced from Mosser, D.M. and J.P. Edwards, *Exploring the full spectrum of macrophage activation*. *Nat Rev Immunol*, 2008. **8**(12): p. 958-69.*

Some authors have argued that the M2 destination has rapidly expanded to include essentially all other types of macrophages than the typically classically activated macrophage (M1) and have used a color wheel to illustrate macrophage plasticity (**Figure 1.2**) [10].

Behind these different forms of macrophage activation lies a wide array of transcription factors, but also epigenetic mechanisms, and post - transcriptional regulators, as well as a network of signaling molecules [12].

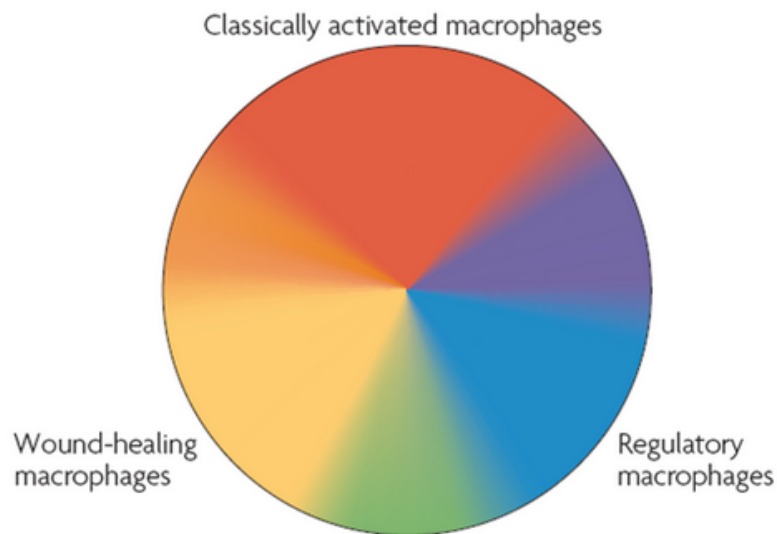


Figure 1.2: Macrophage classification, color wheel: The figure illustrates how Mosser and colleagues proposed to classify macrophages, by using a color wheel. Three populations of macrophages are arranged according to the three primary colors, red color for classically activated macrophages (M1), blue for regulatory macrophages, involved in regulation of immune responses, and yellow for wound-healing macrophages. In the linear classification the two latter types of macrophages would be classified as M2 polarized. The authors argued that the M2 designation has rapidly expanded to include essentially all other types of macrophages, and that a color wheel enhances the illustration of macrophage plasticity. The figure is reproduced from Mosser, D.M. and J.P. Edwards, *Exploring the full spectrum of macrophage activation*. *Nat Rev Immunol*, 2008. **8**(12): p. 958-69 [10].

1.2.1 Classically activated macrophages (M1)

The first and most thoroughly described macrophage phenotype is the classically activated macrophage (M1), which act as an effector cell in T helper cell 1 (Th1) immune responses. The Th1 response is characterized by the production of interferon-gamma (IFN- γ), tumor necrosis factor- α (TNF- α) and interleukin (IL) -2, which activate bactericidal activities of macrophages, and induce B - cells to make opsonizing and complement-fixing antibodies [13].

Macrophages become activated towards an M1 polarization by being exposed to IFN- γ , TNF- α and lipopolysaccharide (LPS), leading to up-regulation of genes shown in **Table 1.1**. IFN- γ is an obligatory first signal that primes the macrophage [14]. The next signals are TNF- α , LPS or other danger signals. Danger signals are molecules of endogenous or exogenous origin that alert the immune system and promote an immune response [15]. LPS acts through Toll-like receptors (TLRs) 2 and 4 [9]. These TLRs are highly expressed in M1 macrophages, where they have fundamental roles in pathogen recognition and activation of the innate immune response. M1 macrophages also express opsonic receptors such as Fc-gamma-receptor-I (CD16),-II (CD32) and -III (CD64) [16]. M1 macrophages exhibit potent microbicidal and

tumoricidal activity, and show high expression of IL-12 and IL-23. These cytokines make the M1 macrophage an efficient producer of toxic intermediates such as reactive oxygen species (ROS), and nitric oxide (NO) produced by inducible nitric oxide synthase (iNOS). M1 macrophages also produce the pro-inflammatory cytokines IL-1 β , TNF- α and IL-6 [17].

Table 1.1: Genes typically expressed in M1 macrophages. The genes are induced by IFN- γ and/or LPS stimulation. The data in the table is collected from [16-31].

Genes expressed	Functions
Cytokines	
TNF- α	Multifunctional cytokine, released in response to LPS and IL-1 [18]. Crucial for initiating innate and adaptive immunity inflammatory responses. Regulates cell proliferation and apoptosis. On macrophages: stimulates phagocytosis, IL-1 and ROS production [19]
IL-6	Multifunctional, pleiotropic, differentiation factor for activated B-cells [20], inducer of the fever response [21], and of angiogenesis by induction of VEGF production [22]
IL-12	Pro-inflammatory cytokine that induces maintenance of naïve CD4 ⁺ T as well as differentiation of these cells to Th1 cells. Blocks Th2 cell responses, and activates NK cells [23]
IL-1 β	Important mediator in the inflammatory response, stimulates thymocyte proliferation and B-cell maturation [24]
IL-23	Pro-inflammatory cytokine closely related to IL-12. Stimulates proliferation and polarization of Th17 cells and proliferation of memory T cells [23]
Cytokine receptors	
IL-1 receptor type I	Receptor for IL-1 α and β , involved in inducing immune and inflammatory responses [25]
Chemokines	
CXCL8 (IL-8)	One of the major mediators of inflammatory responses, act as chemoattractant especially for neutrophils, and induces phagocytosis at the site of inflammation or infection [26]
CXCL9, CXCL10	Both chemokines bind to the same receptor (CXCR3) and is induced by IFN- γ , recruit leukocytes to site of infection and inflammation, and are critical mediators of T-cell dependent immune responses [27]
CCL2-5	CCL2: Chemotactic for monocytes and basophils [28]; CCL3: Involved in inflammatory responses [29]; CCL4: Chemokinetic and inflammatory

	functions [30]; CCL5: Chemoattractant for monocytes, memory T helper cells, and eosinophil granulocytes [31]
Chemokine receptors	
CCR7	Receptor for CCL19 and CCL21. Controls the migration of memory T-cell and dendritic cells to inflamed tissue
Effector molecules	
iNOS	Messenger and effector molecule, induced by TNF- α , IL-1 β and IFN- γ (activation through NF- κ B signaling pathways); iNOS catalyze the breakdown of L-arginine to NO and reactive oxygen species with potent cytotoxic/cytostatic effects (reviewed in [32])

Abbreviations in Table 1.1: VEGF: Vascular endothelial growth factor, Th2: T helper cell 2, NK: Natural killer cells, Th17: T helper 17 cell, NO: nitric oxide

1.2.2 Alternatively activated macrophages (M2)

Macrophages are activated towards an M2 polarization by the Th2 cytokines IL-4 and IL-13 [33]. This phenotype can also be induced by IL-10 or transforming growth factor- β (TGF- β). Depending on the mediators that induce the phenotype, three forms of M2 macrophages have been proposed: 1) M2a, induced by IL-4 or IL-13; 2) M2b, induced by immune complexes and TLR ligands or the IL-1 receptor antagonist (IL-1Ra); and 3) M2c, induced by IL-10 and glucocorticoids [34]. M2 macrophages produce anti-inflammatory cytokines (IL-10 and IL-1Ra), various chemokines and TGF β [35].

M2 macrophages are highly expressed in the wound healing response following inflammation, and are involved in many aspects of this process (**Table 1.2**). By producing TGF- β and platelet derived growth factor (PDGF) they stimulate growth of epithelial cells and fibroblasts [36], whereas tissue remodeling is regulated by enhanced expression of matrix metalloproteinases (MMPs) and tissue inhibitors of metalloproteinases (TIMPs) [36]. Angiogenesis is stimulated through secretion of pro-angiogenic mediators like vascular endothelial growth factors (VEGFs) [37]. M2 macrophages also take part in regulation and resolution of inflammation [38], which will be further discussed in section 1.3.

M2 polarized cells express high levels of scavenger receptors [39] of which stabilin-1 has been recently added to the chart [40]. Scavenger receptors constitute a diverse group of transmembrane receptors that mediate endocytosis of macromolecules with a net negative charge [41]. Ligands for scavenger receptors include oxidized lipoproteins, advanced glycation end products, extracellular matrix (ECM) components, sulphated polysaccharides, nucleic acids, and lipoteichoic acid found in the cell wall of Gram-positive bacteria [42].

Table 1.2: *Processes that include M2 macrophages, a summary*

Process	Mediator	References
Stimulate proliferation of epithelial cells and fibroblasts [34]	PDGF	[34]
Tissue remodeling [34]	MMPs TIMPs	[34]
Angiogenesis	VEGFs	[36]
Immunoregulatory responses, including T cell anergy	IL-10	[43]
Endocytosis of microorganisms and waste products	Scavenger receptors Mannose receptor	[44]

M2 macrophages also express the glucan receptor and the mannose receptor [16] which are lectins that recognize specific carbohydrates on the surface of microorganisms. The mannose receptor also mediates uptake of endogenous molecules, such as lysosomal enzymes and waste products from collagen turnover [13, 45, 46]. The mannose receptor is commonly used as a marker for the M2 phenotype [10].

Metabolically, the M2 macrophages also differ from the M1 phenotype: In M2 cells the arginine metabolism is oriented towards production of ornithine and polyamine (precursors of collagen) instead of production of citrulline and NO, as in the M1 cells [47]. High expression of arginase (**Table 1.3**), which catalyzes the reaction of arginine and water to ornithine and urea, is therefore regarded as a marker of the M2 phenotype, whereas high expression of iNOS is used as a phenotypic marker for M1 cells.

Table 1.3: *Genes typically expressed in M2 macrophages.*

Genes expressed	Functions
Cytokines	
IL-10	Anti-inflammatory, pleiotropic effects in immune regulation and inflammation, down-regulates expression of Th1 cytokines, and MHC class II antigens, and can block NF- κ B activity [48]
IL-1 receptor antagonist	Inhibits the activity and function of IL-1 α and IL-1 β [49]
Cytokine receptors	

Decoy IL-1 receptor type II	Decoy receptor that binds IL-1 α , IL-1 β , acts as a negative pathway regulator of these ligands [50]
Chemokines	
CCL16	Up-regulated by IL-10. Chemotactic activity for lymphocytes and monocytes, suppress proliferation of myeloid progenitor cells [51]
CCL18	Attracts naïve T cells, CD4 ⁺ and CD8 ⁺ T cells [52]
CCL17	Chemotactic for T cells, plays important roles in T cell development in thymus [53]
CCL22	Chemotactic for monocytes, dendritic cells and natural killer cells, attraction of activated T lymphocytes to site of inflammation [54]
Chemokine receptors	
CCR2	Receptor for monocyte chemoattractant protein-1 (MCP-1), involved in monocyte infiltration in acute inflammation, chronic inflammation and tumor tissue [55]
CXCR1, CXCR2	Receptor for IL-8 [56, 57]
Effector molecules	
Arginase	Catalyzes the conversion of arginine and water to ornithine and urea (precursors of collagen) production [47]

Abbreviations in Table 1.3: MHC: Major histocompatibility complex, NF- κ B: nuclear factor kappa-light-chain-enhancer of activated B-cells, MCP-1: monocyte chemoattractant protein-1.

1.3 Macrophage activation and function in inflammation

Macrophages are not only critical for the initiation, but also for the propagation and resolution of inflammation. Evolution has equipped the host with a system that has coupled inflammation and wound healing together [18], and necrosis of host-cells is part of the earliest danger signals to the immune system [58]. Inflammation is also one of the seven hallmarks of cancer [59]. I will therefore start describing macrophage functions in inflammation before I move to their suggested roles in tumors.

Macrophages are recruited to the site of injury and infection due to tissue damage. As mentioned macrophages can be activated by exogenous danger signals or PAMPs (pathogen associated molecular patterns) [18], but macrophages also sense endogenous danger signals

that comes from necrotic tissue due to damage or stress. Some of these endogenous danger signals are called alarmins. These include heat-shock proteins (HSPs) and high-mobility group box1 proteins (HMGB1) [60]. Other endogenous danger signals can be hyaluronan, fibronectin fragments and DNA [18]. Many danger signals binds to the same pattern recognition receptors (PPRs) as PAMPs signal (TLRs, scavenger and lectin receptors) and can activate macrophages [18]. In response to an injury, activated platelets produce TGF- β and PDGF which act as chemo-attractants for leukocytes [61].

The first-responder macrophages that arrive to a site of an injury or infection will have an M1 activation. They act as soldiers, and attack and defend the host from viral and microbial infections by secreting pro-inflammatory mediators such as TNF- α , NO, and IL-1 [17]. TNF- α , and IL-1 contribute to the recruitment of more inflammatory cells and these actions are critical for the elimination of pathogens.

In an acute inflammation macrophages phagocytose foreign material, cellular debris, and dying/dead granulocytes and other inflammatory cells. This phagocytosis stimulates the production of TNF, IL-1 and TGF- β in macrophages. TGF- β will function in resolving the inflammation and initiate the production of ECM components by fibroblasts and thereby initiate the process of wound healing [62]. Damaged and necrotic cells release IL-25, IL-33 and alarmins. This will induce the production of IL-4 and IL-13 in innate and adaptive immune cells [11] which in turn induces M2 polarization of macrophages. A summary of immune- and tissue-derived signals that induce polarization in macrophages is shown in **Figure 1.3**. Alarmins are also potent activator of dendritic cells (DC), which are necessary for a successful immune response.

M2 macrophages produce IL-10 and other anti-inflammatory cytokines. IL-10 acts both in an autocrine and paracrine way, and has immunoregulatory effects, and IL-10 stimulation leads to a down-regulation of many mediators in macrophages, such as MMPs, inflammatory cytokines and chemokines. It also stimulates T cell anergy and induction of regulatory T cells (Tregs) [63], which contributes to the anti-inflammatory effects of IL-10.

When the pathogen or inflammatory stimuli is eliminated, the amount of M1 cells declines. In this later stage of inflammation, M2 macrophages accumulate at the site where they act to balance the action of M1 macrophages [11]. M2 macrophages have the important task of restoring tissue homeostasis. Their down-regulation of the M1 response is essential for the wound healing process to be initiated and for proper tissue repair [64].

In normal circumstances the inflammatory process is self-restricting, but macrophages are potent effector cells and an uncontrolled inflammatory response can produce tissue injury, chronic inflammation and in worst case cancer [58]. M1 and M2 macrophages do not have strict opposing actions at the site of inflammation, but there is a complex interplay between the two phenotypes that is crucial for shaping an appropriate response [65], and for successful resolution of the inflammation.

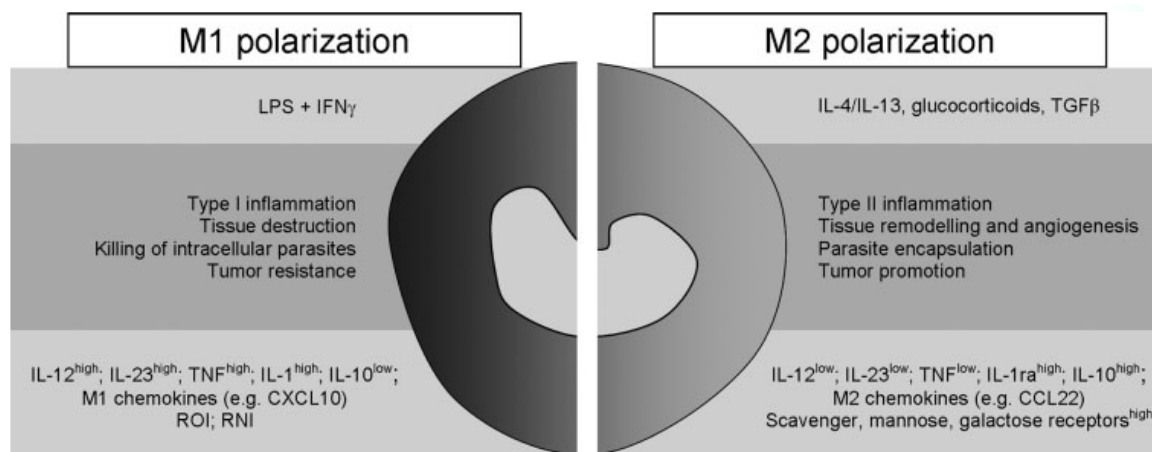


Figure 1.3: **Immune- and tissue-derived signals that induce polarization in macrophages, a simple overview.** The figure illustrates functional programs, chemokines and cytokines that are characteristic for the M1 and M2 phenotype. The figure is collected from **Mantovani, A., A. Sica, and M. Locati**, *New vistas on macrophage differentiation and activation. Eur J Immunol*, 2007. **37**(1): p. 14-6. [66]

1.4 Inflammation and cancer

Inflammation is a characteristic feature of many tumors. The tumor microenvironment consists of, in addition to cancer cells and stromal cells, an abundance of inflammatory cells and their mediators (reviewed in [67]). Inflammation is suggested as the 7th hallmark of cancer [59] together with insensitivity to growth inhibitors, self-sufficiency in growth signals, limitless replicative potential, sustained angiogenesis, evasion of apoptosis, and tissue invasion & metastasis [68]. Epidemiological studies have further shown that chronic inflammation may also in itself predispose for various forms of cancer [59].

1.4.1 Tumor-associated macrophages

Stromal cells like fibroblasts and infiltrating leukocytes can make up a prominent part of solid tumors. Mantovani and colleagues have argued that tumor-associated macrophages (TAMs) are major players of cancer-related inflammation in these tumors (reviewed in [69]). In some cancers, such as invasive breast carcinomas, lung and prostate cancers TAMs represent up to 50% of the tumor mass [69].

TAMs originate from circulating blood monocytes that are recruited to the tumor by chemokine (C-C motif) ligand 2 (CCL2) [70], and other chemokines such as macrophage colony stimulating factors (M-CSF), and VEGF. Monocytes that enter the tumor are influenced by the microenvironment and will differentiate towards an M2 polarization.

Epidemiological studies have shown a connection between numbers of TAMs and poor prognosis in melanoma, breast, prostate, ovarian, cervical and lung cancers [71, 72].

TAMs express a unique transcriptional program. A cDNA microarray study of gene expression profiles of TAMs isolated from murine fibrosarcoma showed unique TAM plasticity in the tumor microenvironment [35]. TAMs had high expression of the immunosuppressive cytokines IL-10 and TGF- β , the pro-inflammatory chemokines CCL2 and CCL5 and the IFN-inducible chemokines CXCL9, CXCL10 and CXCL16. This functional profile was proposed to be associated with defective activation of the transcription factor NF- κ B, full activation of the MyD88-independent interferon regulatory transcription factor (IRF)-3, signal transducers and activators of transcription (STAT)-1 pathway [35]. TAMs also showed a IL-12^{low}, TNF- α ^{low} and nitric oxide synthase 2 (NOS2)^{low} expression profile [73]. An interesting feature with TNF- α is that it shows a biphasic and dosedependent effect in tissues. High doses of TNF- α induce cellular necrosis and have anti-tumor effects, whereas low doses of TNF- α promote tumor development by supporting tumor angiogenesis, tumor growth and metastasis [73].

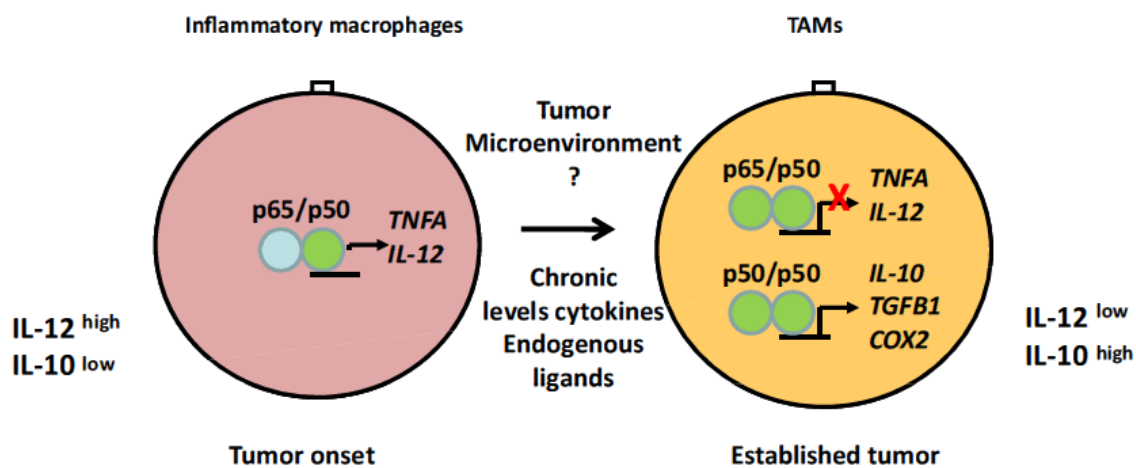
TAMs also express CD81 which is involved in co-stimulation of T cells and is a requirement for the induction of Th2 immune responses [74], which is an anti-inflammatory response. Biswas, et.al showed that TAMs represent an unique population of macrophages that express the key properties of M2 cells, but in addition they also express IFN-inducible chemokines [39].

1.4.2 Molecular mechanisms in tumor - associated inflammation

Signaling in cancer-related inflammation is suggested to go through some of the same signal-transduction mechanisms as infection-related inflammation. In infection toxins and invading organisms are recognized by PRRs of which TLRs are central. TLRs control the activation of many cytokines, chemokines and enzymes and are crucial for correct immune responses [75]. Although TLRs induce several important signaling pathways, signaling leading to NF- κ B activation has a central role in inflammation and innate immunity. The NF- κ B protein family has 5 members: NF- κ B1 (p50), NF- κ B2 (p52), RelA (p65), RelB, and cREL. These members form various dimers (homo- and heterodimers) with different gene regulatory properties [76]. NF- κ B members regulates the expression of many important genes in macrophages including TLR ligands, TNF- α , IL-1, VEGF, IL-6 and COX-2 (reviewed in [77]).

NF- κ B activation occurs in two major pathways. In the classical (canonical) pathway upstream signals leads to the phosphorylation of I κ B kinase (IKK) β and release of p65/p50 NF- κ B heterodimer that translocate to the nucleus and induce the expression of pro-inflammatory genes such as TNF- α , IL-6 and IL-23 (reviewed in [78]). In the alternative (noncanonical) pathway active IKK α homodimers leads to the translocation of p52/ RelB dimers. This pathway has been found to be required for lymphoid organogenesis and maintenance (reviewed in [78]). TAMs have been shown to have a defective activation of

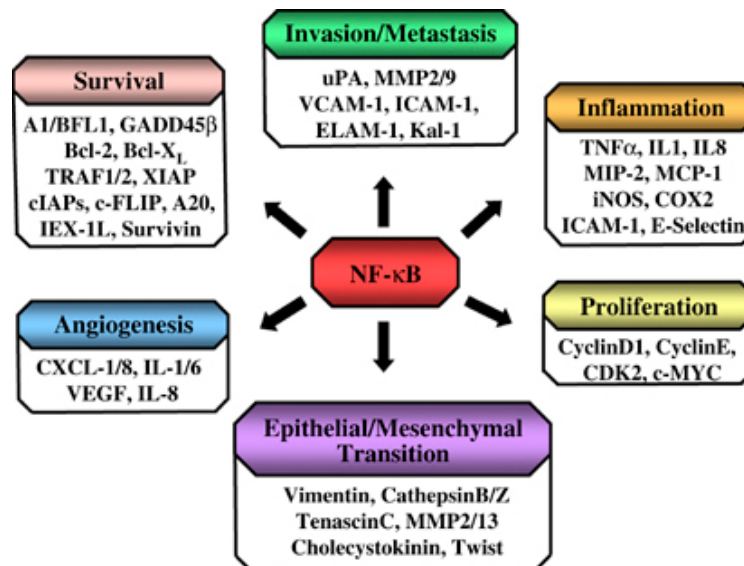
NF- κ B-inducible cytokines (**Figure 1.4**). This defective activation is mediated by the inhibitory p50/p50 NF- κ B homodimer. In murine fibrosarcoma and in human ovarian carcinoma TAMs were found to have a defective response to M1 activation signals due to a massive nuclear localization of p50 NF- κ B homodimers that acts as inhibitor of pro-inflammatory NF- κ B – dependent genes including TNF- α and IL-12 [79]. In the same study TAMs showed a status of tolerance in response to pro-inflammatory signals (especially IL-12 and TNF- α) and the authors argued that p50 may play a pivotal role in tuning of NF- κ B- dependent M1 activation of TAMs. The p50 homodimers have also been shown to be necessary for transcription of COX-2 [80] which is reported to be up-regulated in TAMs [81]. It has also been demonstrated that p50 is crucial in the induction of IL-10 gene expression through the TLR4/TPL2/ERK pathway [82].



*Figure 1.4: Plasticity of NF- κ B activation, as it is believed to function in the onset of cancer and in tumor progression. The figure illustrates what type of NF- κ B members that are activated in macrophages during the course of tumor progression. In the onset of cancer, p65/p50 heterodimers induce the expression of pro-inflammatory genes (IL-12, NOS2 and TNF- α) in M1 cells. In an established tumor TAMs show a defective NF- κ B activation, due to the overexpression of p50/p50 homodimers together with other transcription factors that induce the expression of anti-inflammatory pro-tumoral genes (IL-10, TGF- β , COX-2). The illustration is collected from **Biswas, S.K. and C.E. Lewis**, NF-kappaB as a central regulator of macrophage function in tumors. *J Leukoc Biol*, 2010. **88**(5): p. 877-84 [76].*

NF- κ B inducible pro-inflammatory genes (IL-12 and iNOS) that are associated with the M1 phenotype, have a STAT1/STAT2 binding site at their promoters [83]. IKK β inhibits STAT1 activation in macrophages which results in down-regulation of the M1 associated genes IL-12 and NOS2 [84]. This inhibition of STAT1 by IKK β is also believed to be responsible for the IL-10^{high} / IL-12^{low} expression seen in M2 cells and TAMs [83].

NF- κ B has a complex role in regulating TAM function and operates at many levels. From the studies mention above it becomes clear that NF- κ B has a unique ability to induce or repress different genes in the same cell under different conditions [85] (**Figure 1.5**).



*Figure 1.5: **NF- κ B dependent targets.** NF- κ B is often found to be up-regulated in cancers. Gene expression studies have identified many NF- κ B targets that are linked to an oncogenic phenotype in cancer. NF- κ B support cancer growth and proliferation by activation growth factors like VEGF and by activating cyclin D1 which pushes the cell from G1 phase to S phase. NF- κ B also helps cells avoid apoptosis by induce the expression of Bcl-2 and/or Bcl-xL anti-apoptotic factors and inactivate pro-apoptotic factors like Foxo3a or p53. NF- κ B induces changes in the expression of many genes that are involved in angiogenesis, invasion and metastasis like MMP-2, MMP-9, VEGF, HIF- α and IL-8 (reviewed in [86]). Figure and information is collected from **Basseres, D.S. and A.S. Baldwin**, Nuclear factor-kappaB and inhibitor of kappaB kinase pathways in oncogenic initiation and progression. *Oncogene*, 2006. 25(51): p. 6817-30.*

1.4.3 Role of tumor - associated macrophages in tumor progression

In the onset of cancer, transformed cells are recognized by the immune system that mounts an attack. Natural killer (NK) cells and T-cells produce IFN- γ that initiates the inflammatory signal. Macrophages are attracted to the scene and will first express M1 activation. In most cases the action of the immune system will destroy the transformed cells and the tissue will return back to homeostasis. In the case of cancer formation some transformed cells escape the immune system and will evolve to become cancerous cells. These cells will have the ability to grow and progress, and form a solid tumor [87]. As the tumor grows it influences its microenvironment and TAMs will have a change in phenotype and assume an M2

polarization (reviewed in [88]). TAMs show complex functions in tumor progression (**Figure 1.6**).

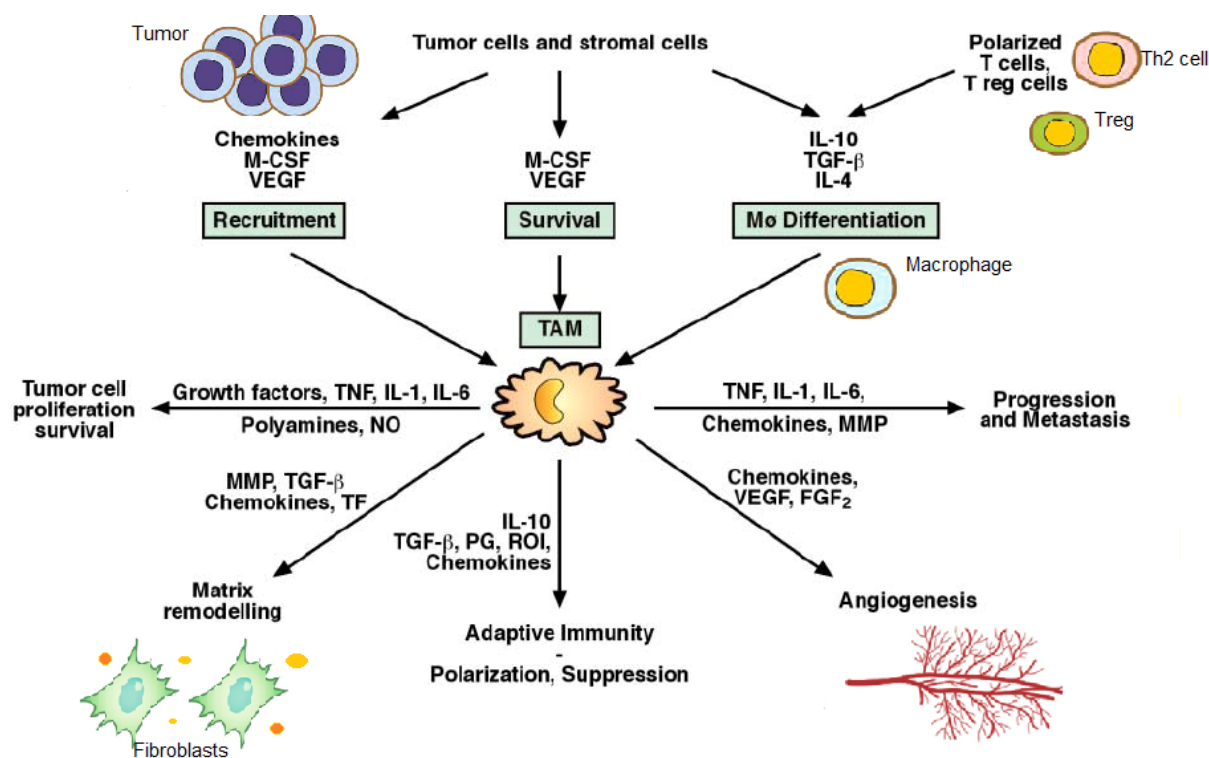


Figure 1.6: The complexity of TAMs function in tumor progression. Monocytes are recruited to the tumor due to tissue damage and tumor-derived chemotactic factors. TAMs are polarized in an M2 direction and are involved in promoting tumor proliferation and survival, matrix remodeling, progression, metastasis and suppressive anti-tumor responses. The figure is modified from **Balkwill, F., K.A. Charles, and A. Mantovani**, Smoldering and polarized inflammation in the initiation and promotion of malignant disease. *Cancer Cell*, 2005. **7**(3): p. 211-7 and **Sica, A., P. Allavena, and A. Mantovani**, Cancer related inflammation: the macrophage connection. *Cancer Lett*, 2008. **267**(2): p. 204-15. [67, 89].

As mentioned in section 1.2.2 M2 macrophages induce angiogenesis. Angiogenesis is important for growth of solid tumors and is therefore a hallmark of cancer [59]. Oxygen in tissue has a diffusion distance of about 100-200 μm and hyperplastic lesions that lack the ability to induce angiogenesis will therefore be restricted in growth to approximately 1-2 mm in diameter (reviewed in [90]). A crucial point in cancer formation is therefore when cancer cells acquire the ability to induce angiogenesis. This is called the angiogenic switch (reviewed in [90]). TAMs have been found to play a key role in inducing and maintain tumor

angiogenesis by producing growth factors (VEGF, FGF and TGF- β), cytokines (IL-8, TNF- α and IL-6) and MMPs [90, 91].

TAMs also contribute to the remodeling of ECM, by production of MMPs. MMPs are involved in many steps of cancer progression: they can release growth factors (e.g. VEGF, TGF- β) that are sequestered by ECM proteins and thereby contribute to tumor growth. They may also contribute to tumor metastasis by helping cancer cells to detach from neighboring cells and ECM, and escape the primary tumor (reviewed in [91]) (**Figure 1.6**).

As mentioned in section 1.4.1 and 1.4.2 M2 polarized TAMs have an immunosuppressive activity that is exerted indirectly by their secretion of cytokines and arachidonic acid metabolites such as PGE₂. Especially TGF- β is a regulatory cytokine that promotes the shift from M1 to M2 polarization in TAMs, and inhibits cytolytic activity in NK cells (reviewed in [92]), as well as dendritic cell migration and antigen presenting activity [93]. TGF- β also promotes CD4⁺ T cells to differentiate into Th2 cells instead of Th1 cells [94] and inhibits CD8⁺ T cell activity [95]. TGF- β therefore has a crucial impact in suppressing anti-tumor activity by immune cells.

IL-10 production by TAMs acts in an autocrine circuit and suppresses the expression of IL-12 [96]. IL-10 also inhibits expression of IFN- γ [43] and dendritic cell maturation [97]. IL-10 has been shown to dampen the antigen presenting ability of dendritic cells and macrophages to present tumor-associated antigens [98].

Prostaglandin endoperoxide H synthase type 2 or cyclooxygenase 2 (COX-2) is an enzyme that converts arachidonic acid into prostaglandin endoperoxide (prostaglandin H₂). COX-2 has been found to be constitutively expressed in many different tumors [99, 100] and TAMs have been found to be one of the major sources of COX-2 [99]. Through the production of prostaglandins, COX-2 has significant immunosuppressive actions, and therefore promotes tumor progression [101].

1.5 The mannose receptor

The mannose receptor (CD206) is a PRR that mediates clathrin-mediated endocytosis of various glycoproteins and non-opsonic phagocytosis of a wide variety of microbes [45, 46]. The receptor is expressed in subsets of tissue macrophages (e.g. M2, TAMs, alveolar macrophages) and is regarded as a hallmark of M2 macrophages [16, 102].

The receptor is also expressed in other highly endocytically active cells, such as the liver sinusoidal endothelial cell [103, 104], immature dendritic cells [105], retinal pigment epithelial cells [106], endothelial cells of lymphatic vessels [107], bone marrow sinusoidal endothelial cells [108], and in the latter cell type the mannose receptor was also reported to mediate lymphocyte binding to the vessel wall [107].

In macrophages, mannose receptor activity is modulated according to differentiation and activation, and the expression of this receptor in macrophages is regulated by cytokines. Studies have shown that mannose receptor synthesis in macrophages is up-regulated by IL-4 and IL-10 [109] and inhibited by IFN- γ [110]. Down-regulation of this receptor by IFN- γ occurs on the protein biosynthesis level, and has been shown to be fully reversible [110], supporting the notion that macrophage function is dependent on a specific balance between signals from different immunomodulators present in the microenvironment.

The mannose receptor is one of four members in the mannose receptor family or subgroup VI of the C-type lectin superfamily [111]. The receptor is a 175-180 kD transmembrane protein, with a short 45 amino acid cytoplasmic tail, and an extracellular region consisting of a cysteine-rich NH₂ - terminal (CysR) domain, a fibronectin type II (FNII) domain, and eight C-type lectin-like domains (CTLDS) [112] (**Figure 1.7**).

The CysR domain, FNII domain and CTLD4 are functional domains active in ligand binding [113]. The CysR domain binds to specific sulfated glycoproteins like SO₄-4-N-acetyl galactosamine (-GalNAc), SO₄-3-GalNAc and SO₄-3-galactose [114]. The FNII domain has its name due to its two fibronectin Type II-like repeats. This is a conserved domain, which binds to different types of denatured collagens [115].

Each CTLD consists of approximately 120 amino acids that are folded into two α -helices and two antiparallel β -sheets. Four of these domains, CTLD4-8, have affinity for carbohydrates in vitro. However, CTLD4 has been found to be the only one active in the cell, with a suggested contribution also of CTLD5 [114]. The CTLDs binding of ligand is calcium dependent, and CTLD4 needs to bind two Ca²⁺ in order to undergo conformational rearrangement in order to bind its ligands which must have either D-mannose, L-fucose, or D-N-acetylglucosamine (D-GluNAc) in terminal position of their sugar side chains [116]. The specificity for D-mannose, L-fucose and D-GluNAc are due to the presence of Glu – Pro – Asn in the ligand-binding site. These amino acids recognize sugars due to the equatorially placed hydroxyl groups in the sugars [117].

The short cytoplasmic tail of the mannose receptor contains di-aromatic motifs that are important in the receptor recycling between the plasma membrane and early endosomes. When the pH inside early endosomes drops, the mannose receptor will dissociate from its ligands and return to the plasma membrane [118].

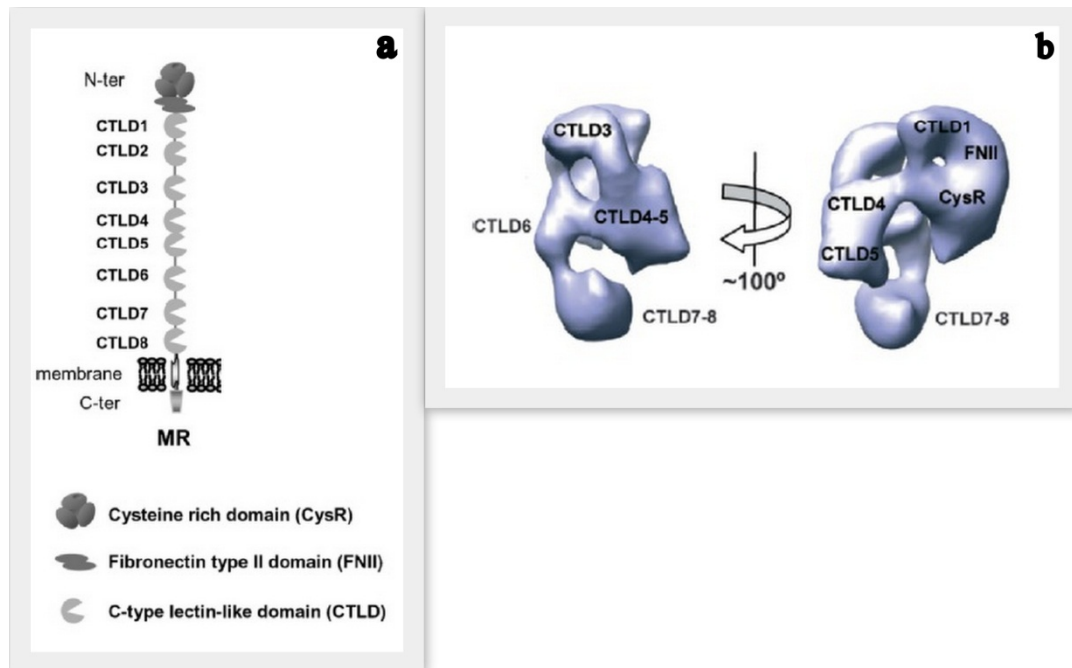


Figure 1.7: Mannose receptor composition. a) The organization of domains of the mannose receptor (MR). Functional domains are the CysR domain, FNII like domain and CTLD4. It is believed that CTLD5 might contribute to ligand recognition of CTLD4 [119]. b) The figure shows the three-dimensional structure of MR. The illustrations are collected from: **Llorca, O.**, Extended and bent conformations of the mannose receptor family. *Cell Mol Life Sci*, 2008. 65(9): p. 1302-10

The mannose receptor is a key player in innate immunity and mediate clathrin-mediated endocytosis of soluble macromolecules and colloidal particles, including virus [45, 120, 121]. In macrophages it also mediates phagocytosis of various bacterial, fungal and protozoan pathogens. As opposed to mammals, terminal mannose, fucose and GluNAc are commonly found on the surface of microorganisms [122], and pathogens as different as yeast cells, which have a cell wall rich in highly mannosylated glycoproteins [123], *Trypanosoma cruzi* (a protozoa), *Streptococcus pneumoniae* [124], *Mycobacterium tuberculosis* [125] and Dengue virus [118] [121] have been found to bind the mannose receptor.

In mammals, lysosomal enzymes and C-terminal procollagen propeptides have terminal mannose in their sugar side chains [44, 126], whereas collagen alpha chains bind to the FNII domain of the mannose receptor [115]. The clearance of such substances may add to the role of this receptor in tumor inflammation.

1.6 Possible functions of the mannose receptor in TAMs

In addition to its well documented role in host defence against pathogens, the mannose receptor has been found to mediate endocytosis/clearance of lysosomal enzymes [44] and ECM components such as collagen alpha chains of collagen types I,II, III, IV, V and XI [104, 115], and C-terminal propeptide of type I and III procollagen (PIPC) [110] which are waste products from collagen synthesis [109]. In accordance with this, mannose receptor- deficient mice have been shown to have elevated levels of lysosomal enzymes, procollagen propeptides, as well as some other molecules that are normally up-regulated during inflammation and wound healing [127].

Cancer cells release various glycoproteins and many cell surface-proteins are heavily glycosylated. In ovarian cancer, one such tumor protein, mesothelin, is reported to be displayed on the cancer cell surface through mannose residue-containing glycolipids (GPI anchors) . These GPI anchors activate the PI3K pro-inflammatory pathway upon interaction with macrophages (reviewed in [128]). Dangaj, D., et al reported that soluble mesothelin binds to the mannose receptor on macrophages and provided evidence for the contribution of this receptor to the M2 phenotype polarization of TAMs [129]. However, this has not been further studied.

Chapter 2

Aim of the study

In the present study, we aimed to examine the role of the mannose receptor in tumor-associated macrophages (TAMs). The key question was: Is the mannose receptor necessary for M2 polarization or is it just a marker of M2 polarized cells?

To assess this question we examined tumor development, TAM infiltration and TAM profiles of primary B16F1 melanomas in mannose receptor knockout (MR-KO) mice (C57BL/6 MR^{-/-}) [127] and in wild-type control mice (C57BL/6).

The B16F1 melanoma primary tumor model is a well-established cancer research model in mouse. The melanoma cells are inoculated subcutaneously in the abdominal region of the animals, and animals euthanized for tumor tissue analysis at various time points after inoculation. More specifically, we aimed to examine and compare:

- Tumor growth rate
- Histological appearance of tumor tissue in small (1-2 mm), middle sized (3-5 mm) and large tumors (> 8 mm)
- Leukocyte infiltration in tumor tissue, with special focus on TAMs
- Activation status of TAMs in tumors of various sizes, to find when the switch from M1 to M2 occurs in wild type mice, and if/when the switch occur in MR-KO mice. This was done by immunohistochemistry using primary antibodies against proteins typically expressed in M1 and M2 polarized macrophages.
- Tumor mRNA expression of M1 and M2 macrophage markers by quantitative real time – polymerase chain reaction method (qPCR).

Chapter 3

Material and Methods

3.1 Ethic statement

The animal experiments were approved by the competent authority under the Norwegian National Animal Research Authority (NARA) and were performed in compliance with the European Convention for the Protection of Vertebrate Animals used for Experimental and Other Scientific Purposes. NARA/FOTS approval IDs: ID-4976 and ID-5948.

3.2 Animals

Wild-type C57BL/6 female mice were obtained from Charles River laboratory (France). Mannose-receptor knock-out (MR-KO) C57BL/6 mice (strain name in the JAX mice database: B6.129P2-*Mrc1*^{tm1Mnz}/J) [127] were originally provided by Professor Michel Nussenzweig, The Rockefeller University, New York, NY, in 2004, and a breeding stock has since then been kept at approved premises the Department of Comparative Medicine (AKM), University of Tromsø. MR-KO status of the mouse strain was tested by polymerase chain reaction [127] as described in **section 3.2**. Only female mice were used in the present experiments.

The wild-type and MR-KO mice used in the experiments were housed in the same room, specially designed for mouse, with 12h/12h day-night cycle, and allowed free access to water and food (standard chow, Scanbur BK, Nittedal, Norway). Each cage had 2-5 mice and had environmental enrichment in form of nest material, house and chewing sticks.

3.3 The B16F1 tumor melanoma model

In 1954, the B16 melanoma arose spontaneously in the skin of the ear of a C57BL/6 mouse [130], and has later been established as an experimental tumor model in this mouse strain. The B16F1 variant of this model is highly tumorigenic and has been used significantly in tumor research [131].

The B16F1 cancer cell line used in the present experiments was obtained from ATCC-Europe (CRL-6323), and was tested, and found free of mouse-pathogens before use in *in vivo* tumor experiments, according to the regulations of Department of Comparative Medicine (AKM), UiT.

3.4 Animal experiments and protocols

Two animal experiments were carried out, and conducted according to approved protocols.

In experiment 1, we harvested tissue for histopathology and immunohistochemical analyses of B16F1 melanomas of various sizes, representing various stages in tumor development. Wild-type (n=15) and MR-KO mice (n=15) were divided into three groups according to the tumor size: small tumors (1-2 mm in diameter, n= 4), medium sized tumors (3-5 mm in diameter, n=7) and large tumors (> 8 mm in diameter, n=4). The newly dead animal was perfusion fixed, the tumor dissected out, and tissues processed for paraffin embedding. A gross examination of the carcass and internal organs was carried out in connection with tumor harvesting.

In experiment 2, we collected tissue for mRNA and protein analyses, and immersion fixed biopsies for histology. The wild-type and MR-KO mice were each divided into two groups according to tumor size: medium sized tumors (3-5 mm in diameter, n=8 per group), and large tumors (> 8mm, n=4 per group). Tumor growth were monitored as in the first experiment, and animals were euthanized when the tumor had reached the specified size (3-5 mm or 9-10 (>8) mm in diameter). A gross examination was done of carcass and internal organs, the tumors were dissected out, one half was harvested for mRNA and protein analysis, and the other half was immersion fixed and processed for paraffin embedding.

Details of the animal experiment protocols are in sections 3.4.2.

I took part in the planning of the in vivo experiments, cell culture and preparing of cells for injection, monitoring of animals, and tissue sampling after euthanasia, whereas the injections and handling of live animals were conducted by my supervisors Jaione Simón-Santamaría and Karen Sørensen, who are licenced for working with laboratory animals in research.

3.4.1 Culturing of B16F1 melanoma cells

Cells from ATCC-Europe-strain (CRL-6323) were used in both animal experiments, and the procedure for culturing of the B16F1 melanoma cells was similar. In the first experiment, cells from passage 32 were used, and in the second experiment cells from passage 33. List of chemicals and equipment are shown in appendix A.2.

General procedure:

- Cryopreserved B16F1 melanoma cells stored in liquid nitrogen were thawed rapidly in a water bath at 37°C for 1-2 min.

- The cells were then gently pipetted into a 50 ml tube, containing 20 ml of pre-warmed growth medium Dulbecco's modified Eagle's medium (DMEM) with 10 % sterile filtered fetal calf serum (FCS).
- The cells were centrifuged gently at 600 rpm for 5 min. The supernatant was removed and 15 ml DMEM with 10% FCS was added.
The cells were transferred to a small Falcon cell culture flask (75 ml) with filter cap and incubated at 37°C.
- After 24 hours the cells had grown to approximately 70% confluence and were split:
 - o The growth medium was removed and the cells washed with 5 ml PBS.
 - o 1.5 ml of trypsin-EDTA 10x (0.5% trypsin, 0.2% EDTA) was added and the cells detached within 3 min.
10 ml of DMEM with 10 % FCS was added and cells were split 1:2, and added to a large Falcon cell culture flask (175 ml) that contained 28 ml of growth medium. The cells were then incubated at 37°C for another 48 hours.
- After 48 hours the cells had reached 75 % confluence and were prepared for injection. The growth medium was removed and cells were washed with 10 ml of PBS.
- 3 ml of trypsin was added and cells detached within 3 min.
- 10 ml of DMEM with 10% FCS was then added to inactivate trypsin.
- The cells were centrifuged at 600 rpm for 5 min and added 20 ml of Roswell Park Memorial Institute (RPMI) medium before the cells were centrifuged again. Before this step, 10 µl of the solution was taken out for cell counting using a haemocytometer.
- Cells were diluted in RPMI-1640 to a final concentration of 1 million cells per ml, and kept on ice until injection in mice (section 3.4.2).

3.4.2 Preparation of animals for experiments, and injection of tumor cells

The day before injection of tumor cells, each animal was individually marked by ear punctures. A 4 cm² area at the right side of the abdomen was shaved to prepare for the injection. All animals were weighed before the start of the experiment.

Each animal was injected with 50 µl of RPMI-1640 containing approximately 50,000 B16F1 in the subcutaneous tissue of the right abdominal wall, approximately 1 cm below the costal arch.

General procedure:

- Immediately before the syringe was filled with cell suspension, the cryotube with cells was turned upside-down to mix the cells well. This is because the melanoma

cells easily sediment. Resuspension by flushing the syringe was avoided because this will mechanically destroy cells due to the fine needle.

- To minimize technical variation, all injections were done by one operator.
- To reduce the eventual effects of decreasing viability of cells, wild-type and MR-KO mice were injected every other time. In experiment 1 this was done on a cage basis, and in experiment 2 on an individual basis (one wild-type mouse, followed by one MR-KO mouse and so on). All injections in each experiment were completed within 1.5 hours after cell splitting.
- After injection, the animals were observed for at least 1 hour to look for any signs of discomfort.
- B16F1 melanoma leftover cells from the same cell suspension that was used for injection was taken back to the cell lab, seeded, incubated at 37°C overnight to test for cell viability (**Figure 3.1**).

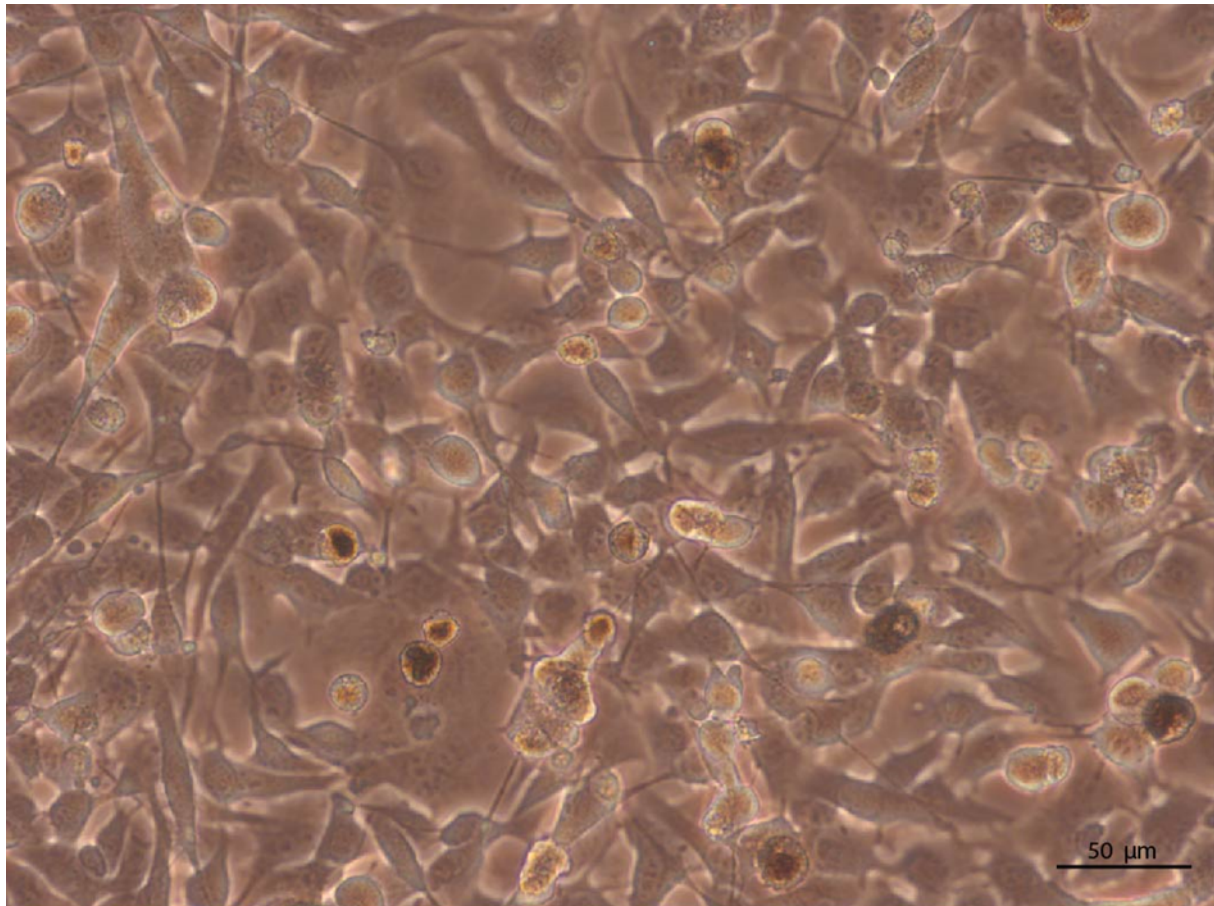


Figure 3.1: The figure shows B16F1 melanoma cells from the viability test in experiment 2. In both viability tests, cells had normal growth rate and grew rapidly to high confluence. B16F1 melanoma cells that were used for inoculation of animals had a confluence of 70 – 75 %.

3.4.3 Monitoring of animals and endpoint criteria

The animals were checked on a daily basis by the researchers, and the body weight and condition of each individual noted on a score scheme (**Appendix C**) at AKM. Human endpoint-criteria define ethical obligations when using animal in research, and was stated in the approved FOTS/NARA applications. The following criteria were implemented: If the tumor diameter reached 12 mm, or there was a weight loss of 10% of body mass, the animal should be euthanized. Any changes in general conditions like signs of discomfort, reduced activity and bristling fur coat were also reasons for euthanasia. The diameter of the tumor was measured every day or every other day by using a digital caliper.

3.4.4 Tissue sampling

The animals were euthanized on different time points according to tumor size.

Adequate fixation is needed in order to preserve tissue architecture and morphology. In experiment 1 this was obtained by perfusion fixation of the newly dead animal with 4% paraformaldehyde (PFA) in PBS with 0.02M sucrose, through the circulatory system. [132].

In experiment 2 the dead animals could not be perfusion fixed since tissues were harvested for mRNA and protein analyses. The tumors were cut in half, one half was immersion fixed in 4% PFA in PBS with 0.02M sucrose, processed and embedded in paraffin and the other half stored in All-protect Tissue Reagent, for later RNA and protein analyses.

In both experiments blood samples were harvested from the right heart chamber. Immediately after euthanasia. The samples were left to clot for 15-30 min, and centrifuged to remove clot. The collected serum was stored at -70°.

General procedure:

Fixative:

4 % PFA in PBS with 0.02 M sucrose (protocol in Appendix B)

Protocol for perfusion fixation:

- The animals were euthanized in a CO₂ chamber, according to the approved protocols for the animal experiments (NARA/FOTS ID-4976 and ID-5948)
- An incision was made through the abdominal wall of the dead animal, below the rib cage, and scissors was used to open the rib cage.
- Blood samples were collected from the right ventricle, for serum sampling.
- Blood was cleared from the general circulation by PBS infusion via the left heart ventricle. To create an outlet, a cut was made in the right atrium.

- 4 % PFA in PBS and 0.02M sucrose was pre-warmed until 37°C. The PFA solution was injected through the left heart ventricle, with outlet through the right atrium. This procedure ensured a rapid fixation of the whole body.
- Tumor tissue from all animals, as well as liver, spleen, kidneys, intestine, heart and lungs from selected animals were collected and stored in fixative at 4°C until processing and embedding in paraffin blocks.

3.5 Testing of gene status of MR-KO mice

In order to confirm the MR-KO gene status of the knockout mouse strain PCR analysis of DNA extracted from white blood cells was conducted. Blood samples were collected from the mice by trained staff at AKM.

DNA was purified by using DNeasy Blood & Tissue Kit from Qiagen (**Appendix A**). Blood samples were collected from breeders, and brothers of the female mice that were used in experiment 2, to avoid stress on the experimental animals. Breeding was carried out as pure knockout-breeding, and thus all siblings have similar gene status.

The kit is designed for rapid purification of total DNA, and suited for working with multiple samples simultaneously. The kit has four steps: blood cell lysis, binding of DNA to the column, washing of column, and elution of DNA. The samples were lysed by adding proteinase K, and then added ethanol that would optimize the binding of DNA to the membrane in the DNeasy mini spin column. The membrane in the columns selectively bind to DNA present in the sample, while the remaining contaminants and enzyme inhibitors can pass through the membrane, and are removed by washing the membrane with washing buffers. In the last step, purified DNA was eluted by using a low-salt buffer.

General procedure:

- Blood samples were collected from the animals using heparin as anti-coagulant
- The blood samples were transferred to 1.5 ml microcentrifuge tubes and 20 µl proteinase K was added. Volume was adjusted to 220 µl with PBS.
- 200 µl of buffer AL was added to the samples and thoroughly mixed by vortexing
- The samples were then incubated at 56°C for 10 min on a heating plate.
- 200 µl of 96% ethanol was added and mixed thoroughly by vortexing.
- The mixture from each sample was pipetted into a DNeasy Mini spin column, placed in a 2 ml collection tube and centrifuged at 8000 rpm for 1 min. Collection tube with flow through was discarded.
- The spin columns were placed in a new collection tube and added 500 µl of buffer AW1 and centrifuge for 1 min at 8000 rpm. Flow-through and collection tube was discarded.

- The spin columns were then placed in a new collection tube, added 500 µl of buffer AW2, and centrifuged for 3 min at 14.000 rpm.
- Flow-through and collection tube was discarded, and the spin columns placed in 1.5 ml microcentrifuge tubes.
- To elute DNA 200 µl of buffer AE was added to the spin columns and incubated for 1 min, before being centrifuged for 1 min at 8000 rpm to elute DNA from the spin columns.

DNA was stored at - 70°C until PCR was conducted.

Mannose receptor PCR

PCR is a method where a specific DNA sequence is amplified by the use of sequence-specific primers and multiple cycles of DNA synthesis, where each cycle is followed by a brief heat treatment to separate complementary strands. The DNA sequence that is amplified by PCR has a limited size of approximately 40 kb. The PCR setup requires components and reagents listed in **Table 3.1 and 3.2**. The MR-KO mouse was made by inserting a stop codon in exon 1 in the Mrc1 gene [127]. Primers, constructed by the group that made the MR-KO mouse model [127] were ordered from Sigma:

Forward primer:

- 5' -GACCTTGGACTGAGCAAAGGGG-3'

Reverse primer:

- 5'-GACATGATGTCCTCAGGAGGACG-3'

PCR products from mouse cells without a functional Mrc1 gene are expected to be approximately 1100 bp, as opposed to a product of approximately 400 bp from mouse cells with intact Mrc1 gene.

Principle: Each thermal cycle in the PCR reaction consists of three temperature steps. In step one the double stranded DNA is denatured by high temperature (94°C) which breaks the hydrogen bonds between complementary strands. In the second step, the temperature is lowered to 70°C to allow the primers to anneal. DNA polymerase binds to the primers and elongation starts. In step three, the temperature is raised to 72°C, which is the optimum temperature for the polymerase to elongate the new strand by adding deoxynucleotides (dNTPs). Every cycle of PCR will double the amount of gene present in the sample if the efficiency of the reaction is 100%. All cycles are with polymerase except step 1, which is a preheating step.

Table 3.1: PCR conditions. One cycle is from step 2 – 4, and is repeated 34 times, for a total of 35 cycles. Step 1 is a preheating step, and therefore do not include polymerase.

Step	Time	Temperature
1	5 min	94°C (without polymerase)
2	35 sec	94°C
3	1 min	70°C
4	1 min	72°C

General procedure:

- Master mixes A and B were prepared in DNA LoBind 2 ml Eppendorf tubes, for a total of 11 samples according to **Table 3.2**, without adding the DNA samples.

Table 3.2: Master mix A and mix B, used for PCR

Master mix A		
Reagent	µl per sample	µl for 11 samples
DNA sample	5	
RNAse free water	33.5	368.5
PCR buffer x 10	4.5	49.5
dNTPs (10 mM)	1	11
Primers (50 µM)	1	11
Total	45	440
Master mix B		
Reagent	µl per sample	For 11 samples, µl
DyNAzyme™ II DNA polymerase	0.5	5.5
PCR buffer x 10	0.5	5.5
RNAase free water	4	44
Total	5	55

- Ten DNA LoBind 0.5 ml Eppendorf tubes were marked
- 40 μ l of the master mix A was first added to each 0.5 ml Eppendorf tube
- 5 μ l of DNA sample was added and samples were placed in the PCR machine for step 1 (**see Table 3.1**); 5 minutes at 94°C.
- 5 μ l of master mix B was added
- PCR reaction was allowed to run for 35 cycles.

Analysis of PCR product

Agarose gel electrophoresis was used to get a visible result from the PCR. In this method, DNA fragments were separated according to size and charge. Tris-borate-EDTA (TBE) buffer was used as a running buffer for the agarose gel electrophoresis, with 1.2% agarose.

General procedure:

- 5x Tris-borate-EDTA buffer (**Appendix B**) was diluted to a concentration of 0.5x (1:10 dilution) with dH₂O.
- 0.9 mg of agarose was added to 75 ml of TBE and heated in a microwave until boiling.
- The gel was left to cool for 5 min before adding 5 μ l of GelRed.
- The gel was poured in into the electrophoresis chamber, and a comb was placed and the gel left to solidify (approximately 20 min).
- The comb was removed, and the gel top filled with 300 ml of dH₂O, and each buffer chamber filled with TBE running buffer.
- 9 μ l of PCR product was added to 0.5 ml micro tubes, 1 μ l of loading buffer was added, and samples were briefly spun down.
- 6 μ l of each sample was loaded on the gel.
- The gel was run at 220V for 20 min.

Testing of gene status in MR-KO mice by immunohistochemistry

In addition to testing the gene status by PCR, we also tested gene status by immunohistochemistry, fluorescence method as described in 3.6.2. Protocol: **Appendix C.1**.

The result from PCR was as expected, all animals had a positive band at 1000 bp in the agarose gel and all animals are therefore homozygotes, MR-KO (**Figure 3.2, A**). Results from immunohistochemistry also supports the findings from PCR, MR is not expressed in liver or tumors (**Figure 3.2, B**).

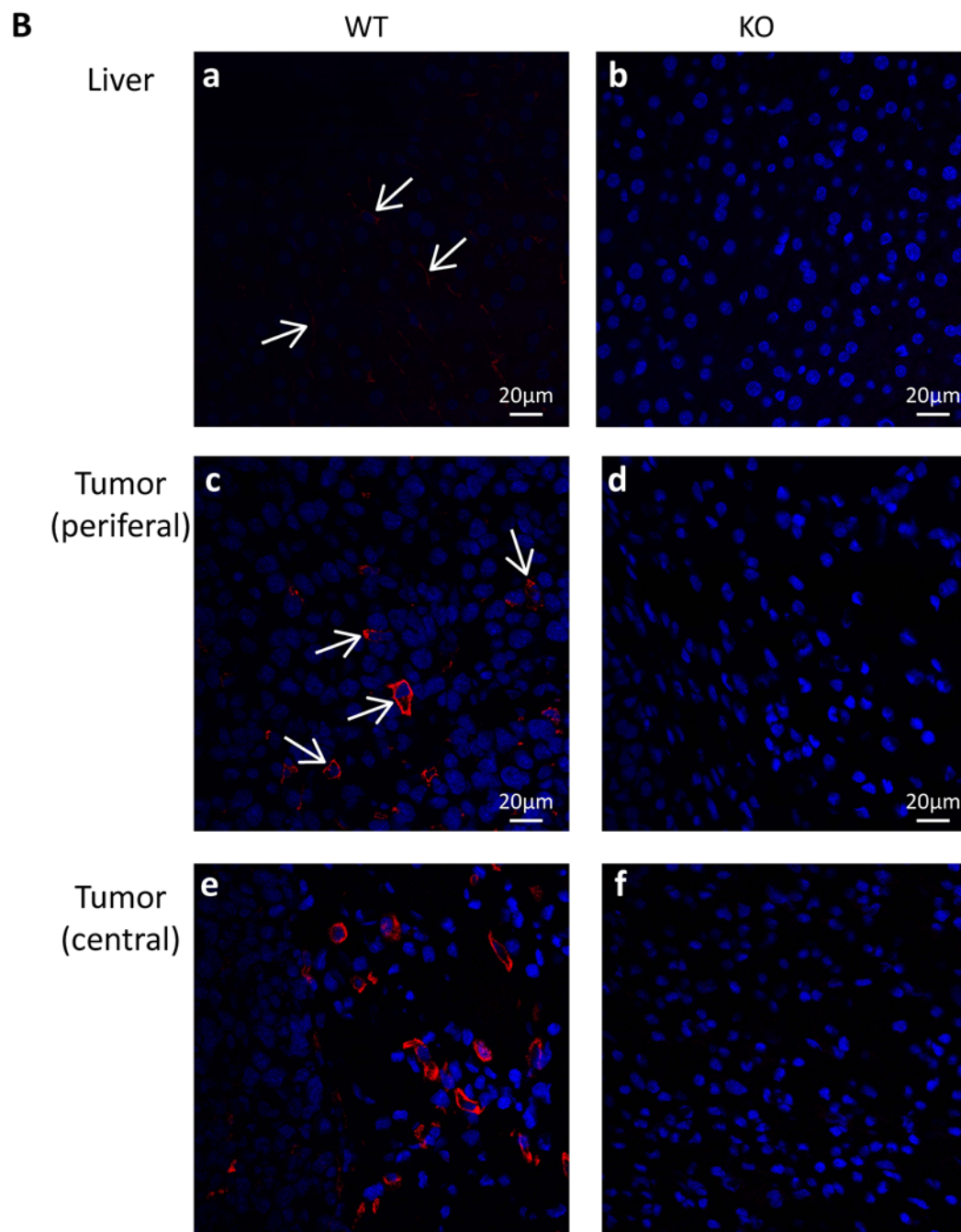
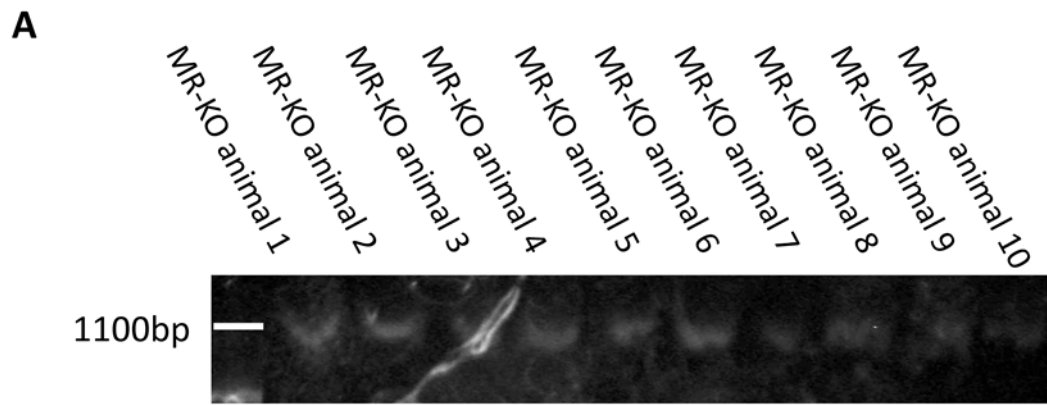


Figure 3.2: Results from A) PCR analysis of gene status of mannose receptor knockout (MR-KO) mice and B) fluorescence staining with a mannose receptor (MR) antibody. A) Results from agarose gel electrophoresis of PCR products of DNA extracted from MR-KO mice. All mice have bands corresponding to 1100 bp, which confirms the gene status of the MR-KO animals. B) Fluorescence staining with MR antibody in wild-type (WT) compared to MR-KO mice. B-a) In liver of WT mice, MR positive staining (red) is seen in liver sinusoidal endothelial cells. B-c and B-e) shows MR positive cells in peripheral and central areas of tumor of the same WT animal. In MR-KO mice, MR staining of livers and tumor tissue was negative (B-b, B-d, B-f).

3.6 Analyses of tumor tissue

Histological analyses of haematoxylin and eosin (H&E) stained tissue sections of tumors were conducted to examine the tumor morphology in wild-type and MR-KO animals, respectively. Measurements of area of necrosis relative to tumor area, and area covered by blood vessels relative to total tumor area were conducted on the same tissue slides.

Immunohistochemistry was used to analyze macrophage infiltration in the tumors, and to reveal the pattern of activation status seen in these cells. Gene expression analyses of macrophage markers were conducted by using q-RT-PCR.

3.6.1 Histological analyses of tumor tissue

Thin sections (approximately 4 μm) of paraffin embedded tissue blocks from experiment 1 were stained with hematoxylin and eosin. The sections were made from the middle part of the tumor, approximately at the widest tumor diameter. One HE stained section from each tumor were photographed for evaluation of tumor histology. From each tumor, 5 pictures were taken by a systematic random sampling approach, according to **Figure 3.3**.

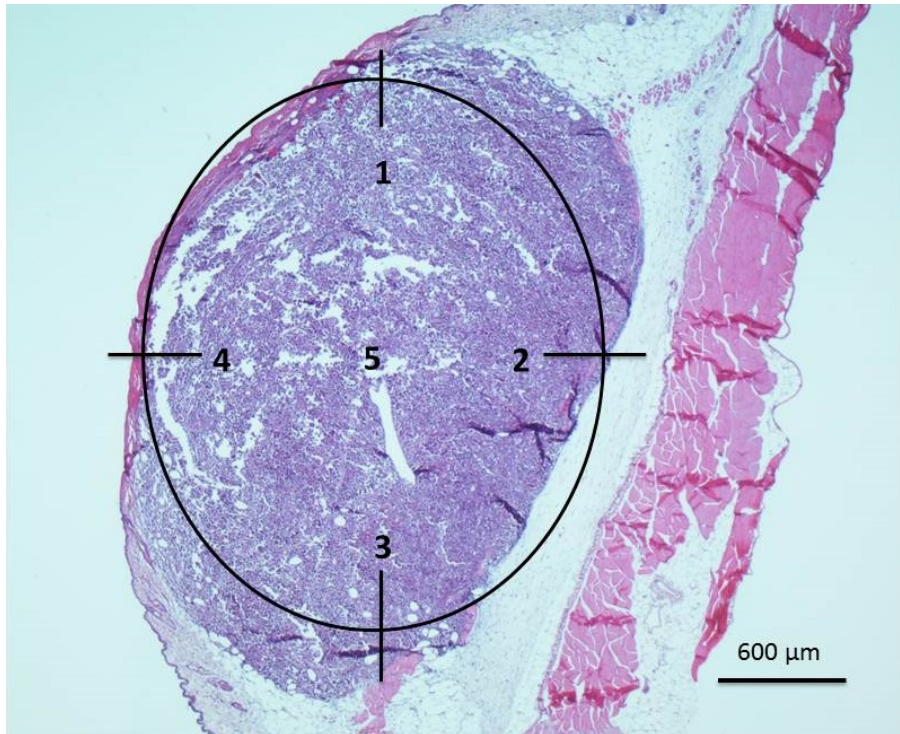


Figure 3.3: Systemic random sampling approach for image collecting. The figure shows a B16F1 tumor with a sketch of the pattern used for image taking of tumor tissue for measurements of necrotic area and tumor area covered by blood vessels. The first image was taken at a random site along the periphery of the tumor tissue proper, and then the other images were taken in a specific pattern in relation to the site of the first image.

For measurements of area of necrosis in % of total tumor area, and area covered by blood vessels in % of total tumor area, a stereology approach was used. ImageJ software [133] (image processing program developed by National Institutes of Health, (USA) was used to superimpose a grid (square lattice) with 80 cross-points to each picture. Then cross-points covering, the total tumor tissue, the necrotic tissue in tumor, and blood vessels in tumor tissue, respectively, were counted. Ratios were then calculated: 1) points per necrotic area / points per total tumor area, and 2) points per blood vessel area / points per total tumor area. According to stereology theory [134], the number of points overlaying the area of the specific structure (i.e. necrosis, blood vessels) divided on the points overlaying the reference area (i.e. melanoma tissue), reflects the relative area covered by the specific structure of interest.

Then the average result for the 5 images from each tumor slide was calculated to find the mean value for this tumor slide (one slide analysed per tumor). The mean results for each animal group and tumor size were calculated as the average of the average value per tumor slide (each representing one animal).

3.6.2 Immunohistochemistry

Theory: Immunohistochemistry (IHC) is a technique used to identify the localization of antigens in a tissue or cell by using antibodies specific to the antigen. The antigen-antibody reaction is visualized by markers like fluorescent dyes or enzymes [135].

Immune labeling can be done in different ways, and both direct and indirect methods are developed. In the direct method the primary antibody is labeled with either a fluorochrome or an enzyme and binding can be visualized directly. In indirect methods several steps are needed to give visualization. In a two-step procedure a secondary labeled antibody is added and binds to the non-labeled primary antibody. If the secondary antibody is linked to an enzyme a substrate is added in addition in order to develop the signal. The advantage of using an indirect method is that the secondary antibody will bind to multiple epitopes on the primary antibody and therefore give signal amplification [135].

In the present study we used both enzyme-based and fluorescence-based indirect staining methods. These involved the HistoMouseTM-Plus Kit (Invitrogen), where the enzyme is horseradish peroxidase (HRP) and the substrate is 3-amino-9-ethylcarbazole (AEC). However as we had problems with one supply of the HistoMouse Plus Kit, which gave unspecific staining of all macrophage like cells, the protocol was changed to a HRP-diaminobenzidine (DAB) method (Appendix D) for one of the antigens (F4/80). For fluorescence labeling we used Alexa Fluor[®] conjugated secondary antibodies from Abcam (**Appendix A**).

When doing immunohistochemistry, negative and positive controls needs to be included in order to validate the staining results. As negative control for polyclonal antibodies, we used non-immune IgG, or non-immune serum to replace the primary antibody. The negative control IgG/serum must have the same animal origin as the primary antibody. For monoclonal antibodies, isotype matched non-immune IgGs were used. Control of unspecific staining of the secondary antibody was checked by excluding the primary antibody. As positive control we used tissue sections known to express the antigen of interest. Mouse liver sections, with abundant Kupffer cells, were used as positive control in most labeling.

Overview of the immune labeling procedure:

- De-paraffinization and rehydration of tissue sections (section 3.6.4)
- Antigen retrieval (section 3.6.4)
- Blocking of endogenous peroxidase and unspecific labeling (section 3.6.5)
- Incubation with primary antibody (section 3.6.6)
- Incubation with secondary antibody and visualization steps (section 3.6.7)
- Counterstaining and mounting of sections (section 3.6.8)

3.6.3 Preparation of tissue for immunohistochemistry

The fixed tumor samples were prepared and casted in paraffin at the Department of pathology at the University Hospital North Norway (UNN). Because paraffin is immiscible with water and to minimize damage to the tissue, the tissue samples were dehydrated through several baths of progressively concentrated ethanol and xylene in the end. The dehydrated samples were placed in melted paraffin, in a mold. Solidified paraffin blocks can be stored in room temperature for years.

3.6.4 De-paraffinization and rehydration of tissue sections, and antigen retrieval

Sections, approximately 4 μm thick, were made by a microtome (Microme HM440E, Medax International, Salt Lake City, Utah), then deparaffinized in xylene, and rehydrated through a graded ethanol series. Then an antigen “retrieval” process was employed to break the cross-linking caused by formalin fixation. The purpose of this step is to make the antigens and epitopes accessible for the antibodies. We used a heat-induced epitope retrieval method where the samples are boiled in citrate buffer in a microwave oven for 10-30 min.

General procedure:

- De-paraffinization and rehydration:
 - 3 x 15 min: Xylene
 - 2 x 10 min: 100 % ethanol
 - 1 x 5 min: 96 % ethanol
 - 1 x 5 min: 79% ethanol
 - 2 x 5 min: Milli-Q water

- Antigen “retrieval”, by 10-30 min microwaving in citrate buffer (pH 6):
 - Sections were placed in pre- warmed buffer (95°C), and microwaved 6 x 5 min, or 2x 5 min depending on antigen, at 750 Watt.
 - Sections were left to cool for 20 min at room temperature, and then washed in Milli-Q water for 3 x 2 min.
 - A circle was made around the tissue section by using a PAP pen (DAKO, Glostrup, Denmark)

3.6.5 Blocking of unspecific staining

Background staining is a frequent problem in IHC. This staining can be unspecific or specific. All antibodies have the ability to bind unspecifically if the concentration is sufficiently high, and proper titration to find the concentration that gives the best signal to noise ratio is essential. Polyclonal antibodies tend to cause background staining more often than monoclonal because they target more epitopes. Because unspecific binding often is weaker than the antibody-antigen binding it can be blocked. The most common cause of unspecific binding is due to hydrophobic and electrostatic forces. These problems can be solved by increasing the pH in the washing buffer and by adding a detergent, as Tween20. Unspecific binding can also occur if the primary antibody reacts with similar epitopes found on several antigens. Necrotic areas are known to bind antibodies avidly and give specific background staining [135].

Blocking of endogen peroxidase activity

Both AEC and DAB are frequently used as a precipitable peroxidase substrate for IHC. Because many cells and tissues contain endogenous peroxidase, e.g. liver cells, macrophages, and neutrophil granulocytes, and therefore may react with AEC or DAB, it is necessary to block this reaction to avoid high background staining and false-positive staining. The reaction can be efficiently blocked by using hydrogen peroxidase (H_2O_2) that inactivates any peroxidase present in the tissue [135].

General procedure:

- Peroxidase quenching solution: 1 part of 30 % H_2O_2 was added to 9 parts of cold absolute methanol, and mixed well
- Approximately 100 μ l of this solution was added per slide to cover the tissue, and slided incubated at room temperature for 10-15 min.

Blocking of unspecific binding of antibody

The antigen “retrieval” step will unmask many different epitopes in the sample and these needs to be blocked to avoid unspecific labeling with antibodies. We used a blocking buffer with 1 % bovine serum albumin (BSA), which binds to different epitopes and free aldehyde groups that may react with the antibodies. The blocking buffer will not affect the high affinity binding between the specific antibody and antigen [135].

The buffer used for making the blocking buffer was also used as a buffer for the washing steps. Depending on the method, both TBS and/or PBS were used in our protocols. Tris-buffered saline (TBS), pH 8.4, were used in most protocols as this gave a cleaner staining

than PBS, pH 7.2. The advantage of the higher pH is that it reduces unspecific binding of antibodies [135]. TBS has a good buffer capacity in the pH range of 7-9.2, whereas PBS is working at pH 7 to 7.6. In some steps, TBS with 0.05% tween20 (TBS-T) were used. Tween20 is a detergent that contributes to a cleaner wash.

General procedure:

Fluorescence method:

- Blocking buffer: 1 % BSA (**Appendix B**) in TBS (pH 8.4).
- 100 µl or enough to cover the tissue, was added to each section.
- Sections were incubated 30 min at room temperature.

HRP/AEC method:

Reagent 1A (Histokit™): BEAT™ blocking solution (ready to use)

- 2 drops or enough to cover the tissue were added to each section.
- Sections were incubated 30 min at room temperature, then washed 3 x 2 min in Milli-Q water.

Reagent 1B (Histokit™): BEAT™ blocking solution (ready to use)

- 2 drops or enough to cover the tissue were added to each section.
- Sections were incubated 10 min at room temperature, then washed 3 x 2 min in Milli-Q water, and 3 x 2 min in TBS-T.

HRP/DAB method:

- Blocking buffer: 1 % BSA in PBS.
- Sections were incubated 30 min at 4°C at room temperature.

3.6.6 Primary antibody

Antibodies can be monoclonal or polyclonal. In a normal immunological response several B-cells are activated and these will produce antibodies against several epitopes on the antigen. This serum is called polyclonal as the serum is heterogeneous and contains antibodies with different specificity and epitope affinity. The advantage of polyclonal antibodies is that they can enhance a weak signal and they are more robust to small changes in the epitope. Monoclonal antibodies are produced by the fusion of isolated B-cells and myeloma cells. These hybridoma cells produce identical antibodies that have identical epitope specificities. The advantage of monoclonal antibodies is that they are absolutely specific, but they are

sensitive for any epitope changes that may occur by fixation. Primary antibodies used in this study, see **Table 3.3**.

General procedure:

Fluorescence method:

- The primary antibody was diluted in blocking buffer (1% BSA in TBS-T).
- 100 µl or enough to cover the tissue was added to each section.
- The sections were incubated in a moist chamber at 37°C for 60 min or overnight.
- The sections were then washed in TBST for 3 x 2 min.

HRP/AEC method:

- The primary antibody was diluted in blocking buffer (1% BSA in TBS-T)
- 100 µl or enough to cover the tissue was added to each section.
The sections were incubated in a moist chamber at 37°C for 60 min or overnight
- The sections were then washed in TBST for 3 x 2 min, and then in PBS for 3 x 2 min

HRP/DAB method:

- The primary antibody was diluted in blocking buffer (1% BSA in PBS)
- 100 µl or enough to cover the tissue was added to each section.
- The sections were incubated in a moist chamber at 4 °C overnight.
- The sections were then washed 3 x 5 min in PBS.

Table 3.3: Primary antibodies used for testing on B16F1 melanoma tumor sections. The Information is collected from the antibody datasheets. The dilution giving the best signal to noise ratio after titration of the antibodies is shown.

Antibody	Producer	Dilution used		Staining method
Goat anti-human mannose receptor (CD206) Polyclonal antibody	R&D Systems, (AF2534)	1:200	Expressed on tissue macrophages and is a marker for M2 macrophages. Also expressed on liver and lymphatic endothelial cells.	Fluorescence
Rabbit anti- human Arginase I Polyclonal antibody	Santa Cruz (H-52) sc-20150	1:100	Expressed in liver and in macrophages with an M2 polarization. Enzyme that catalyzes conversion of arginine to ornithine and urea.	HRP/AEC
Rabbit anti-human Stabilin 1 Polyclonal antibody	Millipore (AB6021)	1:2000	Transmembrane receptor expressed in endothelial cells in liver sinusoids, spleen, and lymphoid tissue; reported to be expressed on M2 macrophages.	HRP/AEC
Rabbit anti-mouse iNOS Polyclonal antibody	Abcam (ab15323)	1:100	Expressed in liver, retina, and M1 macrophages where it has tumoricidal and bactericidal actions.	HRP/AEC
Rat anti- mouse CD68 Monoclonal antibody	Abcam (ab53444) [FA-11]	1:100/1:150	Transmembrane protein specifically expressed by macrophages, Langerhans cells and at low levels by dendritic cells. Possible functions in clearance, phagocytosis, mediating recruitment and activation of macrophages.	Fluorescence, HRP/AEC
Mouse anti-rat CD163 Monoclonal antibody	AbD Serotec (MCA342EL) [ED2]	1:50/1:100	Expressed exclusively by monocytes and macrophages. Acute phase-regulated receptor, involved in the clearance of hemoglobin, and protection from free hemoglobin-mediated oxidative	Fluorescence, HRP/AEC

			damage.	
Rat anti-mouse F4/80	AbD Serotec (MCA49RT) [CI:A3-1]	1:50/1:100	Cell surface glycoprotein. Expressed on tissue macrophages, Kupffer cells and Langerhans cells. Biological function has not yet been determined.	Fluorescence, HRP/DAB
Mouse anti-rat CD11b/c	Cedarlane (CL042B-5)	1:150	Cell surface protein, implicated in various adhesive interactions of monocytes and macrophages. Mediating uptake of complement coated particles.	HRP/AEC
Rabbit anti-human CD3	DAKO	1:150	Cell surface, a T-cell co-receptor to generate an active signal in T lymphocytes.	Fluorescence, HRP/AEC
Rabbit anti-human Ki67	Abcam	1:150	Ki-67 is a nuclear protein expressed only in proliferating cells, preferentially expressed in late G1, S, M and G2 phase. Not expressed in G0 phase.	HRP/AEC

Abbreviations: HRP, horse reddish peroxidase; DAB, diaminobenzidine ; AEC, 3-amino-9-ethylcarbazole.

3.6.7 Secondary antibody labeling and visualization

Fluorescence labeling

Fluorescence staining produces an instantly visible signal that is seen against a black non-fluorescent background. The secondary antibody is conjugated with a fluorescent tag that will be excited by a light of particular wavelength, and in response emits light that is visible in a fluorescence microscope, such as the confocal laser scanning microscope (used in this study). The confocal microscope uses a laser to excite fluorescence molecules and a detector that captures the emitted light. In front of this detector there is a pin – hole which function is to eliminate all of the out-of-focus light. The advantage of using a confocal microscope is that it will focus the laser light on one specific point and depth of the sample, thus creating a sharper image than a conventional fluorescence microscope. Fluorochromes are available with different emission spectra and therefore allows for the detection of two or more

antigens in the same sample. We used Alexa Fluor® conjugated secondary antibodies from Abcam (**Appendix A**).

General procedure:

- All incubations steps were carried out under aluminium foil to protect the samples from light and avoid bleaching
- The secondary antibody was diluted in 1 % BSA in TBS-T buffer, and added to cover the tissue sections labeled previously with primary antibody or non-immune IgG.
- Sections were then incubated for 60 min in room temperature, followed by a 3 x 5 min wash in TBS-T, and 2 x 5 min wash in PBS.

Enzyme labeling

Antibodies conjugated with enzymes needs to react with a substrate and a chromogen to yield a colored precipitate. The most popular enzyme used for immunohistochemistry is peroxidase. The HistoMouse™- Plus kit from Invitrogen is a broad spectrum kit that will react with primary antibodies from mouse, rabbit, guinea pig and rat primary antibodies [136]. The secondary antibody in this kit is biotinylated, which means that the secondary antibody is conjugated with a linker molecule biotin. After incubation with the secondary antibody the samples are treated with a secondary conjugate of streptavidin and HRP. Streptavidin is a protein that has a strong affinity to bind to biotin and therefore also enables signal amplification. The last step is to add the substrate AEC that reacts with HRP. The dark red end-product is visible in a light microscope.

In the DAB method, which was employed in the F4/80 labeling procedure in the present study, DAB works as a chromogen and H₂O₂ is used as a substrate. The secondary antibody used in this method is conjugated with HRP. When DAB is then added it will be oxidized in the presence of HRP resulting in a brown precipitate that is insoluble in alcohol.

General procedure:

HRP/AEC method:

Reagent 1C (Histokit™): Biotinylated secondary antibody (ready to use)

- 2 drops or enough to cover the tissue were added to each section.
- The sections were incubated 30 min at room temperature, and then washed in PBS for 3 x 2 min.

Reagent 2 (Histokit™): Streptavidin-peroxidase conjugate (ready to use)

- 2 drops or enough to cover the tissue were added to each section.
- The sections were incubated 20 min at room temperature, and then washed in PBS for 3 x 2 min.

Reagent 3 (Histokit™): AEC single solution chromogen (ready to use)

- 2 drops or enough to cover tissue, of cold AEC solution was added to each section. The AEC has to be stored cold and were immediately returned to the fridge. The sections were incubate 15 min at room temperature, and then washed in Milli-Q water.

HRP/DAB method

Secondary antibody:

- Secondary antibody was diluted in 1% BSA in PBS, and added to each section
- The sections were incubated at room temperature for 45 min, and then washed in PBS for 4 x 5 min

Substrate solution DAB:

- The substrate solution DAB was added to each section, and incubated until formation of brown color could be seen (empiric: 5 seconds to 2 min)

3.6.8 Counterstaining and mounting

Counterstaining provides contrast and makes it easier to localize tissue structures.

Counterstaining for fluorescence was done with Draq5, and 4', 6-diamidino-2-phenylindole (DAPI). Draq5 is a fluorochrome that binds to nucleic acids and makes the cell nucleus visible in the confocal microscope. DAPI stains double stranded DNA and has a blue fluorescence color under UV excitation.

The red end-product from the AEC staining is soluble in organic solutions and needs to be counterstained and mounted in an aqueous-based medium. Hematoxylin is a common nuclear stain used for immunohistochemistry, histology and histopathology. Hematoxylin stains the nucleus and some other structures like keratohyalin granules and calcified material. The initial color from hematoxylin is red but it turns blue when exposed to pH 5.4 to 9.8.

General procedure:

Fluorescence:

- All work was done under aluminium foil to protect the sample from light.

- Approximately 100 µl of DAPI in PBS (dilution 1:50 000) was added to each section, and sections incubated 5 min at room temperature, and then washed 2 x 2 min in PBS.
- The sections were then incubated with Draq5 in PBS (dilution 1:1000), 5 min at room temperature, and washed 2 min in PBS, then 2 x 2 min in Milli-Q-water.
- The sections were mounted in Dako fluoromount, and coverslips sealed with nail polish.

The sections were examined in a confocal laser-scanning microscope, Zeiss LSM 510 microscope (Zeiss, Germany), by using a 40x water objective.

HRP/AEC staining:

Reagent 4 (Histokit™): Hematoxylin counterstaining (ready to use)

- 2 drops or enough to cover the tissue was added to each section.
- The sections were incubated 4 min at room temperature.
- Sections were then placed in tap water, and then in in PBS until blue colour appeared, approximately after 30 sec.
- The sections were then rinsed with Milli-Q- water, and mounted with Dako Faramount aqueous mounting medium (ready to use), and coverslips sealed with nail polish.

Sections were examined in a Zeiss Axiophot light microscope (Zeiss, Germany). Objectives used: 2.5x, 10x, 20x, 40x, 63x in addition to 10x in the eyepiece, giving final magnifications: 25x, 100x, 200x, 400x, and 630x.

HRP/DAB method:

Reagent 4 (Histokit™): Hematoxylin counterstaining (ready to use)

- 2 drops or enough to cover the tissue was added to each section.
- The sections were incubated 4 min at room temperature.
- Sections were then placed in tap water, and then in in PBS until blue colour appeared, approximately after 30 sec.
- The sections were then rinsed with Milli-Q- water
- Before mounting the sections were t dehydrated in a graded ethanol series as follows:
 - o 75 % EtOH 5 min
 - o 90 % EtOH 5 min
 - o 100 % EtOH 5 min
 - o Xylene 2 min
- The sections were then mounted in a xylene based mounting medium (Histokit).

Sections were examined in a Zeiss Axiophot light microscope. Objectives used: 2.5x, 10x, 20x, 40x, 63x in addition to 10x in the eyepiece, giving final magnifications: 25x, 100x, 200x, 400x, and 630x.

3.6.9 Evaluation of IHC staining results

The amount of positively stained non-tumor cells in the tumor tissue proper and adjacent connective tissue was evaluated by a scoring system, graded from 0-3 as illustrated in **Table 3.4**. The staining intensity of positive cells was evaluated by using a scoring system graded from 1-3 (**Table 3.4**). The scoring scheme is in **Appendix C.2**. The evaluation was done blinded by three researchers (Iselin Rønningen, Jaione Simón-Santamaría, and Karen Sørensen), first independently, then together. There were only small differences in the evaluation done by the different researchers, and a consensus was made on these sections.

Table 3.4: Scoring system for evaluating positively stained cells and staining intensity.

Amount of positive cells (non-tumor cells)	
Score	
0	No positive cells
1	Few positive cells
2	Moderate number of positive cells
3	High number of positive cells
Assessment of staining intensity in positive cells	
1	Weak staining intensity
2	Moderate staining intensity
3	Strong staining intensity

3.7 Gene expression analysis

One cycle of PCR can be basically be divided in three phases, exponential phase, linear phase and plateau phase which is the end-point of the reaction. In traditional PCR detection and quantification is done after the reaction has reached its end-point. The exponential phase is the most optimal phase for analyzing data and to do quantifications, due to fact that DNA is

doubled with each cycle and quantification is therefore very accurate. Real time quantitative RT-PCR (qPCR) is therefore a powerful technique used in quantitative gene expression analysis. We did a two-step qPCR, which means that the cDNA reaction and the qPCR are done in two different steps.

For accurate measurements of gene expression, the results from qPCR need to be normalized to reference genes, which are genes who are not affected by the experimental conditions.

3.7.1 RNA isolation and stabilization

During tissue harvesting, changes in gene expression pattern will rapidly occur due to the actions of specific and nonspecific RNA degradation. In order to obtain reliable results from gene expression analyses, RNA needs to be effectively stabilized immediately after harvesting. For this purpose we used the Allprotect tissue reagent kit from Qiagen (**Appendix A**). The kit provides immediate preservation of DNA, RNA and proteins in tissue samples. Tissue samples (maximum thickness 5 mm) were submerged in > 10 x volume of Allprotect tissue reagent according to the protocol by the manufacturer. The samples were stored overnight at 2-8 °C, and then at minus 20°C until further processing.

3.7.2 Isolation of total RNA from tumor biopsies

In order to isolate RNA from tumor biopsies the tissue needs to be homogenized. For this purpose we used the Precellys 24 (Bertin Technologies). The tumor biopsies were placed in MagNA Lyser Green beads – tubes. These tubes are 2 ml screw tubes filled with 1.4 mm ceramic beads. The principle behind homogenization is the fast-moving, oscillating reciprocal motion of the MagNA Lyser Instrument which will disrupt the tissue without the use of lysing enzymes or grinding. The collision between the ceramic beads and the tissue sample makes cells disrupt and results in a homogenized sample [137].

RNeasy Mini kit from Qiagen was first tested for the isolation of total RNA. This kit is designed to purify RNA from small amounts of starting material. The kit use RNeasy Mini spin column with a silica-based membrane that binds RNA. Contaminants are then washed away by the use of a specialized high-salt buffer system.

The amount of RNA isolated by the RNeasy Mini kit from Qiagen was low, and we suspected that the tissue was not homogenized properly. We then tested RNeasy Fibrous Tissue Mini kit (Qiagen), which gave a much higher yield of isolated RNA than the first kit. The same principle for RNA isolation is the same as for the RNeasy Mini kit, in addition includes a step with proteinase K for removing abundant protein in fiber-rich tissue.

A NanoDrop spectrophotometer was used to measure RNA concentrations, which has an absorbance at 260 nm (A260), and protein concentration, which has an absorbance at 280 nm (A280). These values are also used to calculate the sample purity which is given by the ratio of the A260/A280 values. The value for good quality RNA will ideally be 2.0.

General procedure:

Disruption and homogenization of tumor biopsies:

- The tissue sample was weighed in order to calculate the proper amount of RLT buffer.
- 6 μ l of 3 M dithiothreitol (DTT) was added per 350 μ l of buffer RLT.
- MagNA Lyser Green beads – tubes were marked and added the proper amount of RLT buffer according to the protocol provided by the manufacturer.
- Tissue sample was removed from the Allprotect Tissue reagent using sterile forceps, and placed in their respective MagNA Lyser Green beads – tubes.
- The homogenization was done by using Precellys tissue homogenizer (Bertin technologies): for 40 seconds at 5000 Hz
- Samples were then centrifuged at max speed for 3 min, and the supernatant collected. The next step was isolation of total RNA.

Isolation of total RNA from tissue homogenate:

RNeasy fibrous tissue mini kit:

1. 590 μ l of RNase-free water was added to each sample, together with 10 μ l of proteinase K. Samples were mixed, and incubated at 55 °C for 10 min.
2. Supernatant was transferred to a new tube and added 0.5 volumes of 96% ethanol and then mixed.
3. 700 μ l of sample was added to a RNeasy Mini column which was placed in a 2 ml collection tube, lid closed, and column centrifuged for 15 sec at 8.000 rpm. Flow through was discarded.
4. This step was repeated until complete lysate was used.
5. 350 μ l of buffer RW1 was added to the column, lid closed, and column centrifuged for 15 seconds at 8.000 rpm. Flow-through was discarded.
6. 10 μ l of DNase stock solution with 70 μ l of buffer RDD was added to the column, and column incubated at 20-30 °C (room temperature) for 15 min.
7. 350 μ l of buffer RW1 was added to the column, lid closed, and column centrifuged for 15 seconds at 8.000 rpm. Flow-through was discarded.

8. 500 μ l of buffer RPE was added to the column, lid closed, and column centrifuged for 15 seconds at 8.000 rpm. Flow-through was discarded.
9. Step 8 was repeated, and column was centrifuged for 2 min at 8.000 rpm.
10. Column was placed in a 2 ml collection tube, and centrifuged at full speed for 1 min.
11. Column was placed in a 1.5 ml tube, and 40 μ l of RNase-free water was added, lid closed and column centrifuged for 1 min at 8.000 rpm.
12. Samples were kept on ice, and RNA concentration was measured by the NanoDrop method.
13. RNA was then stored at -70°C until further analyses.

3.7.3 RNA integrity test

In addition to testing of RNA concentration and purity, we also conducted a high resolution integrity test of RNA from each sample using The Experion automated electrophoresis station (BIO-RAD), which performs all the steps of gel-based electrophoresis: electrophoresis, staining, destaining, band detection and imaging in one 30 min step, in one unit. Gel solution was loaded onto an Experion Analysis Chip, before standards and samples were added to wells located on the chip. The chip was placed in The Experion automated electrophoresis station, which applies voltage and thereby separation of the RNA. A fluorescent dye, which is bound to the RNA in the sample, is excited by a laser and the sample is detected and quantified simultaneously. The detection signal provides a peak in the Experion Software, and can in addition display the data in a traditional gel view. The sample information is collected in a results-table which provides a fast and direct view of sample characteristics like molecular weight, RNA concentration and ribosomal RNA ratio which indicates RNA quality. RNA quality is scored by RNA quality indicator (RQI) function, which gives a numerical value from 1 (lowest) to 10 (highest) for total RNA quality.

The RNA integrity test was performed by Hagar Taman from the Microarray Resource Centre Tromsø, Institute of Clinical Medicine, UiT.

3.7.4 First strand cDNA synthesis

Of the total amount of RNA in a cell, there is only a small percentage of mRNA. After the RNA isolation by the RNeasy fibrous tissue mini kit, the mRNA needs to be reversely transcribed in order to become stable double stranded DNA. cDNA is a more convenient way to work with the coding sequence in the mRNA, as RNA are easily degraded by RNAases present in the surroundings. For this purpose we used a kit, QuantiTect Reverse Transcription kit from Qiagen. The kit contains gDNA wipeout buffer which effectively eliminates any genomic DNA contamination present in the RNA samples.

General procedure:**Genomic DNA elimination reaction**

- RNA samples stored at -70 °C were thawed on ice.
- gDNA wipeout buffer, quantiscript reverse transcriptase (RT), quantiscript RT buffer, RT primer mix and RNase-free water was thawed in room temperature.
- Each solution was mixed by flicking the tubes, and briefly centrifuged and stored on ice.
- Master Mix 1 was prepared according to **Table 3.5** and stored on ice.
- Individual 0.2 ml PCR tubes were marked and 5 µl of Master Mix 1 was added.
- The amount of template RNA to add to the reaction was 1 µg, which was calculated from the RNA concentration.
- RNase-free water was then added to a total of 14 µl.
- Samples were incubated for 2 min at 42°C, and then immediately placed on ice.

Table 3.5: Master Mix 1 for genomic DNA elimination reaction

Master Mix 1	
Component	Volume added (per sample)
gDNA Wipeout Buffer	2 µl
RNase-free water	3 µl
Total volume	5 µl

Reverse-transcription reaction

- Master Mix 2 was prepared according to **Table 3.6**
- After Genomic DNA elimination reaction, Master Mix 2 is added to the samples
- Incubate at 42°C for 15 min
- Incubate at 95°C for 3 min, to inactivate Quantiscript Reverse Transcriptase

Table 3.6: Master Mix 2, for reverse-transcription reaction

Master Mix 2	
Component	Volume added (per sample)
Quantiscript Reverse Transcriptase	1 µl

Quantiscript Reverse Transcriptase buffer	4 μ l
Reverse Transcriptase Primer Mix	1 μ l
Total volume	5 μl

3.7.5 Real time PCR

Materials needed for qPCR is FastStart SYBR Green Master (Roche), Sybr green Primers (Primerdesign Ltd). FastStart SYBR Green Master is a master mix that contains all the reagents that is needed for qPCR; FastStart Taq DNA polymerase, reaction buffer, nucleotides and SYBR green I. The FastStart Taq DNA polymerase is a chemically modified form of the well-known Taq DNA polymerase. The FastStart Taq DNA polymerase is active only at high temperature (over 75°C), where primers no longer can bind non-specifically. The enzyme is activated in a pre-incubation step (95°C, 10 min) before cycling begins. The FastStart SYBR Green Master also contains ROX reference dye. ROX is used to normalize the non-PCR related fluctuations in the fluorescence signal. The fluorescent dye, SYBR Green I binds double stranded DNA with great affinity, and absorbs blue light and emits green light which is detectable. The use of multiple reference genes is generally accepted for RT-qPCR, and four reference genes were selected.

Genes that have been tested:

- Beta actin (ACTB) – reference gene
- Glyceraldehyde-3-phosphate dehydrogenase (GAPDH) – Reference gene
- Beta-2 microglobulin (B2M) – reference gene
- Phospholipase A2 (YWHAZ) – reference gene
- CD68 – Pan macrophage marker
- iNOS – M1 macrophage marker
- Arginase I – M2 macrophage marker

General procedure:

- One master mix was prepared for each gene (**Table 3.7**)
- The plate setting was designed.
- 17 μ l from master mix was added to each well, following the design
- 3 μ l of each cDNA (or water) in the correspondent well
- The plate was sealed and centrifuged
- Running of qPCR was done by Roche Lightcycler 9, conditions in **Table 3.8**

Table 3.7: *Preparations of Master Mix for RT-PCR*

Component	Amount per sample
FastStart SYBR Green Master	10 μ l
Primer	1 μ l
RNase free water	6 μ l
Total	17 μl

Table 3.8: *The RT-PCR conditions used (set-up recommended by the producer)*

	Temperature ($^{\circ}$ C)	Duration (seconds)
Pre-incubation		
1 cycle	95	600
3-step amplification		
45 cycles	95	10
	60 (primer dependent)	10
	72	10
Melting		
1 cycle	95	10
	65	60
	97	1

3.8 Statistical analyses and software

Statistical analyses were done by Microsoft Excel 2013 (Microsoft, Redmond, WA), and IMB SPSS Statistics 21 (SPSS Inc., Chicago, IL)

Differences between means were tested for significance by Student's t-test (normally distributed data) and Mann Whitney U test (non-normally distributed data). Two sided p-values below 0.05 were considered statistically significant.

Image panels were made by using Adobe Illustrator CS6 (Adobe Systems Inc., San Jose, CA), and graphs were made by using Microsoft Excel 2013, and GraphPad Prism 4 (GraphPad Software Inc., San Jose, CA).

Image J, a public domain image processing program developed by National Institutes of Health, USA [133], was used for morphometric analyses of necrosis and blood vessels in tumor tissue sections [133].

Chapter 4

Results

4.1 In vivo tumor experiment

The experimental tumor studies were conducted as described in the Material and Methods, according to approved protocols by NARA. In both experimental series, the animals showed no immediate signs of discomfort after inoculation of tumor cells in the abdominal wall. The animals were examined daily during the experimental period, and seemed to be unaffected by the growing tumor and had a good general condition.

4.1.1 Time from inoculation of tumor cells to visible tumor growth

All mice in both experimental series developed tumors. After injection the tumor first appeared as small black spots, approximately 0.5-1 mm in diameter, in the skin. The time from inoculation to first visible tumor (“tumor take”) is shown in **Figures 4.1 and 4.2**.

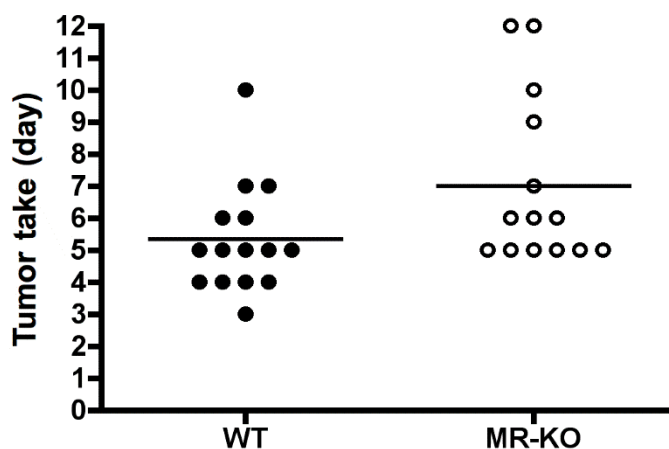


Figure 4.1: The first day of visible tumor (“tumor take”) in wild-type (WT) and mannose receptor knockout (MR-KO) animals in experiment 1. Mean value for tumor take is presented by horizontal lines. The difference between the WT and MR-KO group was borderline significant by the Mann Whitney U test ($p=0.051$).

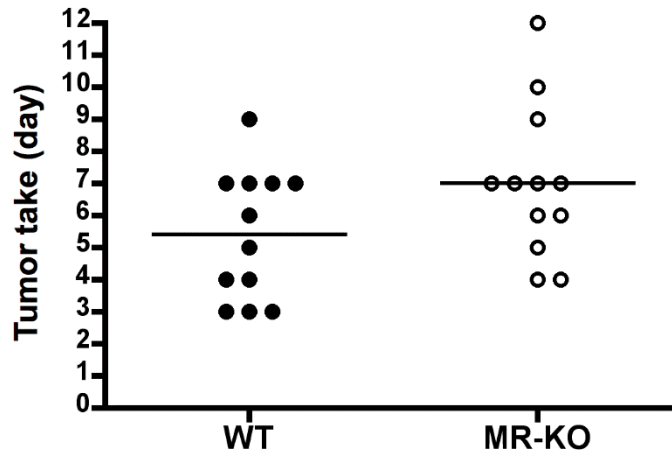


Figure 4.2: **The first day of visible tumor (“tumor take”)** in wild-type (WT) and mannose receptor knockout (MR-KO) animals in experiment 2. Mean value is presented by horizontal lines. The difference between the WT and MR-KO groups was not statistically significant (p -value=0.14).

In wild-type mice, the mean time to tumor take was 5.3 days in experiment 1 and 5.4 days in experiment 2, while the mean time to tumor take in MR-KOs were 7 days in both experiments. Median values were 5 days for wild-type (WT), and 6 days for MR-KO mice in experiment 1, and 5.5 days and 7 days for WT and MR-KO, respectively, in experiment 2. This difference was borderline significant in experiment 1 (Mann Whitney U test, p -value = 0.51), but not statistically significant in experiment 2 (p -value = 0.14).

4.1.2 Rate of tumor growth in vivo

The tumor diameter was measured daily by a digital caliper. Data for wild-type and MR-KO animals in experimental 2 are presented in **Figure 4.3**. The data were normalized to the day of first visible tumor, and growth curves constructed. Similar results were obtained from experiment 1. Although day of tumor take differed between wild-type and MR-KO mice, tumors from then on grew at similar rate in both groups.

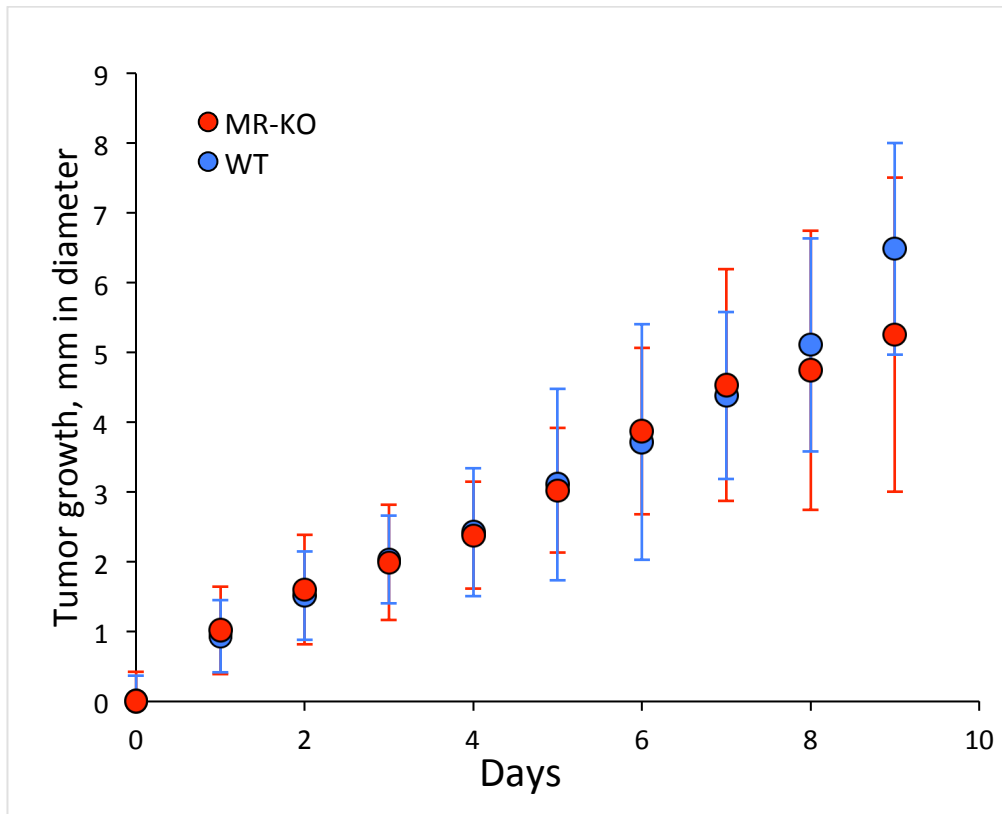


Figure 4.3: Growth curve for wild-type (WT) (blue) and mannose receptor knockout (MR-KO) (red) animals in experiment 2. Starting point (0) is the first day that the tumor was visible by inspection. As animals were taken out of the experiment when the tumor had reached a certain size, the numbers vary at the different times points as follows: WT: Day 0 – 7: n=12, day 8: n =11, day 9: n=8. MR-KO: Day 0-7: n=12, day 8: n=10, day 9: n=7.

4.2 Tumor morphology

B16F1 melanoma typically forms a solid tumor that appears to be soft and glossy, and the color is dark, often black [131]. In the present in vivo experiments, B16F1 melanoma tumors first appeared as small dark spots under the skin of the mouse. The tumors showed different shapes as they grew, many were round (most common), but some were more elongated, or flattened. It was often observed that more than one tumor formed after injection and that these would often fuse and form one tumor. We also observed that with time; the color of some of the tumors changed to a lighter brown at gross morphology. In our studies metastases were not observed at necropsy, but 3 animals (1 MR-KO and 2 WTs) had to be excluded from experiment 2 in the end because cells had been accidentally injected into the peritoneal cavity, leading to tumor development in the visceral peritoneum, as well.

Perfusion fixed tumor tissue from experiment 1 was used for evaluation of tumor morphology on hematoxylin and eosin (H&E) stained sections and for IHC (Chapter 4.2.2).

In H&E sections the B16F1 melanoma cells appeared as round, oval, or elongated cells with variable amount of pigments. In both animal groups, middle sized tumors (3-5 mm in diameter) and large tumors (>8 mm) were richly vascularized (**Figure 4.4**).

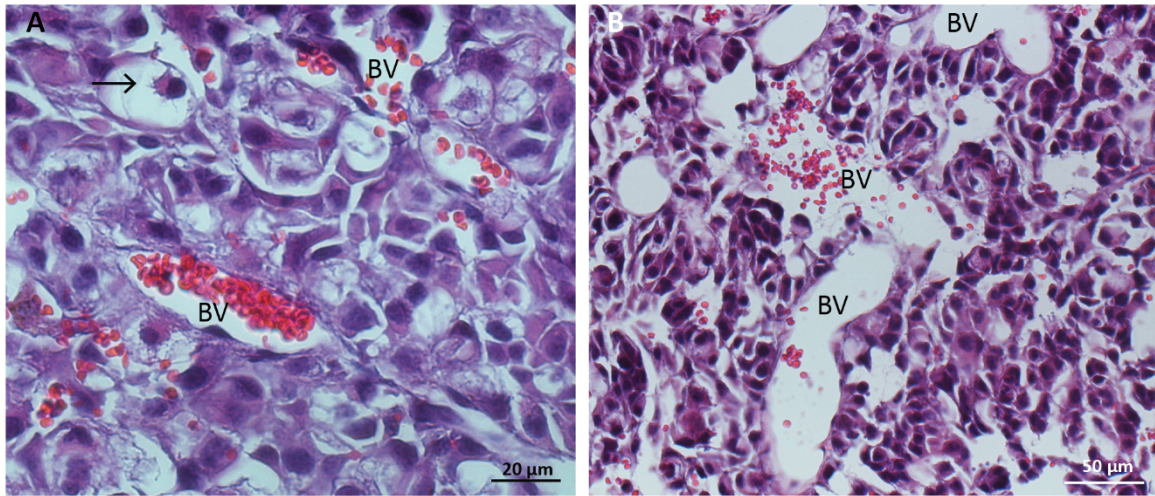


Figure 4.4: Morphology of the tumor tissue of the B16F1 melanomas. The figure shows H&E stained sections of B16F1 tumor tissue proper from **A**) middle sized tumor (3-5 mm in diameter) from a mannose receptor knockout mouse, and **B**) a large size (> 8 mm) tumor from a wild-type mouse. Tumor cells are stained dark purple/blue. In **A**), arrow points to a B16F1 cell with dendritic extensions. The tumor tissue in **A**) and **B**) is highly vascularized, and blood vessels (BV) show an irregular structure, size and shape.

The smallest tumors (1-2 mm in diameter; 4 from wild-type, and 4 from MR-KO mice) appeared as dark, purple/blue stained spots in the hypodermis, with some tumors also located in the underlying muscle layer (**Figure 4.5**). Tumor necroses were not observed in these tumors. The connective tissue surrounding the small tumors contained some infiltration of neutrophil granulocytes and mononucleated macrophage-like cells, indicating a mild inflammatory reaction (**Figure 4.5, E and F**).

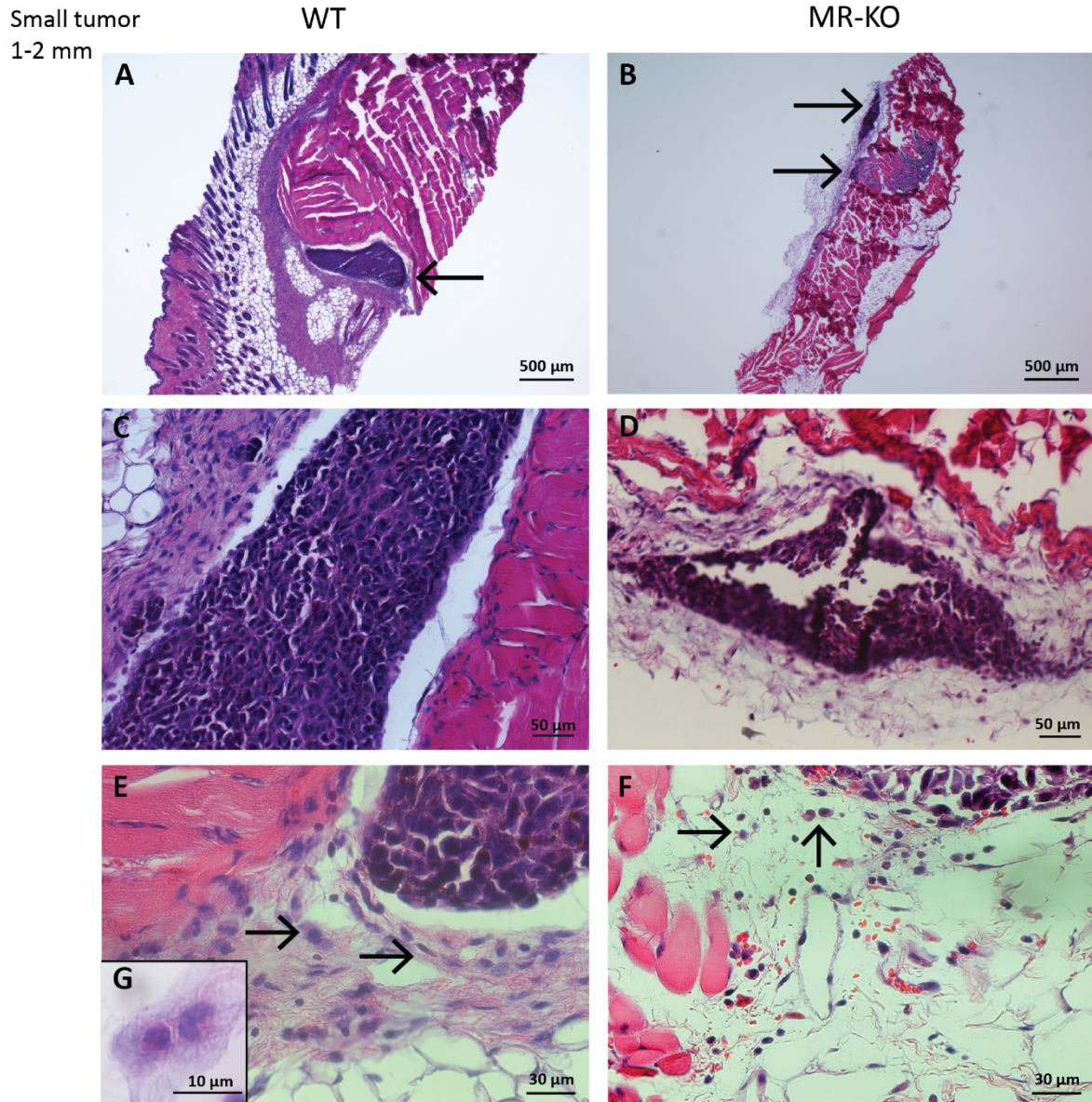


Figure 4.5: Tumor morphology of small tumors, 1-2 mm in diameter (H&E stained sections). The small tumors were located in the hypodermis (arrow in **A**, upper arrow in **B**), or partly also in the muscle layer underneath the hypodermis (lower arrow in **B**). Necrosis or large blood vessels were not observed inside the tumors (**C** and **D**). In the peri-tumoral connective tissue (**E** and **F**), infiltrating leukocytes are visible (arrows). Close up of infiltrating inflammatory cells (**G** and **H**)

The middle sized tumors (3-5 mm in diameter; 7 from wild-type and 7 from MR-KO mice), were all somewhat different from each other in shape, structure and morphology. However, the tumor tissue proper appeared more disorganized than in the smallest tumors, and they all had areas of necrosis (**Figure 4.6**). Size and shape of necrotic area in sections were very different between individual tumours, as presented later in this chapter. The tumors were well vascularized, but the pattern of blood vessels seemed rather disorganized (**Figure 4.6**,

C). A more pronounced infiltration of immune cells, in particular mononuclear cells were seen in the connective tissue surrounding the middle sized tumor, compared to the small tumors (Figure 4.6, E and F).

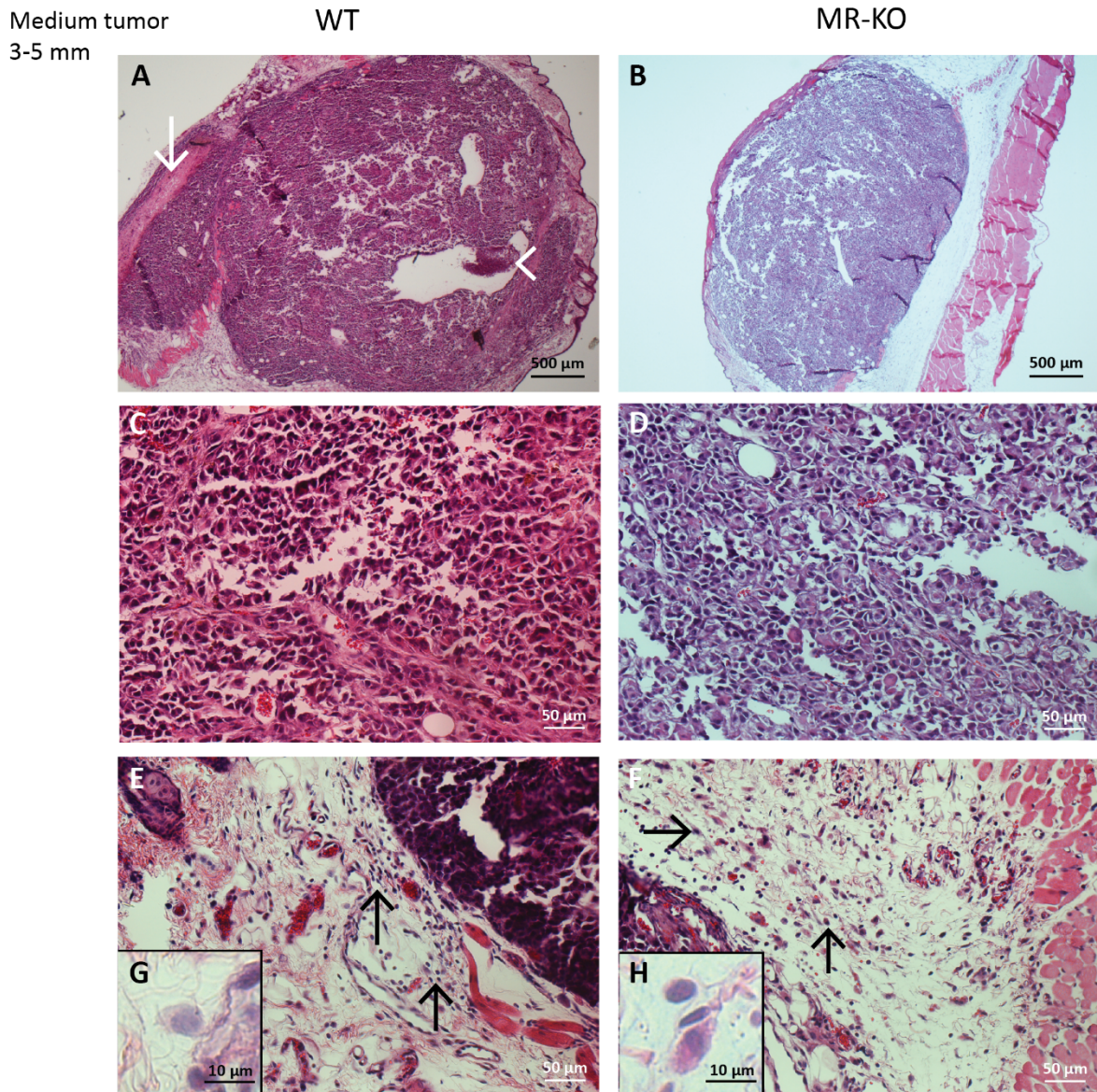


Figure 4.6: **Tumor morphology of medium sized** (approximately 3-5 mm) tumors (H&E stained sections). In **A**, arrow - head points to bleeding in tumor, and the arrow to an area with necrosis. Tumor vasculature is visible in **C** and **D** (arrows). The connective tissue surrounding the tumor has many infiltrating inflammatory cells (**E** and **F**; close ups in **G** and **H**).

In the large sized tumors (> 8 mm in diameter; 4 from wild-type and 4 from MR-KO mice), the tumor tissue proper was highly chaotic, and contained many areas of necrosis and bleedings (**Figure 4.7, A, B**). Blood vessels could be seen in close connection to and even inside necrotic areas, suggesting a dysfunctional tumor vasculature.

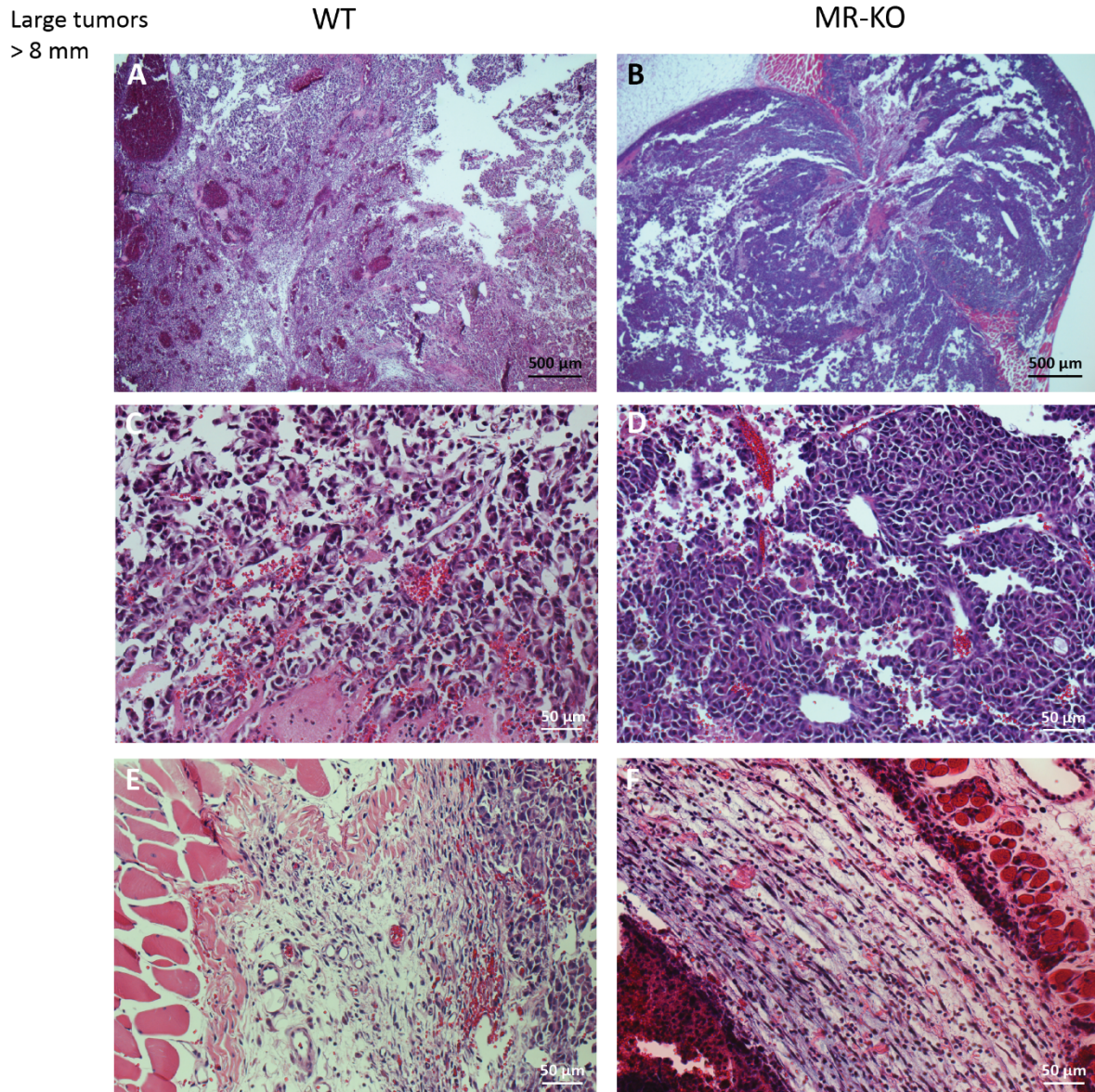


Figure 4.7: Tumor morphology of large sized (> 8 mm in diameter) tumors (H&E stained sections). The large tumors had a far more chaotic morphology than the small and medium sized tumors. Large blood filled vessels, and multiple bleedings and necrotic areas were visible at low magnification (**A** and **B**), details are shown in (**C** and **D**). Many inflammatory cells, especially mononuclear cells, were seen both inside the tumors (**C, D**), and in the connective tissue area surrounding the tumor (**E** and **F**).

4.2.1 Quantitative analyses of tumor tissue in H&E stained sections

In order to examine whether there were any differences between the tumors from wild-type and MR-KO mice, pictures were taken of H&E stained sections (five images per section) from all tumors in experiment 1, by a systematic random sampling approach, as described in material and methods (Chapter 3, section 3.6). The pictures were used to calculate the total area covered by necrosis and blood vessels in each section, in % of tumor area (described in material and methods). The H&E stained sections, one per tumor, were made approximately from the middle area of the tumors.

Tumor necrosis

The section area covered by necrosis, in % of total tumor area, did not differ significantly between wild-type and MR-KOs in either medium sized (3-5 mm diameter) or large tumors (> 8 mm) (**Figure 4.8**). On average, the relative area covered by necrosis decreased as the tumor grew from a medium size to a large size both in WT and MR-KO mice. However, this decline was not statistically significant.

Of note, measurements of tumor necrosis could sometimes be a challenge because the distinction between necrotic and intact tumor tissue were difficult to distinguish.

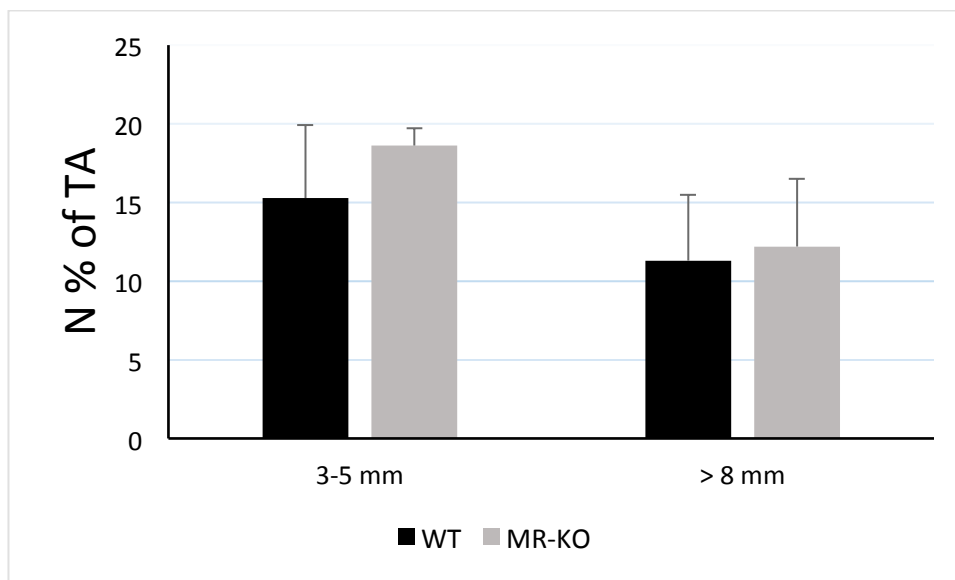


Figure 4.8: Necrosis (N) in % of tumor area (TA). The figure shows area covered by necrosis in % of tumor area in H&E sections from medium sized (3-5 mm) and large (> 8 mm) tumors from wild-type (WT; black) and mannose receptor knockout (MR-KO; grey) mice. Group sizes: medium sized tumors: WT : n=7, MR-KO: n=7. Large sized tumors: WT: n=4, MR-KO: n=4. Error bars: SEM.

Blood vessels in tumors

The number and size of blood vessels seen in individual tumors varied considerably. In some tumors, blood vessels were more distinguishable than in others. Most blood vessels observed in the H&E stained tumor sections had a “simple construction”, with a vascular wall consisting mainly of one layer of endothelial cells, lacking a distinct smooth muscle cell layer, and thus resembling a dilated capillary or sinusoidal structure, or venule-like structure.

For measurement of blood vessel area in percentage of tumor area, a stereology approach was used as described in chapter 3, section 3.6.1. For the medium sized tumors, the area covered by blood vessels in tumors was similar in wild-type and MR-KO mice, making up approximately 7 % of tumor area in both animal groups (**Figure 4.9**). In large tumors the tumor area covered by blood vessels was slightly lower in the MR-KO group, however, the difference was not statistically significant.

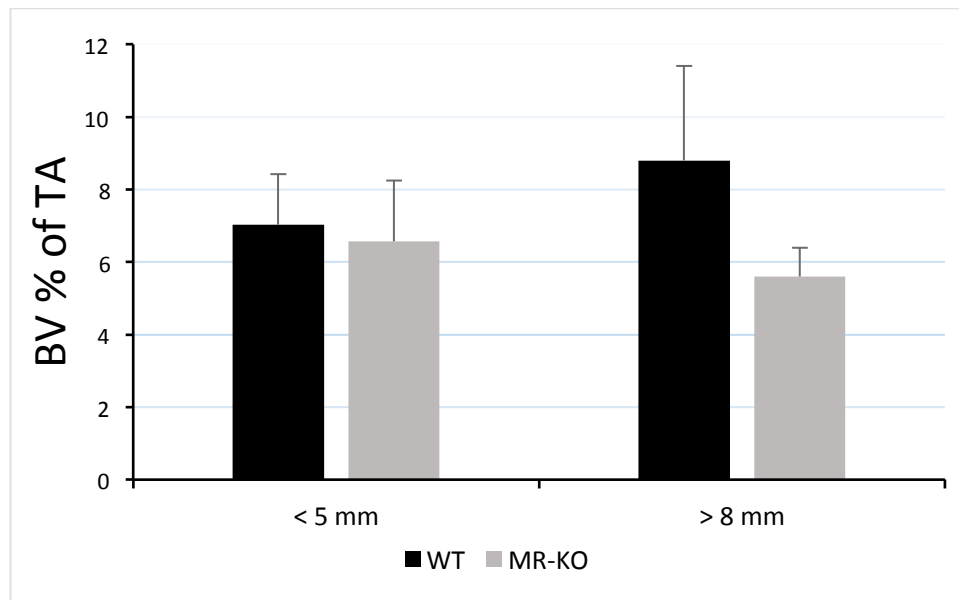


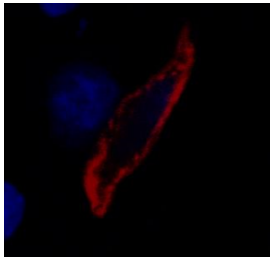
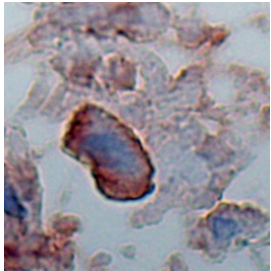
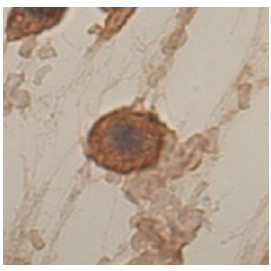

Figure 4.9: Blood vessels (BV) in % of tumor area (TA). The figure shows area covered by blood vessels in % of total tumor area in H&E sections of medium sized tumors (3-5) and large sized tumors (> 8 mm) from wild-type (WT; black) and mannose receptor knockout (MR-KO; grey) mice. Group sizes: Medium sized tumors; WT: n=7, MR-KO: n=7; Large tumors: WT: n=4, MR-KO: n=4. Error bars: SEM.

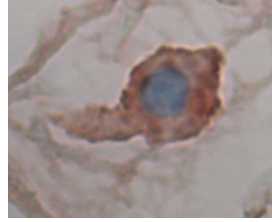

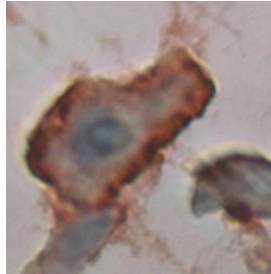
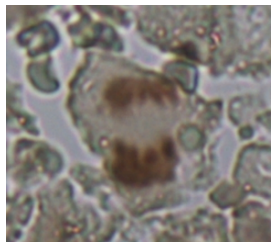
4.3 Immunohistochemistry

To try to answer the question raised in aims whether the mannose receptor is necessary for M2 polarization or just a marker for M2 polarized cells we did a immunohistochemical screening for the expression of M1 and M2 macrophage markers on paraffin sections of B16F1 melanomas of various sizes harvested from wild-type and MR-KO mice in experiment 1.

However, before this screening could be done the antibodies had to be tested and titrated. In addition to macrophage markers, we also tested a general T-cell marker in order to get more information about tumor associated inflammation, and a proliferation marker to look for eventual differences in mitosis frequency between tumors from the two animal groups. This testing was done as described (chapter 3, page 36) on sections from a large tumor (> 8 mm) from a wild-type mouse. Some markers were also tested in tumor sections from MR-KO mice. The results of the antibody testing are summarized in **Table 4.1**, whereas final antibody concentrations are given in **Table 3.3** (page 42, 43) and **Appendix A3**.

Table 4.1: The table summarizes the testing results of antibodies on B16F1 melanoma sections.

Marker	Antibody	Stains	Staining results	
Mannose receptor	Goat anti-human mannose receptor (CD206) <i>R&D systems</i>	M2 macrophages	Good staining of cells in WT mice; no staining in tumors from MR-KOs. Tested with fluorescence method)	
Arginase I	Rabbit anti-human Arginase I <i>Santa cruz</i>	M2 macrophages	Good staining; Tested with Histomouse™ and fluorescence methods	
Stabilin 1	Rabbit anti-human Stabilin 1 <i>Millipore</i>	M2 macrophages	Good staining; tested with Histomouse™	
iNOS	Rabbit anti-mouse iNOS <i>Abcam</i>	M1 macrophages	Good staining with Histomouse™. Did not function with fluorescence staining	
CD68	Rat anti-mouse CD68 <i>Abcam</i>	Macrophages	No staining; tested with Histomouse™ or fluorescence	

CD163	Mouse anti-rat CD163 <i>AbD Serotec</i>	Tissue macrophages	Good staining with Histomouse™	
F4/80	Rat anti-mouse F4/80 <i>AbD Serotec</i>	Macrophages	Good staining; Tested with HRP/DAB method	
CD11b/c	Mouse anti-rat CD11b/c <i>Cedarlane</i>	Monocytes, macrophages, dendritic cells	Good staining; Tested with Histomouse™	
CD3	Rabbit anti- human CD3 <i>DAKO</i>	Pan T-cell marker	No staining; Tested with Histomouse™, and fluorescence	
Proliferation marker	Rabbit anti- human Ki67 <i>Abcam</i>	Proliferating cells	Good staining; Tested with Histomouse™	

4.3.1 IHC screening of macrophage markers in tumors

As summarized in **Table 4.1**, most antibodies worked, and the macrophage markers all gave positive staining of mononuclear macrophage-like cells, as shown in the images in the right column of the table. However, the antibodies tested for CD68 (monoclonal, Abcam) and CD3

(polyclonal, DAKO) did not work on paraffin sections, at least not with our protocols. CD68 is a scavenger receptor expressed by many macrophages, and is commonly used as a pan macrophage marker [138]. The choice for a pan macrophage marker therefore fell on F4/80, which is another commonly expressed antigen in mouse tissue macrophages, where it is located in the plasma membrane [11]. The F4/80 antibody (CL:A3-1, AbD Serotec) gave very good staining of all macrophage-like cells in the B16F1 tumor tissue tested, and was therefore regarded as well suited for the screening of macrophages in the tumors.

To answer the question of macrophage polarization, we choose to test for iNOS, which is highly expressed in M1 macrophages, and arginase I, which is expressed in M2 macrophages and in TAMs (Chapter 1, section 1.2.1 and 1.2.2). The iNOS antibody (polyclonal, Abcam) gave good specific staining of macrophage-like cells with Histokit™, but not with the fluorescence method used, whereas the Arginase I antibody (polyclonal, Santa Cruz) worked well with both staining methods.

In addition to these markers, Stabilin 1 and mannose receptor was chosen. Stabilin 1 has recently been reported to be expressed in subsets of M2 macrophages [40], and also to be expressed in brain tumors like glioblastoma [40]. The mannose receptor is commonly used as a hall-mark for TAMs, and we therefore used the mannose receptor antibody as a TAM marker.

The scoring system for amount of positive non-tumor, macrophage-like cells in the tumor tissue proper and adjacent connective tissue, and the staining intensity is described in Section 3.6.7. Examples of how the staining intensity was scored is shown in **Figure 4.10**.

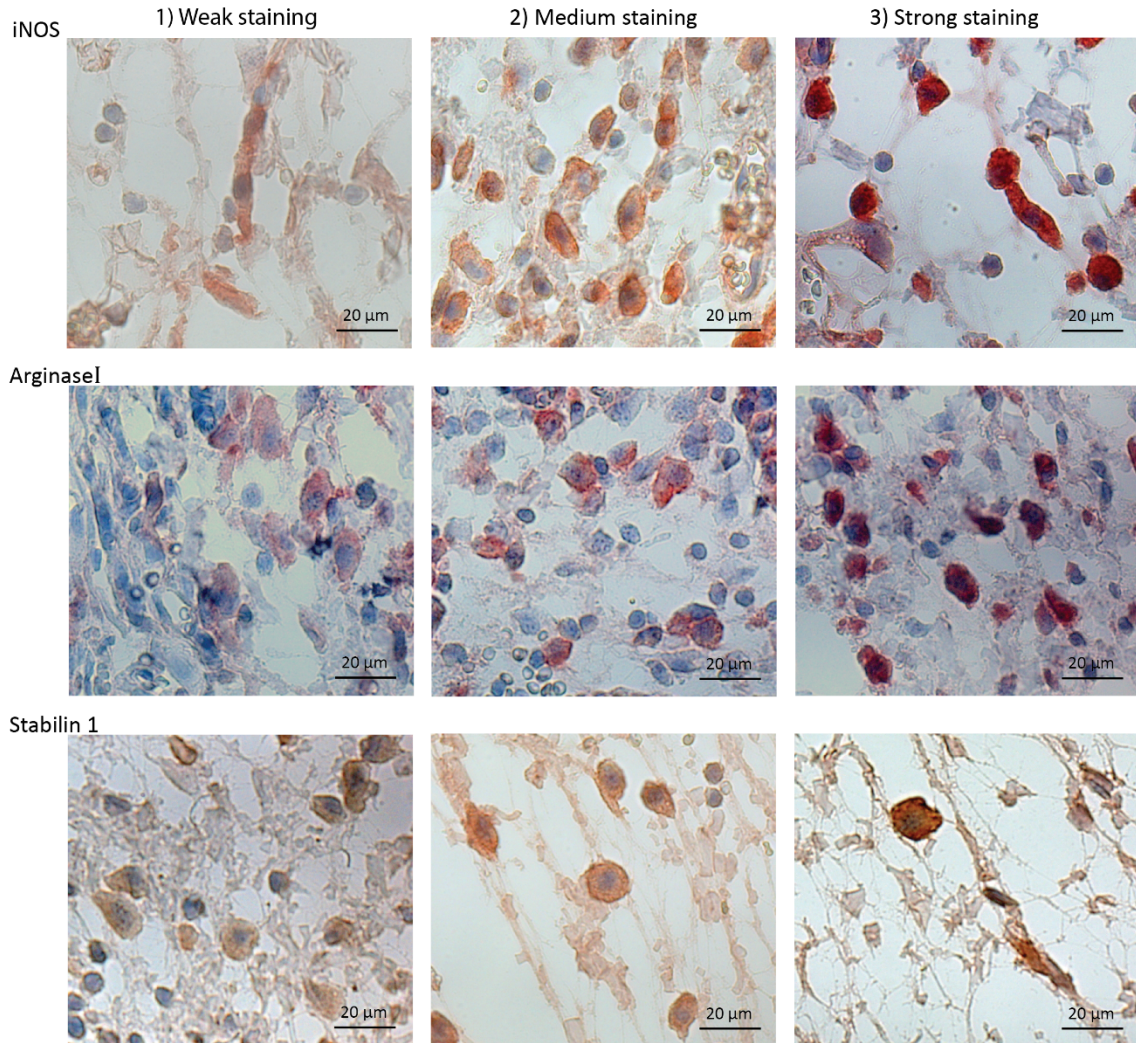


Figure 4.10: Examples of how scoring intensity was evaluated for iNOS, Arginase I and Stabilin 1. The staining intensity was scored on a scale from 1 to 3, where 1 represented weak, 2 medium, and 3 strong intensity of staining, respectively.

The tumor biopsies were roughly divided into three areas; tumor central area (TC), tumor peripheral area (TP) and tumor associated extra cellular matrix (ECM) (**Figure 4.11**). The tumor peripheral area was defined as the edge part of the solid tumor. The tumor associated ECM was defined as the matrix surrounding the tumor with border to the tumor tissue proper.

Screening for F4/80 positive cells

Screening of F4/80 was conducted with the HRP/DAB-method on sections from all animals in experiment 1. The end-result of positive DAB staining was a dark-brown color that was easy distinguishable from other structures. Results for small, medium sized and large tumors are represented in **Figures 4.11, 4.12 and 4.13**, respectively.

Already in the small tumors there was a high amount of F4/80 positive macrophages in central and peripheral parts of the tumor tissue proper and in the connective tissue surrounding the tumor. This was seen in both animal groups. The exception was one tumor from a MR-KO mouse, which only showed a few positive cells in the central part of the tumor. However, in all tumors F4/80 positive cells showed strong staining intensity.

Small tumors
1-2 mm

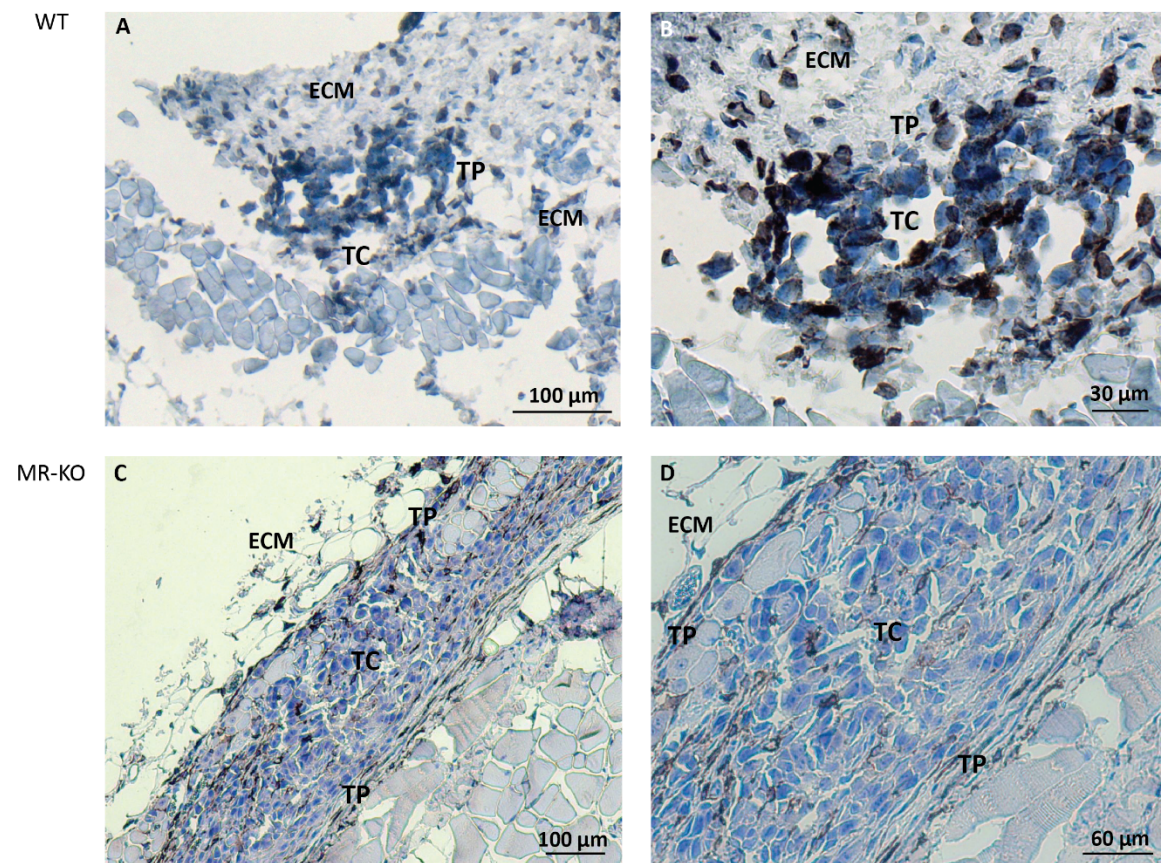


Figure 4.11: F4/80 screening of small tumors (1-2 mm). F4/80 positive cells (brown) were found in tumors from wild-type (WT) mice (A, magnified image in B), and in tumors from mannose receptor knockout (MR-KO) mice (C, magnified image in D). F4/80 positive cells were seen both in tumor central (TC), and tumor peripheral (TP) parts and in the extracellular matrix (ECM) surrounding the tumor (B and C).

In the medium sized tumor group, there was a high amount of strongly stained F4/80 positive cells both in the central and peripheral part of the tumor and in the tumor associated connective tissue. The amount of positive cells and staining intensity were the same for wild-type and MR-KO tumors (**Figure 4.12**).

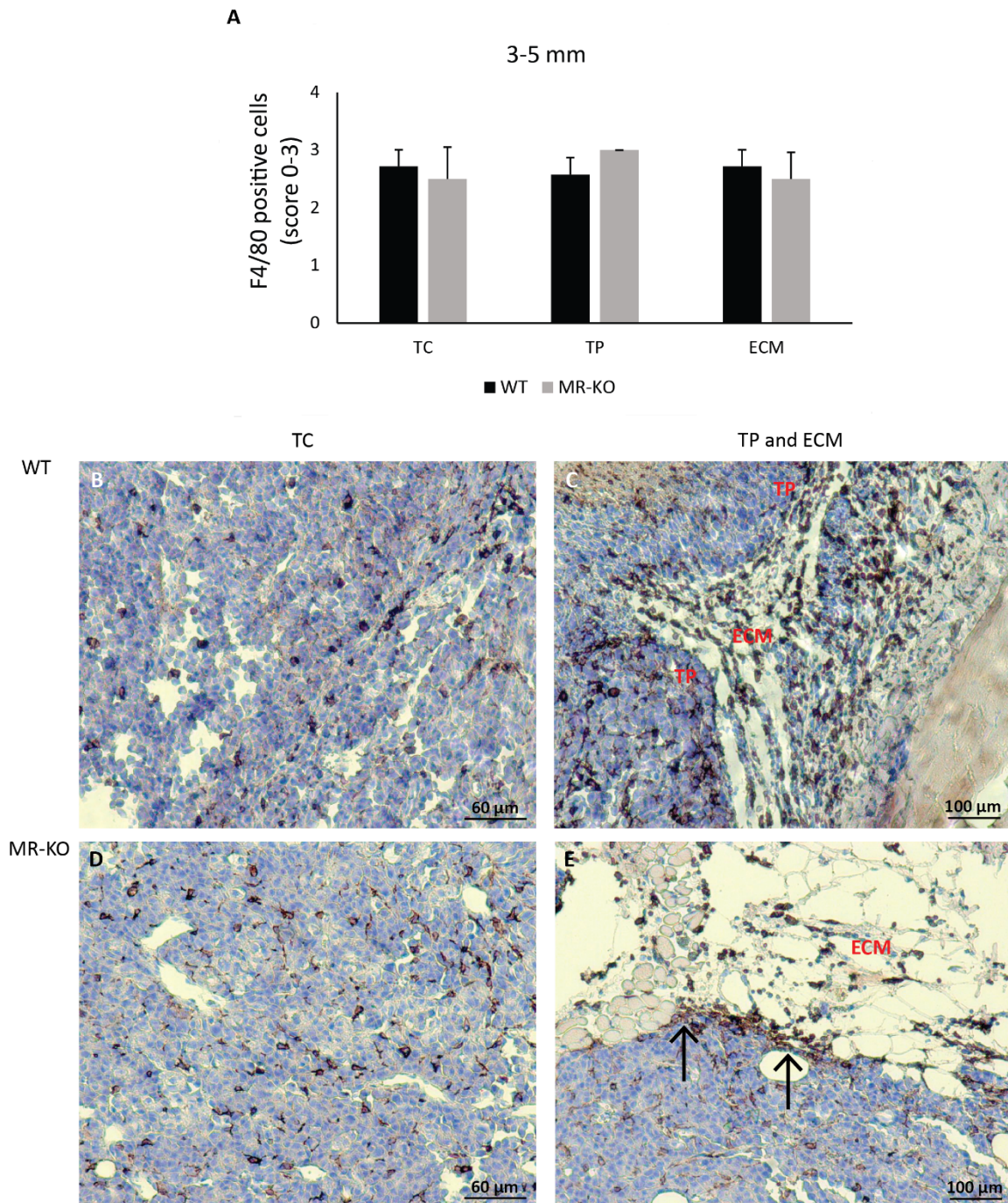


Figure 4.12: F4/80 labeling of medium sized (3-5mm) tumors. A) Scoring results for F4/80 positive cells in tumor central area (TC), tumor peripheral area (TP) and in the extracellular matrix (ECM) surrounding the tumors. **B-E)** Positively stained (dark brown precipitates) macrophages are seen throughout the whole tumor (TC and TP parts) and in the extracellular matrix (ECM) of tumors from

wild type (WT, **B-C**) and mannose receptor knockout (MR-KO, **D-E**) mice. Arrows in **E** point to accumulation of F4/80 positive macrophages along the border between ECM and the tumor tissue. Error bar in **A**: SEM; WT n=7; MR-KO, n=7.

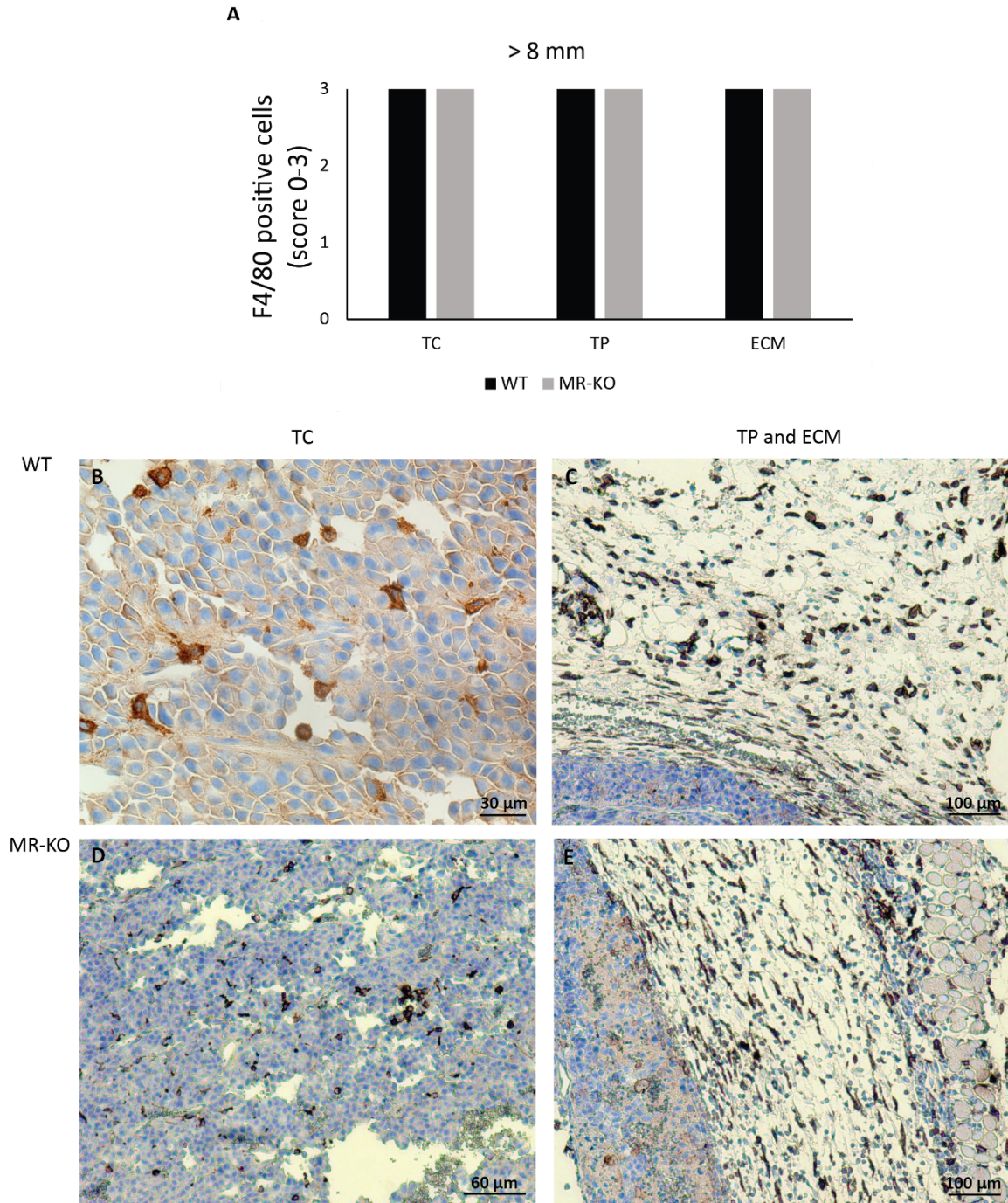


Figure 4.13: F4/80 labeling of large size (> 8 mm) tumors. **A**) Scoring results for F4/80 positive cells in the tumor central part (TC), peripheral part (TP) and extracellular matrix (ECM). **B-E**) Positively stained (dark brown precipitates) macrophages are seen throughout the whole tumor (TC and TP parts) and in the extracellular matrix (ECM) of tumors from wild type (WT, **B-C**) and mannose receptor knockout (MR-KO, **D-E**) mice. WT, n=4; MR-KO, n = 4.

The amount of F4/80 positive cells in large tumors, and tumor-associated connective tissue was even higher than in medium sized tumors (**Figure 4.13**).

To sum up the highest density of F4/80 positive macrophages were seen in the largest tumors, and the lowest in the smallest tumors, however, the staining intensity was strong in all tumors (**Table 4.2**).

Table 4.2: Staining intensity of F4/80 positive cells. Average scoring values (SD) for staining intensity seen in F4/80 positive cells in melanomas from wild-type (WT) and mannose receptor knockout (MR-KO) animals. Small size tumors (1-2 mm) WT: n=4, MR-KO: n=4. Medium sized tumors (3-5 mm) WT: n=7, MR-KO: n=7. Large size tumors (>8 mm) WT: n=4, MR-KO: n=4. Standard deviation: SD (in brackets)

Score: 1-3 (SD)			
	Tumor - central part	Tumor – peripheral part	Extracellular matrix
Tumor size: 1-2 mm			
WT	3 (0)	3 (0)	3 (0)
MR-KO	3 (0)	3 (0)	3 (0)
Tumor size: 3-5 mm			
WT	3 (0)	3 (0)	3 (0)
MR-KO	2.5 (1.5)	3 (0)	3 (0)
Tumor size: > 8 mm			
WT	3 (0)	3 (0)	3 (0)
MR-KO	3 (0)	3 (0)	3 (0)

Screening for of iNOS positive cells

Immune labeling for iNOS positive cells was conducted on sections from all animals with medium sized and large tumors in experiment 1. The Histomouse™ method was used for visualization of positive staining. Results are presented in **Figures 4.14** and **4.15**, and in **Table 4.3**.

In the medium sized tumor group no iNOS positive cells were seen inside the tumors from either wild-type or MR-KO mice. In the tumor peripheral area, a few positive cells with low staining intensity were observed in both animal groups (**Figure 4.14, C, F; Table 4.3**). A moderate number of iNOS positive macrophage-like cells were observed in the connective tissue surrounding the tumor, and these cells had a moderate staining intensity. The amount of positive cells and staining intensity were the same for wild-type and MR-KO tumors.

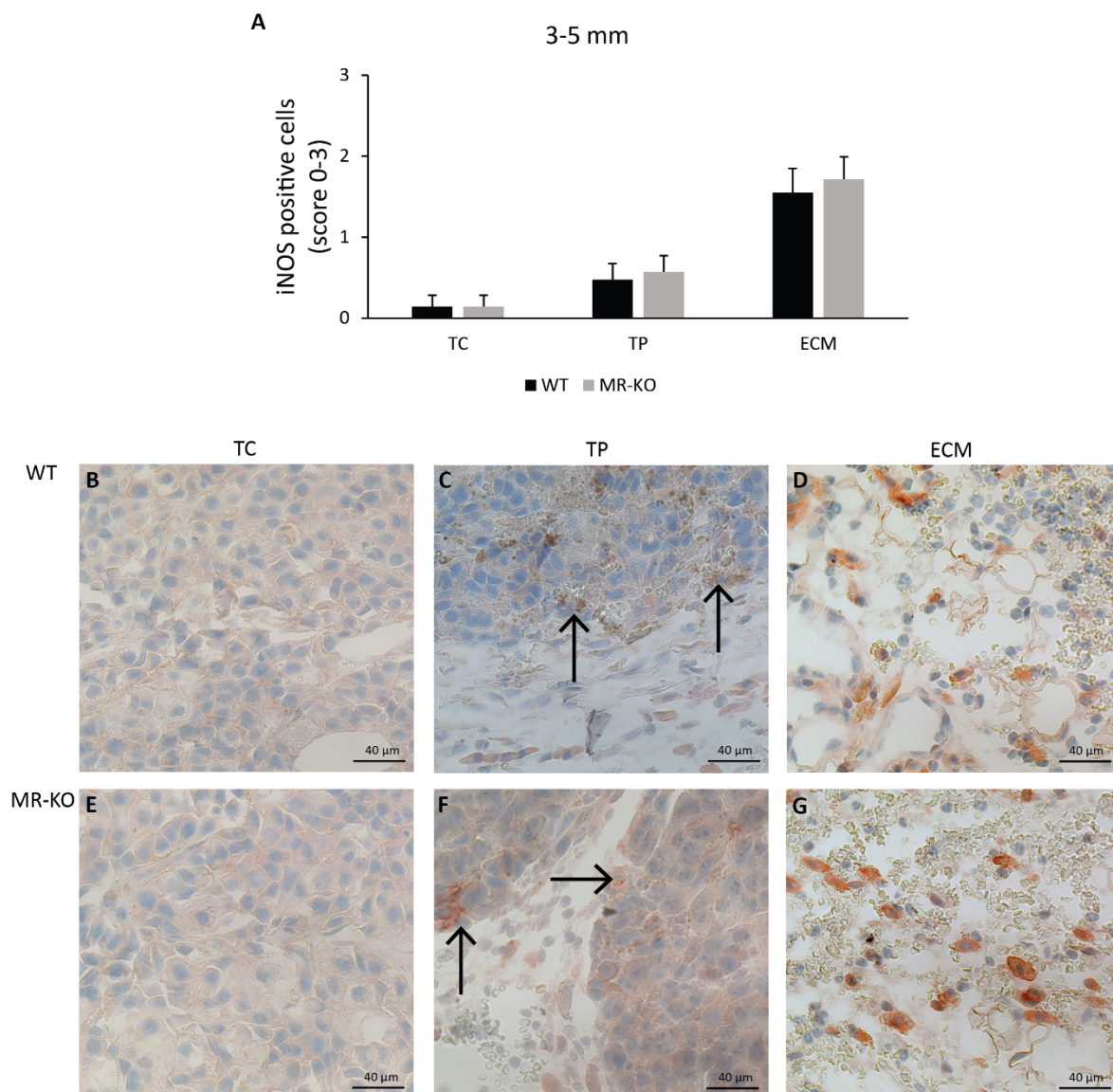


Figure 4.14: The figure shows results from the screening for iNOS expression in medium sized melanomas (3-5 mm in diameter). **A)** Graph showing the scoring results for iNOS. **Panel B-D** shows

the staining pattern in a representative tumor from wild-type mouse (WT), and panel E-G the results from a mannose receptor knockout mouse (MR-KO). TC: Central part of tumor; TP: peripheral part of tumor; ECM: extracellular matrix surrounding the tumor tissue proper. Error bars in A: SEM, WT, n=7; MR-KO, n=7.

In the large tumors, very few iNOS positive cells were observed inside the tumors (**Figure 14.15**) and fewer cells were seen in the tumor associated connective tissue (ECM), than in the medium sized tumors. There were more iNOS positive cells in the ECM of wild-type tumors than in tumors from MR-KOs, and these cells also had a stronger staining intensity than in the latter animal group (**Table 4.3**).

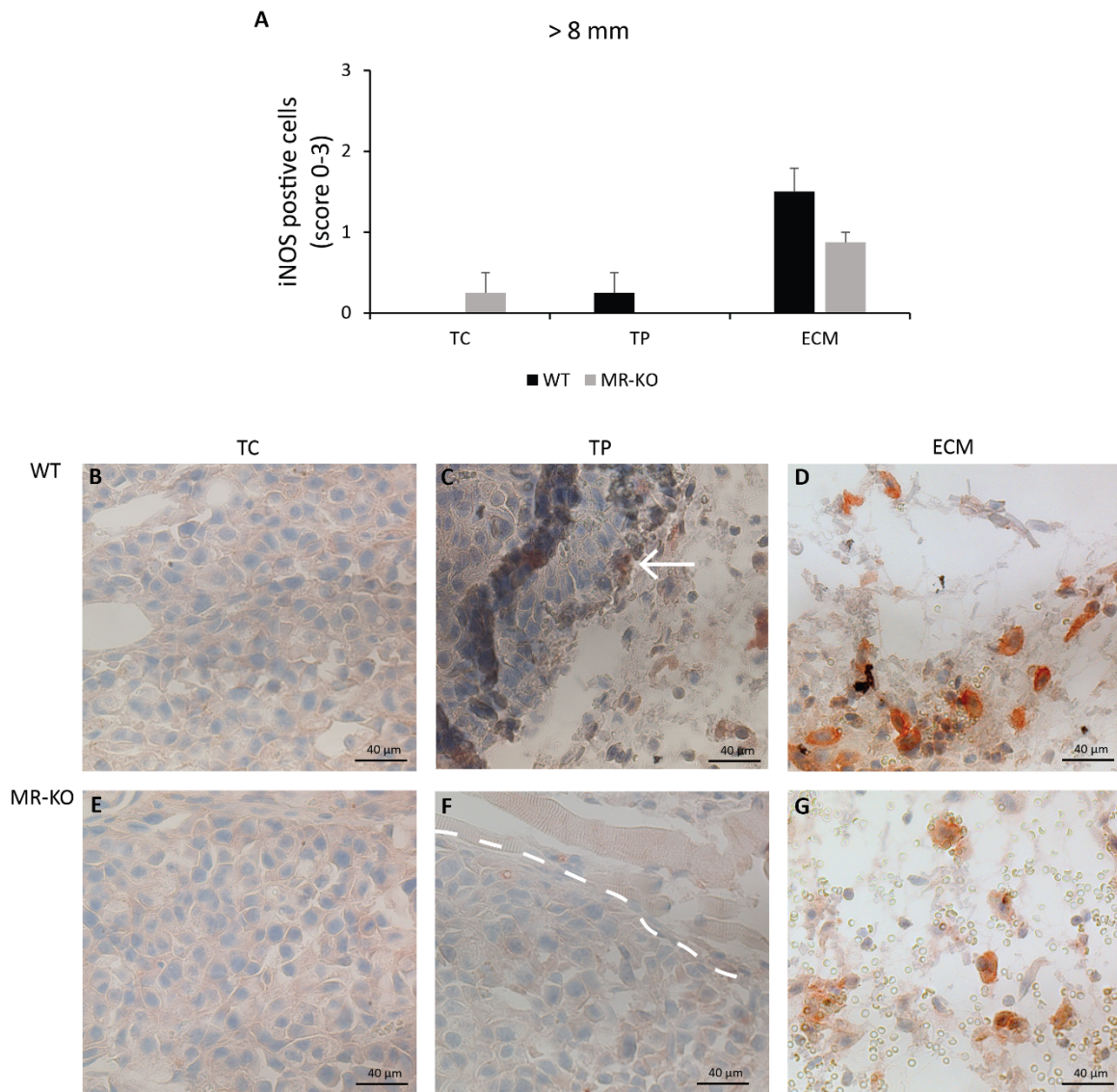


Figure 4.15: The figure shows results from the screening for iNOS expression in large sized melanomas (>8 mm in diameter). A) Graph showing the scoring results for iNOS positive cells. Panel B-D shows the staining pattern in a representative tumor from a wild-type mouse (WT), and panel E-G

the results from a mannose receptor knockout mouse (MR-KO). Positive staining is seen as red cytoplasmic staining. TC: Central part of tumor; TP: peripheral part of tumor; ECM: extracellular matrix surrounding the tumor tissue proper. Discontinuous line marks the border between tumor peripheral area and surrounding tissue. You may insert an arrow in C, pointing to one of the few positive cells there. Error bars in A: SEM; WT, n=4; MR-KO, n = 4.

Due to limited time and problems encountered with the last batch of the Histomouse Plus kit (high unspecific staining), iNOS staining was not done on sections from small tumors.

The staining intensity of the positive cells in the iNOS screening is shown in **Table 4.3**.

Table 4.3: Staining intensity of iNOS positive cells. Average values (SD) for staining intensity of iNOS positive cells in melanomas from wild-type (WT) and mannose receptor knockout (MR-KO) animals. Medium size tumors (3-5 mm) WT: n=7, MR-KO: n=7. Large size tumors (>8 mm) WT: n=4, MR-KO: n=4. Of note, as iNOS positive cells were hardly detected in tumor tissue proper, no values are given.

Score: 1-3 (SD)			
	Tumor - central part	Tumor - peripheral part	Extracellular matrix
Tumor size: 3-5 mm			
WT	-	-	2.1 (0.9)
MR-KO	-	1 (1)	2.4 (0.5)
Tumor size: > 8 mm			
WT	-	-	2 (0.8)
MR-KO	-	-	1.4 (0.5)

Screening for Arginase I positive cells

Screening for arginase I was conducted on sections from all animals with medium sized and large tumors in experiment 1. The Histomouse™ kit was used for visualization of positive labeling. Results are presented in **Figures 4.16** and **4.17**.

In the medium sized tumor group, arginase positive cells were observed in the central and peripheral parts of the tumor tissue both in wild-type and MR-KO mice. The highest density of arginase positive cells was found in the connective tissue surrounding the tumor. There

was no difference in the amount of positive cells (**Figures 4.16**) and staining intensity (**Table 4.4**) between wild-type and MR-KO mice tumors.

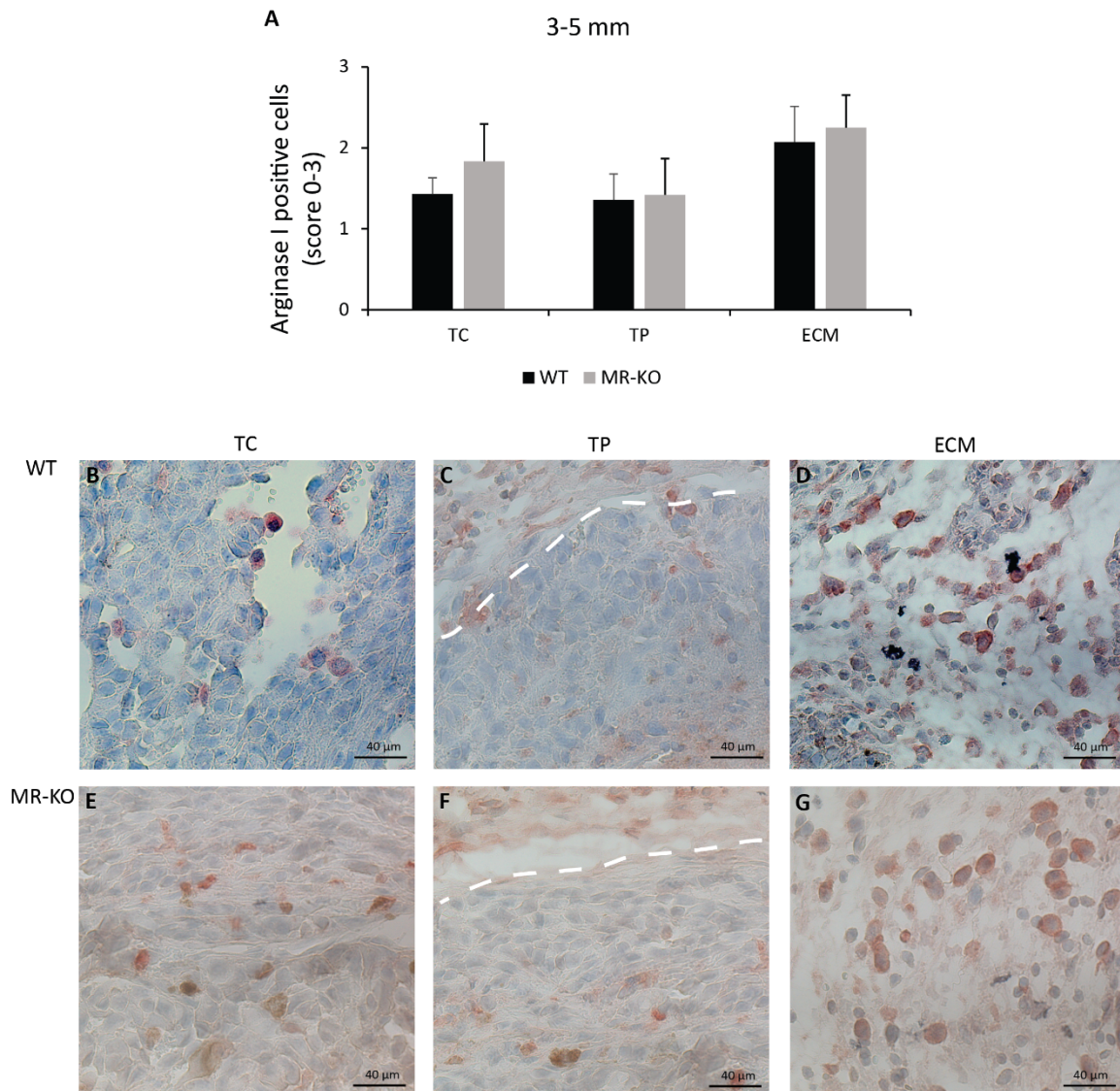


Figure 4.16: The figure shows results from the screening for arginase I expression in medium sized melanomas (3-5 mm in diameter). A) Graph showing the scoring results for arginase I. **Panel B-D** shows the arginase staining pattern in a representative tumor from wild-type (WT) mouse, and **panel E-G** the staining pattern in tumors from a mannose receptor knockout (MR-KO) mouse. TC: Central part of tumor; TP: peripheral part of tumor; ECM: extracellular matrix surrounding the tumor tissue proper. Error bars in A: SEM; WT, n = 7; MR-KO, n= 7.

In both wild-type and MR-KOs there were more arginase positive cells in the central part of the large tumors than in the medium sized tumors (**Figures 4.16 A, 4.17A**). A high amount of positive cells were also seen in the tumor associated connective tissue of the large tumors, and these cells showed a stronger staining intensity in large melanomas from wild-type animals than in melanomas from MR-KO animals (**Table 4.4**), however, the results were not statistically significant (p -value=0.23).

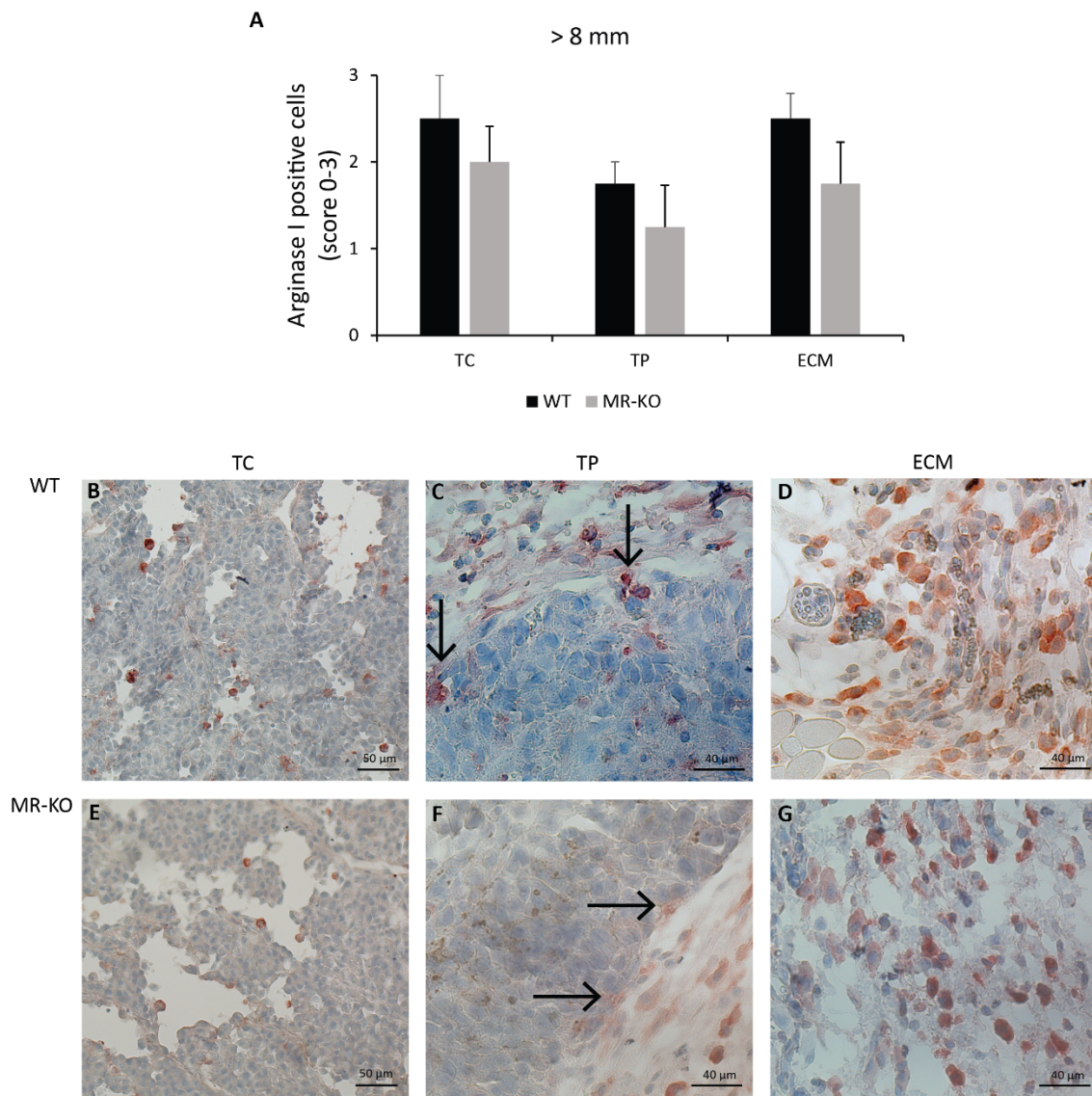


Figure 4.17: The figure shows the results from the screening for arginase I expression in large sized B16F1 melanomas (>8 mm). A) Graph showing the scoring results for arginase I. Panel B-D shows the staining pattern in a representative tumor from a wild-type (WT) mouse, and panel E-G a tumor from a mannose receptor knockout (MR-KO) mouse. TC: Central part of tumor; TP: peripheral part of

tumor; ECM: extracellular matrix surrounding the tumor tissue proper. Arrows: positive cells in TC (B and E), and TP (C and F). Error bars in A: SEM; WT, n=4; MR-KO, n=4.

Due to limited time and problems encountered with the last supply of Histomouse Plus kit, arginase I staining was not done on sections from small tumors.

Table 4.4: Staining intensity of arginase I positive cells. Average values (SD values) for staining intensity of arginase I positive cells in melanomas from wild-type (WT) and mannose receptor knockout (MR-KO) animals. Medium sized tumors (3-5 mm in diameter) WT: n=7, MR-KO: n=7. Large size tumors (>8 mm) WT: n=4, MR-KO: n=4

Score: 1-3 (SD)			
	Tumor - central part	Tumor - peripheral part	Extracellular matrix
Tumor size: 3-5 mm			
WT	1.9 (0.7)	1.6 (1)	1.9 (1.1)
MR-KO	2 (1)	1.5 (0.8)	2.4 (0.6)
Tumor size: > 8 mm			
WT	2.8 (0.5)	1.5 (0.6)	2.8 (0.5)
MR-KO	2 (1.2)	1.3 (1)	1.8 (0.5)

Screening for Stabilin-1 positive cells

Screening of stabilin-1 was conducted on sections from all animals with medium sized and large tumors in experiment 1. The histomouseTM method was used for visualization. Results are presented in **Figures 4.18** and **4.19**, and in **Table 4.5**.

Stabilin-1 positive cells were very rarely seen inside the tumors in either wild-type or MR-KO mice, independent of tumor size (**Figure 4.18** and **4.19**). Far more cells were observed in the tumor associated connective tissue, with the highest amount seen in large tumors from wild-type mice (**Figure 4.19**). Staining intensity was mostly weak, except for stabilin 1 positive cells in ECM associated with large tumors in wild -type mice which showed a moderate to strong staining intensity (**Table 4.5**).

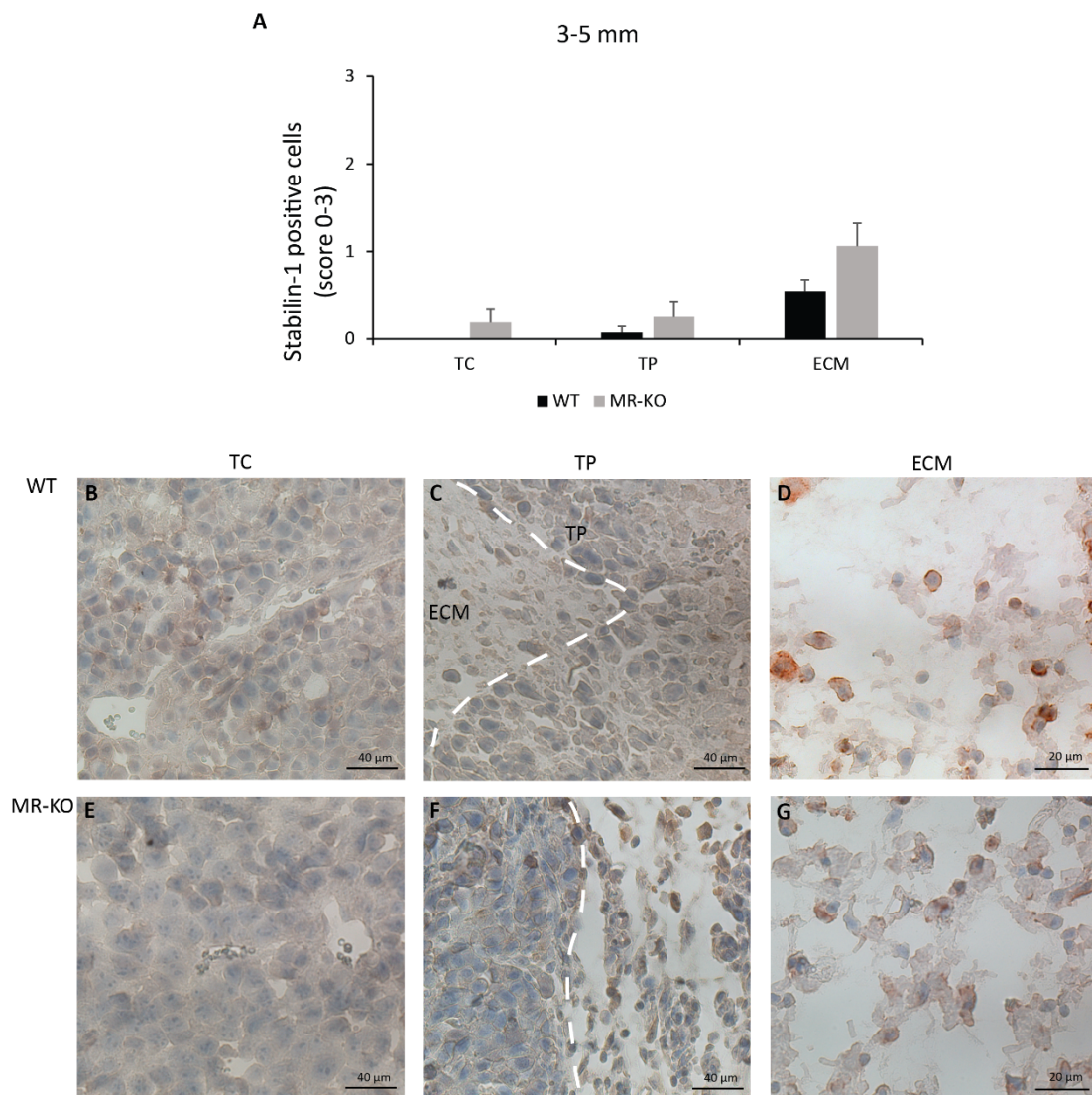


Figure 4.18: The figure shows results from the screening for stabilin-1 expression in medium sized melanomas (3-5 mm in diameter). A) Graph showing stabilin-1 positive cells scored on a scale from 0-3. Panel B-D shows the staining pattern in a tumor from wild-type mouse (WT), and panel E-G from a mannose receptor knockout mouse (MR-KO). TC: Central part of tumor; TP: peripheral part of tumor; ECM: extracellular matrix surrounding the tumor tissue proper. Discontinuous lines in C and F divide tumor peripheral area from ECM. Error bars in A: SEM; WT, n=7; MR-KO, n=7.

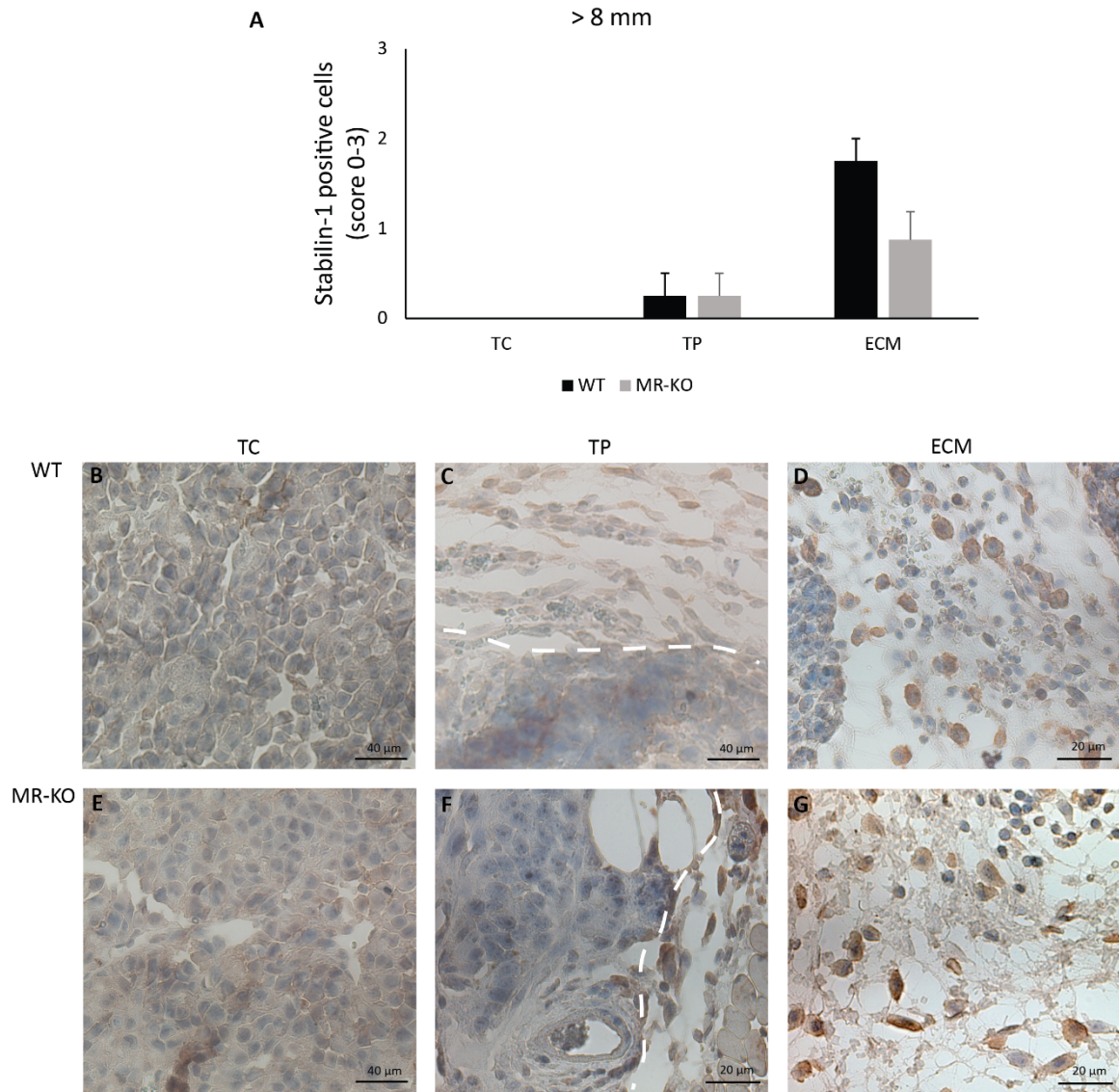


Figure 4.19: The figure shows results from the screening for stabilin-1 expression in large melanomas (>8 mm). A) Graph showing average number of stabilin-1 positive cells. Panel B-D shows the staining pattern in a tumor from wild-type mouse, and panel E-G staining results from a mannose receptor knockout mouse (MR-KO). TC: Central part of tumor; TP: peripheral part of tumor; ECM: extracellular matrix surrounding the tumor tissue proper. Discontinuous lines in C and F mark the border between ECM and the tumor peripheral part. Error bars in A: SEM; WT, n=4; MR-KO, n=4.

Table 4.5: Staining intensity of stabilin-1 positive cells. Average values (SD) for stabilin-1 staining intensity in positive cells in melanomas from wild-type (WT) and mannose receptor knockout (MR-KO) animals. Medium size tumors (3-5 mm) WT: n=7, MR-KO: n=7. Large size tumors (>8 mm) WT: n=4, MR-KO: n=4. Of note, as very few stabilin-positive cells were observed inside the tumors, no values are given.

Score: 1-3 (SD)			
	Tumor - central part	Tumor – peripheral part	Extracellular matrix
Tumor size: 3-5 mm			
WT	-	-	1 (0.5)
MR-KO	-	-	1.4 (1)
Tumor size: > 8 mm			
WT	-	-	2.8 (0.5)
MR-KO	-	-	1 (0)

Testing of mannose receptor in tumors

In order to find out when the shift from M1 to M2 macrophages starts to occur in the B16F1 melanomas, we compared the expression of the mannose receptor, which is a hallmark of M2 polarized TAMs, with that of the pan-macrophage marker F4/80 in parallel sections from small, medium sized and large tumors from wild-type animals (2 tumors tested per size group). The results are presented in **Figures 4.20, 4.21** and **4.22**.

In the small tumors some mannose receptor positive cells were observed inside the tumors and in the tumor periphery. However, the majority of positive cells were found in the connective tissue surrounding the tumor. The F4/80 labeling showed far more macrophages both in the tumor and in the ECM, than seen in parallel sections stained for the mannose receptor suggesting that most infiltrating macrophages were not yet M2 polarized at this stage (**Figure 4.20**).

In the medium sized tumor group, there were almost as many MR positive cells in the tumor tissue proper as F4/80 positive cells, and there was also a high amount of MR positive cells in the connective tissue surrounding the tumor (**Figure 4.21**).

The large tumors also had a large number of mannose receptor positive cells in the tumor and surrounding connective tissue, much corresponding to the staining pattern of F4/80 in these tumors (**Figure 4.22**).

Small tumors
1-2 mm

F4/80

MR

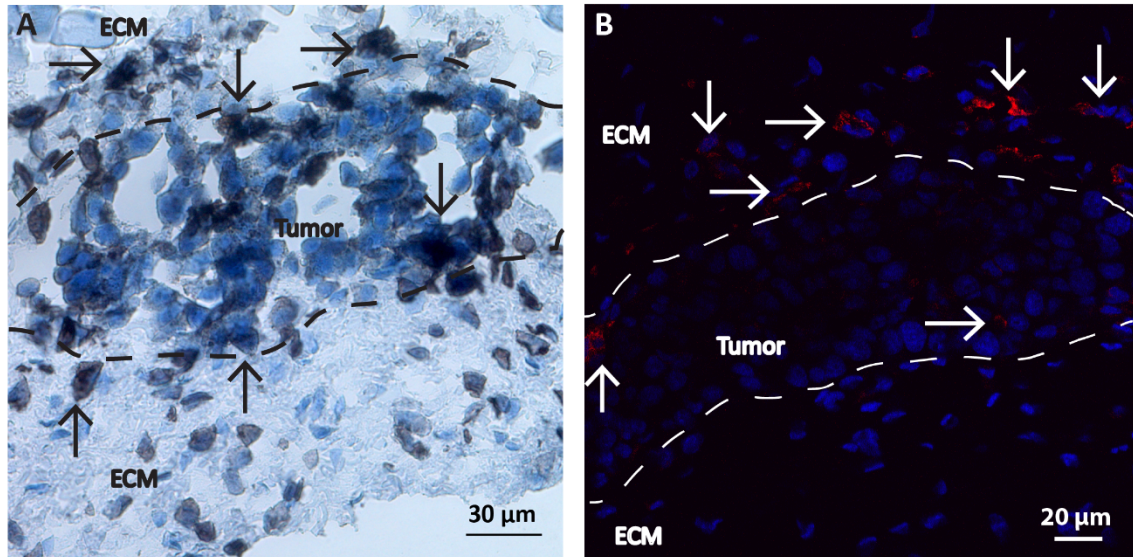


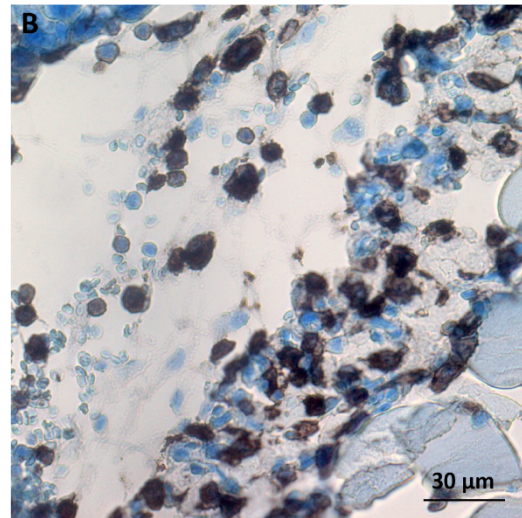
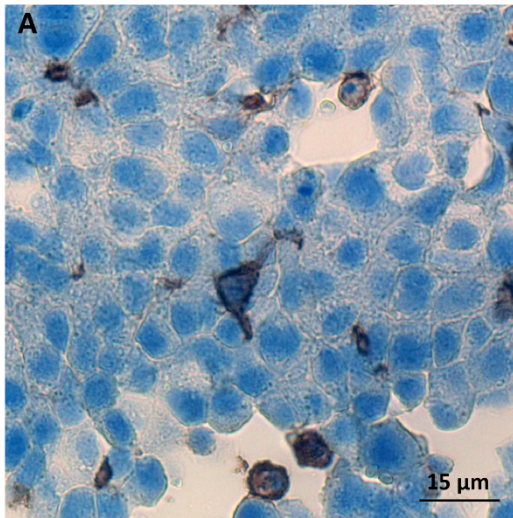
Figure 4.20: The figure shows F4/80 and mannose receptor (MR) expression in a small sized melanoma (1-2 mm). Picture in A) shows F4/80 positive cells (dark brown/black), and B) shows MR positive cells (red fluorescence) in a parallel section from the same tumor. Arrows point to MR positive cells. TC: Central part of tumor; TP: peripheral part of tumor; ECM: extracellular matrix surrounding the tumor tissue proper. Discontinues line mark the tumor border towards the ECM.

Medium tumors
3-5 mm

F4/80

TC

ECM



MR

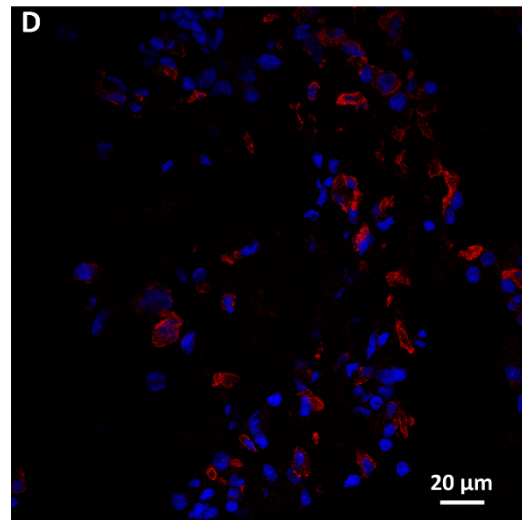
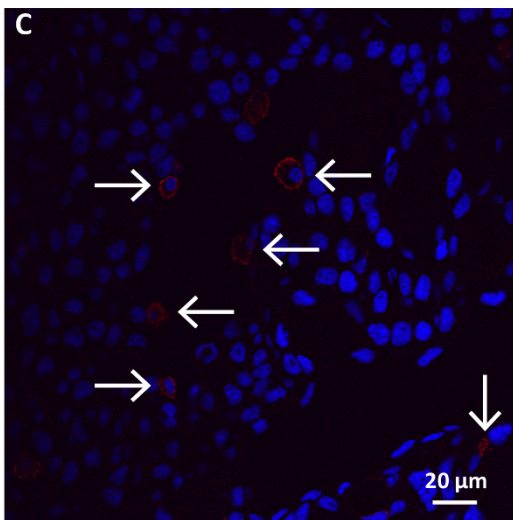


Figure 4.21: The figure shows F4/80 and mannose receptor (MR) expression in medium sized melanomas (3-5 mm). A) Picture shows F4/80 positive cells (dark brown/black) in the central part of tumor (TC), and (B) in the extracellular matrix (ECM) surrounding the tumor. C) Picture shows mannose receptor (MR) positive cells (red, arrows) in TC and (D) in ECM.

Large tumors
> 8 mm

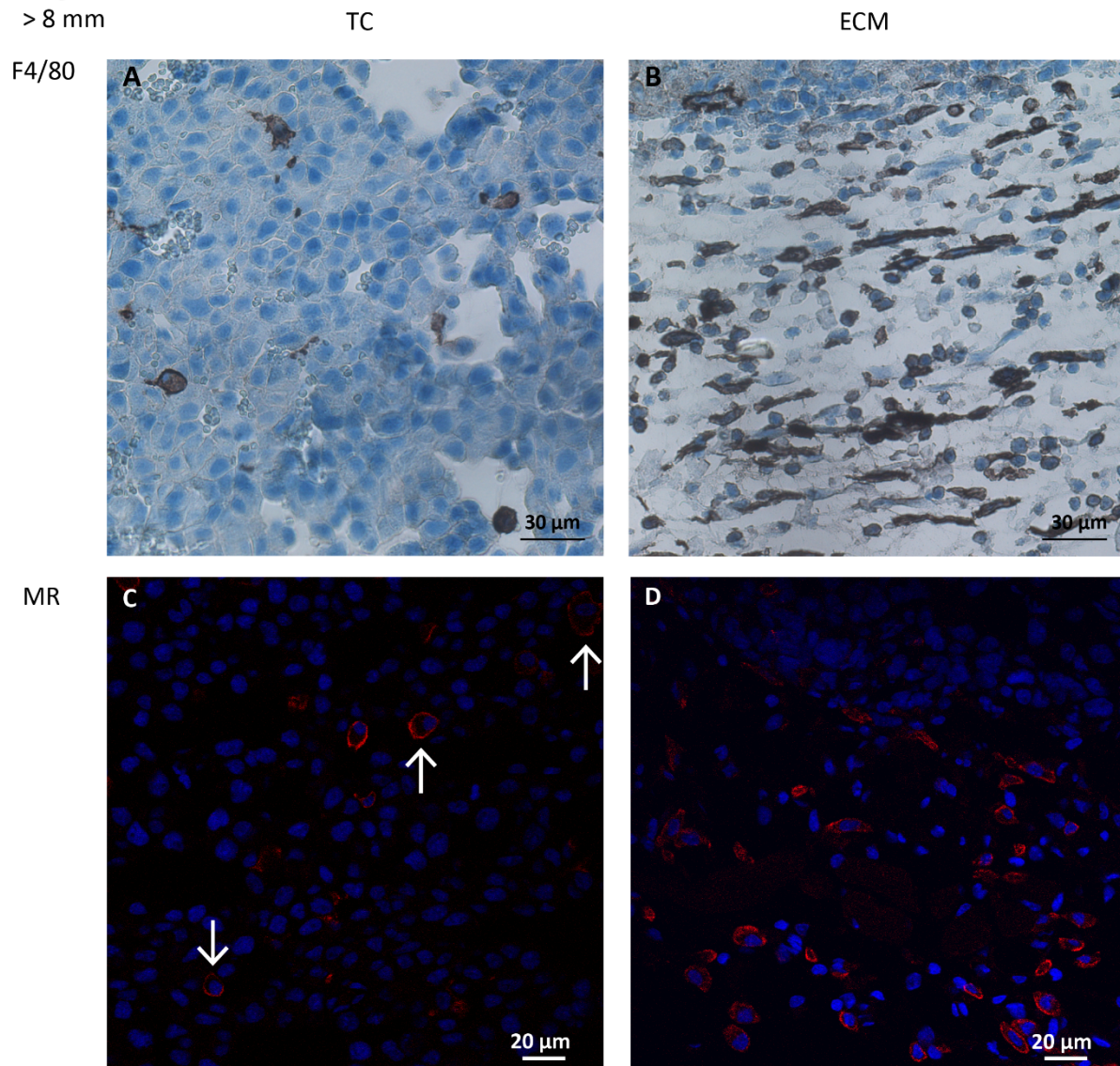


Figure 4.22: The figure shows F4/80 and mannose receptor (MR) expression in large sized melanomas (> 8 mm). A) F4/80 positive cells in the central part of tumor (TC), and (B) in the extracellular matrix (ECM) surrounding the tumor. C) Mannose receptor (MR) positive cells (red; arrows) in TC and (D) in ECM.

4.2.3 Gene expression analysis – qPCR

Gene expression analysis was conducted as described in section 3.7. Due to limited time four MR-KO samples and four wild-type samples from medium sized tumors were chosen for a preliminary study. Sample purity and RNA integrity was good (**Table 4.6**). We tested 4 reference genes preselected from the provider – some of which had been used in melanoma studies by others. As CD68 is expected to be expressed by all or most macrophages in the tumor, this was also tested as a possible reference gene for normalizing M1 and M2 marker gene expression.

Unfortunately, the variation in gene expression of the reference genes was too high for proper normalization. In order to partially analyze the reference gene results, we chose one of the wild-type samples (WT 3) as a reference sample, and gave this the value 1, and normalized the other against this sample (**Table 4.7**). As Beta-2 microglobulin (B2M) showed the least variation, the results from qPCR of the target genes Arginase I, iNOS and CD68 were normalized to this gene (**Figure 4.23**). Two MR-KO samples had to be excluded because of too low amplification product of the target genes and B2M. Because of the problems with the reference genes, and few samples tested, the results in **Figure 4.23** are at best only indicative.

Table 4.6: Results from RNA isolation. Sample concentration and sample purity was evaluated by using Nanodrop, and Experion RNA integrity test (RQI).

Sample	ng/ul	Sample purity (260/280)	RQI
WT 3	1295.11	2.11	9.1
WT 9	2.13	2.23	9.6
MR-KO 14	914.79	2.11	9.4
WT 15	2435.26	2.08	9.2
MR-KO 18	199.52	2.11	ND
WT 21	1487.11	2.11	9.5
MR-KO 22	904.69	2.13	9.6
	1478.88	2.11	9.6
MR-KO 24	1140.90	2.08	9.1

Table 4.7: Results from qPCR with normalization to WT 3. Due to high variation in the reference genes, and in pan macrophages marker CD68, the expression was normalized to results from WT 3. Values below than 1 reflect lower expression than in WT 3, values above than 1 reflect higher expression than in WT 3. Samples from 2 MR-KO animals were excluded because of low detection (not shown in the table).

Sample	Beta actin (ACTB)	Glyceraldehyde -3-phosphate dehydrogenase (GAPDH)	Beta-2 microglobulin (B2M)	Phospholipase A2 (YWHAZ)	CD68
WT 3	1	1	1	1	1
WT 9	ND	ND	0.08	0.13	0.11
WT 15	1.41	0.62	0.70	0.62	0.88
WT 21	1.29	0.65	0.36	0.32	0.22
KO 14	0.77	0.27	0.23	0.40	2.51
KO24	ND	ND	0.76	2.40	1.84

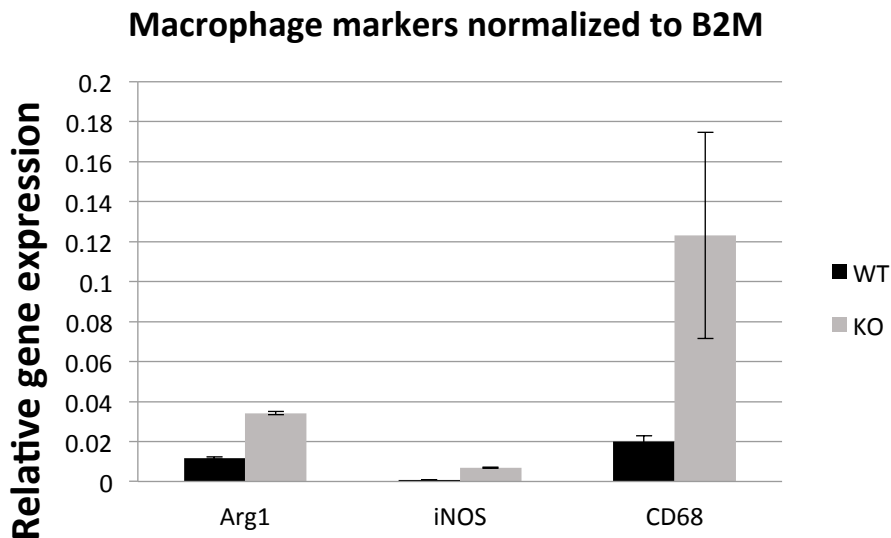


Figure 4.23: Preliminary results from qPCR of target genes: Arginase 1 (Arg1), iNOS and CD68. Gene expression was normalized to Beta-2 microglobulin (B2M). Wild-type (WT): n=4; MR-KO: n=2.

Chapter 5

Discussion

In the present study we used a mannose receptor knockout mouse model [127] to study the role of the mannose receptor in polarization of TAMs and tumor development in experimental B16F1 skin melanoma. The key question raised was whether the mannose receptor is necessary for M2 polarization of TAMs, and thus is likely to also influence tumor development, or just a marker for M2 polarized macrophages.

The data presented suggest that the mannose receptor may be involved in early stages of melanoma growth, as mice deficient in this receptor showed a delayed tumor take, with a 1.6-1.7 day difference in mean values, and a 1-1.5 day difference in median values, in two independent experiments. This difference was borderline significant in the first experiment (Mann Whitney U test, $p=0.051$) and not statistically significant in the latter ($p=0.14$) due to large variations between animals. However, as a delay in mean and median tumor take was noted in two different experiments it may point to a trend. When the tumors became visible, they grew in the similar rate in both animal groups.

The reason for the delay in tumor take seen in MR-KOs is unknown, but differences in T-cell immunity may be involved. *Dan, J.M., et al.*, reported that this mouse strain has a decreased number of T cells [139], and in the same study it was suggested that the mannose receptor on dendritic cells have a non-redundant role in priming of specific CD4⁺ T-cell responses in vivo. Naïve T cells will differentiate in response to an antigen-presenting cell, and become activated. *Lee, S.J., et al.* on the other hand reported that there were no difference in the number or the type of inflammatory cells at the site of inflammation in candida infections in MR-KO and wild-type control mice [140]. Except from reduced plasma clearance of glycoproteins with high-mannose and N-acetylglucosamine residues, and collagen alpha chains [44, 104, 127], the MR-KO mouse strain is healthy and the mice do not show behavioural of physical abnormalities [141].

The production of subsets of mannose-bearing serum glycoproteins, are under normal circumstances up-regulated during inflammation. As the clearance of these substances is impaired in the MR-KO mice strain, serum levels of these proteins are elevated during inflammation [142]. One may speculate whether the delay in the day of visible tumor seen in MR-KO mice may be related to the clearance function of MR, by macrophages and dendritic cells in tumors. Inoculation of tumor cells produces an acute inflammation, which in its earliest stage is dominated by M1 activated macrophages [17]. M1 macrophages secrete inflammatory mediators and subsequently maintains the acute inflammatory response [17]. This acute phase will gradually have a shift towards a healing phase, with a corresponding

shift from M1 to M2 polarization of macrophages. Tumors resemble “wounds that never heals”, and many of the processes that are active during wound healing are also active during tumor progression. MR-KO mice have been shown to have defective plasma clearance of glycoprotein with mannose and N-acetylglucosamine residues [44, 127] and therefore have elevated levels of several glycoproteins, including lysosomal enzymes, C-terminal procollagen propeptides, and the acute phase protein alpha-fetuin. An impaired clearance of glycoproteins up-regulated during inflammation, by liver sinusoidal endothelial cells (in the general circulation) and by macrophages and dendritic cells (in tumor) might result in increased levels of these substances, and a prolonged or more pronounced acute inflammation, which may delay the start of the tumor growth. However, this has to be further explored.

The B16F1 melanoma tumor model is a well established model in cancer research, and the tumor morphology in the present experiments corresponded to the morphology described earlier [131]. The tumor shows a rapid growth, and is regarded as an aggressive tumor type [143].

Necrosis is a feature associated with the aggressiveness of the tumors, together with formation of blood vessels. In melanomas, tumor necrosis is associated with tumor progression [143]. In the present project, blood vessels and necrotic tissue in tumors were quantified on tissue sections using a stereological approach. Stereology is a method where data is gathered effectively and efficiently, and produces results that are unbiased [134].

Tumor necrosis, measured as area in % of total area covered by the tumor on tissue sections was only observed in medium sized and large sized melanomas, and was similar in wild-type animals and MR-KO, and in medium sized or large sized melanomas.

The relative amount of blood vessels was also quite similar in wild-type and MR-KO tumors, and did not differ between medium sized and large tumors. The tumor vasculature is distinct from normal vasculature, as it lacks hierarchical organization, and it is clearly disorganized and tortuous [144] These characteristics were also noted in the melanomas analysed in the present study, in both animal groups.

The B16F1 melanoma is a fast growing tumor model, and it is known that the growth of these tumors is largely dependent on the expression and secretion of VEGFs by the cancer cells [145]. This mechanism is crucial for inducing tumor angiogenesis, and it is known that a rapid - growing tumor is more susceptible for necrosis, than a slow – growing tumor [145]. The relative areas covered by necrosis in the different tumors varied from almost zero to almost 70%. Also blood vessel formation differed. The differences seen in necrosis and blood vessel formation between individual tumors, may be related to tumor heterogeneity [146].

Even though all inoculated B16F1 cells have the same origin, each tumor formation is a single event. Functional heterogeneity may arise among cancer cells within the same tumor, and consequently the tumor’s ability to induce angiogenesis might be different.

To answer the question about macrophage polarization in B16F1 melanomas, IHC screening of macrophage marker expressed in tissue sections from small (1-2 mm), medium sized (3-5 mm) and large (>8 mm) tumors were carried out. Included in the study were markers for M1 and M2 macrophages and markers expressed by most macrophages – so called pan macrophage markers. A titration study prior to the screening showed that the markers chosen were expressed by large mononuclear cells, resembling macrophages.

Due to macrophage plasticity and heterogeneity, the choice of a pan macrophage marker was important. CD68 and F4/80 are commonly used as such macrophage markers as they are expressed by most tissue macrophages [147-149]. *Khazen, W., et al.* found that CD68 antibodies may also bind fibroblast-like cells (adipoblasts), preadipocytes and adipocytes [147]. In the present study, the F4/80 antibody tested showed a strict specificity for mononuclear, macrophage-like cells in the melanoma tissue sections, as well as for Kupffer cells in mouse liver slides, and the specificity of this antibody for monocytes and tissue macrophages has also been reported by others [147]. As the CD68 antibody did not function on paraffin sections, the choice fell on F4/80 as a pan macrophage marker.

Using this marker we found that macrophage infiltration was high already in the small sized tumors. The smallest tumor in the study (figure 4.11, A-B) was barely visible to the naked eye, but compared to the tumor size, there was a rather high infiltration of macrophages. Mannose receptor labelling of parallel sections from wild-type mice revealed that some cells inside the small tumors already expressed this receptor. The majority of the mannose receptor positive cells were, however, seen in the connective tissue adjacent to the tumor tissue proper. Although we cannot distinguish mannose receptor expressing macrophages from dendritic cells that may also express this receptor, without double-labeling with a dendritic cell marker, these results indicate that M2 polarized macrophages are present already at this early stage of tumor progression, and that the shift towards an M2 polarization starts early.

In all tumor size groups, macrophages were found in all parts of the tumor; including central and peripheral parts of the tumor tissue proper and in the adjacent connective tissue. The latter is where the majority of macrophages were located. The accumulation of TAMs in this area might be related to the TAMs secretion of ECM- degrading enzymes e.g. MMPs, proteases and other proteolytic enzymes (Chapter 3, paragraph 1.2.2), as it enables the fast growing tumor to invade locally [75].

The amount of macrophage infiltration in melanomas are reported to be as high as 30-50 %, and macrophage density is reported to increase as the tumor grows (reviewed in [150]). These reports are consistent with our findings. Staining of slides from the medium sized and large sized tumor groups showed that as the tumors grew, the amount of infiltrating macrophages increased, as well as the proportion of macrophages expressing M2 markers (mannose receptor and arginase I). The macrophage population was clearly dominated by

M2 polarized macrophages in medium sized and large sized tumors, whereas iNOS positive cells (M1 macrophages) were scarce in these tumors.

Screening for iNOS expression in medium sized and large B16F1 melanoma showed low amounts of positive cells inside the tumors, with almost similar results observed in wild-type and MR-KO animals, suggesting that M1 macrophages are hardly found in central parts of B16F1 melanomas at these stages of tumor development. In the connective tissue, iNOS positive cells were still present, but in a lower amount than arginase I positive cells. Furthermore, macrophages with a high expression of iNOS were located further away from the tumor, than the arginase-positive M2 polarized cells.

As opposed to iNOS, arginase I positive macrophages were abundant in the central parts of medium sized and large tumors, with the highest amount observed in the latter. As mentioned in the introduction, arginase I catalyse the reaction of arginine and water to ornithine and urea. Ornithine is further used to produce polyamines, glutamate and proline. The latter is critical for the regulation of wound healing through synthesis of collagen [151], and polyamines are essential for cell growth and therefore supports tumor growth and invasion (reviewed in [152]). In addition arginase 1 is important for the down regulation of inflammation (by preventing formation of NO from arginine through iNOS), and contributes to the resolution of inflammation by inhibiting CD4⁺ T [153].

Stabilin 1 is a scavenger receptor, which among other ligands, binds receptor for secreted protein acidic and rich in cysteine (SPARC), a matricellular protein, which is a soluble non-structural component of the ECM. SPARC plays a role in tissue remodelling, angiogenesis and wound healing [142]. M2 polarized cells in skin were recently shown to express stabilin-1, where the receptor is involved in the clearance of “unwanted selfs” and therefor has a role in the maintenance of tissue homeostasis [142]. Only a few studies have been done on the role of stabilin-1 in TAMs and cancer progression. A recent study in mouse glioblastoma showed that in early tumor progression there was an up-regulation of stabilin-1 expression in TAMs, but as the tumors grew stabilin-1 expression decreased [40]. The finding of low expression of stabilin-1 in murine TAMs is consistent with our results, where stabilin-1 positive cells were found almost exclusively in the connective tissue around the tumor, and the staining intensity of these cells was weak, compared to the positive control (liver sinusoidal endothelium on liver slides).

In this study we further wanted to investigate mRNA expression by qPCR of macrophage markers in medium sized tumors to compare the expression pattern on transcriptomic and proteomic levels. The macrophage markers that were chosen for this purpose was iNOS, and Arginase, with CD68 as pan macrophage marker. Due to limited time, the qPCR study was not finished, and only one test round was conducted. The expression of reference genes diverged too much among samples, and this issue has to be solved before further analyses can be done of macrophage marker expression in the melanomas. There may be many reasons for the varying reference gene expression. It can be due to low amount of DNA in

the reaction. It may also be that the ready-made primers were not well designed. Even though we used the recommended settings from the provider, the qPCR settings need to be re-evaluated. Furthermore, tissue heterogeneity may be a problem. The tissue analysed is a heterogeneous tissue, which can be a challenge when doing qPCR, due to the presence of many different cell types. Although conclusions cannot be drawn from a few samples and one test round, the preliminary results showed the same pattern of iNOS and arginase I expression in the tumor biopsies tested as in the IHC study, with a lower expression of iNOS than of arginase. The results need to be repeated with more biological replicas, several different primer sets and optimized reference genes.

To sum up, our study showed heavy infiltration of macrophages in B16F1 melanomas. The majority of TAMs in B16F1 melanomas sized 3-5 mm in diameter or more, had an M2 polarization, based on their expression of the mannose receptor (in wild-type) and arginase I (in both wild-type and MR-KO mice). M2 polarized TAMs, evidenced by mannose receptor positive mononuclear macrophage-like cells, are found already in small (1-2 mm) tumors, suggesting an early shift in macrophage polarization from M1 to M2 in B16F1 melanomas.

Macrophage infiltration is described as a double-edge sword in tumor biology, as they can both promote and inhibit tumor progression [154]. The microenvironment is created by the tumor, which manipulates the normal plasticity of the macrophages as they exploits the physiological functions of wound healing, to serve the tumors best interest [68]. The divergent expression of arginase I and iNOS has contributed to the dichotomous nomenclature of macrophages [154], and TAMs are often referred to exhibit two opposing phenotypes, M1 or M2, however it is important to keep in mind that macrophages are highly plastic cells and they can display a spectrum of phenotypes (Chapter 1, section 1.2).

Even though TAMs made up a significant portion of the tumor associated leukocytes, other inflammatory cells, in particular small mononuclear cells, resembling lymphocytes, were present in the tumor stroma and connective tissue. T cells are known to be present in melanomas [68] and staining with a T-cell marker such as CD3, and eventual markers for subsets of T-cells, such as T regulatory cells, should be included in further investigations. As the mannose receptor is also expressed in dendritic cells, further immunohistochemical screening with a marker for dendritic cells should be conducted.

Screening of small tumors for iNOS and arginase expression by IHC should also be conducted in order to get a better picture of the activation status of macrophages in this tumor size group. The smallest tumors were in the borderline of what was possible to use for IHC, as the tumors were barely visible and therefore challenging to cut. Transmission electron microscopy is a method that allows smaller tissue samples to be studied. Ultrathin sections can be cut of snap frozen and low-vicryl embedded tissue by ultramicrotomes, and labelled for both light and electron microscopy, which allow for more thorough studies of leukocyte infiltrates and inflammation in early tumors

Conclusion and further aspects

The aim for this study was to investigate the mannose receptor's role in polarization of tumor-associated macrophages (TAMs) and in tumor development. This was done by comparing tumor growth, leukocyte infiltration and activation status of TAMs in B16F1 primary melanomas from mice lacking mannose receptor expression (MR-KO mice) and in wild-type mice of the same mouse strain (C57BL/6).

The study was divided into the following sub-projects:

- Is there a difference in rate of tumor growth between MR-KO mice and wild-type mice?

Main result:

There was a 1.6-1.7 days delay in the mean day of first visible tumor (tumor take) in MR-KO mice compared to wild-tumor control mice. This difference was borderline significant in experiment 1 and not statistically significant in experiment 2 due to large variation between animals, but may still be seen as a trend as the same finding was observed in two independent experiments. The reason for this difference in the initial phase of tumor growth is not known. When tumors were visible in the skin, they grew at the same rate in both animal groups. Our data therefore suggest that the mannose receptor may be involved in the early stage of tumor growth; but does not have a major role in regulating the further tumor growth of B16F1 skin melanoma.

- Is there a difference in the histological appearance of tumor tissue in MR-KO mice compared to wild-type mice?

Main result:

There was no difference in the histological appearance of tumor tissue in the three tumor size groups examined from MR-KO mice and WT control mice. Blood vessels started to appear in the small tumors, but necrosis was not observed at this stage. There was no significant difference in necrotic area or blood vessels in tissue sections from melanomas in MR-KO mice and wild-type mice.

- Is there a difference in the amount of leukocyte infiltration in MR-KO tumors, compared to wild-type tumors?

Main result:

There was no difference in the amount of macrophage infiltration in tumors in MR-KOs, compared to wild-type controls. Macrophages and other mononuclear cells dominated in the infiltrates. However, eventual differences in numbers of T-cells, or dendritic cells were not examined. The relative amount of leukocyte infiltrate in tumors corresponded to the tumor size. The larger the tumor, the larger the amount of infiltrating leukocytes, this was also observed in tumor associated connective tissue.

- Activation status of TAMs, when do the switch from M1 to M2 occur?

Main result:

Macrophages were abundant in the tumor tissue proper, and in tumor associated connective tissue both in small, medium sized and large melanomas. In the small tumors some of the TAMs already expressed the mannose receptor, indicating that that shift from M1 polarization to an M2 polarization is likely to start earlier, before the tumor become visible in the skin.

Main conclusion:

The shift in macrophage polarization occurs very early in the tumor development. Since polarization of macrophages towards M2 happened in both MR-KO and wild-type mice it is likely that the MR is not a driver for polarization. However, it may have a role in early tumor development.

Future aspects:

- Immunohistochemical analyses of the small, 1-2 mm tumors are underway. Especially screening for iNOS and Arginase I expression will be of interest to get a clearer picture of the activation status of macrophages at this stage in both MR-KO and control mice.
- To get a deeper understanding of the ongoing inflammation in the B16F1 melanomas, screening for additional macrophage markers, T cell markers, including T-cell subsets, and dendritic cells markers would be interesting.
- Double immune labelling with M1 and M2 markers may give a better picture of how TAMs are modulated by the melanomas.
- The qRT-PCR analyses should be replicated with a larger number of biological samples.

- It may be interesting to test the role of MR in the development of a more slowly growing tumor model, as the aggressiveness of the B16F1 melanoma model may have obscured finer details.

Bibliography

1. Gordon, S., *Elie Metchnikoff: father of natural immunity*. Eur J Immunol, 2008. **38**(12): p. 3257-64.
2. Tan, S.Y. and M.K. Dee, *Elie Metchnikoff (1845-1916): discoverer of phagocytosis*. Singapore Med J, 2009. **50**(5): p. 456-7.
3. Young, B., et al., *Wheater's Functional Histology: A text and colour Atlas*. fifth ed. 2006, USA: Elsevier.
4. Davies, L.C., et al., *Tissue-resident macrophages*. Nat Immunol, 2013. **14**(10): p. 986-95.
5. Naito, M., et al., *Differentiation and function of Kupffer cells*. Med Electron Microsc, 2004. **37**(1): p. 16-28.
6. Theurl, M., et al., *Kupffer cells modulate iron homeostasis in mice via regulation of hepcidin expression*. J Mol Med (Berl), 2008. **86**(7): p. 825-35.
7. Bowden, D.H., *The alveolar macrophage*. Environ Health Perspect, 1984. **55**: p. 327-41.
8. Miyamoto, T. and T. Suda, *Differentiation and function of osteoclasts*. Keio J Med, 2003. **52**(1): p. 1-7.
9. Verschoor, C.P., A. Puchta, and D.M. Bowdish, *The macrophage*. Methods Mol Biol, 2012. **844**: p. 139-56.
10. Mosser, D.M. and J.P. Edwards, *Exploring the full spectrum of macrophage activation*. Nat Rev Immunol, 2008. **8**(12): p. 958-69.
11. Murray, P.J. and T.A. Wynn, *Protective and pathogenic functions of macrophage subsets*. Nat Rev Immunol, 2011. **11**(11): p. 723-37.
12. Sica, A. and A. Mantovani, *Macrophage plasticity and polarization: in vivo veritas*. J Clin Invest, 2012. **122**(3): p. 787-95.
13. Parham, P., *The Immune System*. 7th ed. 2009, United States of America: Garland Science, Taylor & Francis Group, LLC.
14. Nathan, C., *Mechanisms and modulation of macrophage activation*. Behring Inst Mitt, 1991(88): p. 200-7.
15. Shi, Y., J.E. Evans, and K.L. Rock, *Molecular identification of a danger signal that alerts the immune system to dying cells*. Nature, 2003. **425**(6957): p. 516-21.
16. Mantovani, A., et al., *Macrophage polarization: tumor-associated macrophages as a paradigm for polarized M2 mononuclear phagocytes*. Trends Immunol, 2002. **23**(11): p. 549-55.
17. Edwards, J.P., et al., *Biochemical and functional characterization of three activated macrophage populations*. J Leukoc Biol, 2006. **80**(6): p. 1298-307.
18. Zhang, X. and D.M. Mosser, *Macrophage activation by endogenous danger signals*. J Pathol, 2008. **214**(2): p. 161-78.
19. Tayal, V. and B.S. Kalra, *Cytokines and anti-cytokines as therapeutics--an update*. Eur J Pharmacol, 2008. **579**(1-3): p. 1-12.
20. Hirano, T., et al., *Complementary DNA for a novel human interleukin (BSF-2) that induces B lymphocytes to produce immunoglobulin*. Nature, 1986. **324**(6092): p. 73-6.
21. LeMay, L.G., A.J. Vander, and M.J. Kluger, *Role of interleukin 6 in fever in rats*. Am J Physiol, 1990. **258**(3 Pt 2): p. R798-803.
22. Nakahara, H., et al., *Anti-interleukin-6 receptor antibody therapy reduces vascular endothelial growth factor production in rheumatoid arthritis*. Arthritis Rheum, 2003. **48**(6): p. 1521-9.
23. Hamza, T., J.B. Barnett, and B. Li, *Interleukin 12 a key immunoregulatory cytokine in infection applications*. Int J Mol Sci, 2010. **11**(3): p. 789-806.
24. Reference, G.H., *IL-16*. U.S National Library of Medicine, 2013.

25. *IL-1R1 Interleukin 1 receptor, type I*. 2013, Pubmed: National Center for Biotechnology Information.
26. *IL8 Interleukin 8*. 2013, National Center for biotechnology Information: Pubmed.
27. *Chemokine (C-X-C Motif) Ligand 9*. 2013: www.genecards.org.
28. *CCL2 chemokine (C-C motif) ligand 2*, in Pubmed. 2013, National Center for biotechnology Information.
29. *CCL3 chemokine (C-C motif) ligand 3*. 2013, National Center for biotechnology Information

Pubmed

30. *CCL4 chemokine (C-C motif) ligand*. 2013, National Center for biotechnology Information: Pubmed.
31. *CCL5 chemokine (C-C motif) ligand 5*. 2013, National Center for biotechnology Information

Pubmed.

32. Lechner, M., P. Lirk, and J. Rieder, *Inducible nitric oxide synthase (iNOS) in tumor biology: the two sides of the same coin*. *Semin Cancer Biol*, 2005. **15**(4): p. 277-89.
33. Gordon, S. and F.O. Martinez, *Alternative activation of macrophages: mechanism and functions*. *Immunity*, 2010. **32**(5): p. 593-604.
34. Mantovani, A., et al., *The chemokine system in diverse forms of macrophage activation and polarization*. *Trends Immunol*, 2004. **25**(12): p. 677-86.
35. Biswas, S.K., et al., *A distinct and unique transcriptional program expressed by tumor-associated macrophages (defective NF-kappaB and enhanced IRF-3/STAT1 activation)*. *Blood*, 2006. **107**(5): p. 2112-22.
36. Roberts, A.B., et al., *Transforming growth factor type beta: rapid induction of fibrosis and angiogenesis in vivo and stimulation of collagen formation in vitro*. *Proc Natl Acad Sci U S A*, 1986. **83**(12): p. 4167-71.
37. Tonnesen, M.G., X. Feng, and R.A. Clark, *Angiogenesis in wound healing*. *J Investig Dermatol Symp Proc*, 2000. **5**(1): p. 40-6.
38. Noel, W., et al., *Alternatively activated macrophages during parasite infections*. *Trends Parasitol*, 2004. **20**(3): p. 126-33.
39. Martinez, F.O., et al., *Transcriptional profiling of the human monocyte-to-macrophage differentiation and polarization: new molecules and patterns of gene expression*. *J Immunol*, 2006. **177**(10): p. 7303-11.
40. David, C., et al., *Stabilin-1 expression in tumor associated macrophages*. *Brain Res*, 2012. **1481**: p. 71-8.
41. Matsumoto, A., et al., *Human macrophage scavenger receptors: primary structure, expression, and localization in atherosclerotic lesions*. *Proc Natl Acad Sci U S A*, 1990. **87**(23): p. 9133-7.
42. Navarre, W.W. and O. Schneewind, *Surface proteins of gram-positive bacteria and mechanisms of their targeting to the cell wall envelope*. *Microbiol Mol Biol Rev*, 1999. **63**(1): p. 174-229.
43. Sica, A., et al., *Autocrine production of IL-10 mediates defective IL-12 production and NF-kappa B activation in tumor-associated macrophages*. *J Immunol*, 2000. **164**(2): p. 762-7.
44. Elvevold, K., et al., *Liver sinusoidal endothelial cells depend on mannose receptor-mediated recruitment of lysosomal enzymes for normal degradation capacity*. *Hepatology*, 2008. **48**(6): p. 2007-15.
45. Sorensen, K.K., et al., *The scavenger endothelial cell: a new player in homeostasis and immunity*. *Am J Physiol Regul Integr Comp Physiol*, 2012. **303**(12): p. R1217-30.
46. McGreal, E.P., L. Martinez-Pomares, and S. Gordon, *Divergent roles for C-type lectins expressed by cells of the innate immune system*. *Mol Immunol*, 2004. **41**(11): p. 1109-21.
47. Mills, C.D., *Macrophage arginine metabolism to ornithine/urea or nitric oxide/citrulline: a life or death issue*. *Crit Rev Immunol*, 2001. **21**(5): p. 399-425.

48. *IL10 Interleukin 10*. 2013, National Center for Biotechnological Information: Pubmed.
49. *IL1RN interleukin 1 receptor antagonist*. 2013, National Center for Biotechnology Information: Pubmed.
50. *IL1R2 Interlukin 1, type II*. 2013, National Center for Biotechnology Information: Pubmed.
51. *CCL16 chemokine (C-C-motif) ligand 16*. 2013, National Center for Biotechnology Information: Pubmed.
52. *CCL18 Chemokine (C-C motif) ligand 18*. 2013, National Center for Biotechnology Information: Pubmed.
53. *CCL17 chemokine (C-C motif) ligand 17*. 2013, National Center for Biotechnology Information: Pubmed.
54. *CCL22 chemokine (C-C motif) ligand 22*. 2013, National Center for Biotechnology Information: Pubmed.
55. *CCR2 chemokine (C-C motif) receptor 2*. 2013, National Center for Biotechnology Information: Pubmed.
56. *CXCR1 Chemokine (C-X-C motif) receptor 1*. 2013, National Center for Biotechnology Information: Pubmed.
57. *CXCR2 Chemokine (C-X-C motif) receptor 2*. 2013, National Center for Biotechnology Information: Pubmed.
58. Nathan, C. and A. Ding, *Nonresolving inflammation*. Cell, 2010. **140**(6): p. 871-82.
59. Colotta, F., et al., *Cancer-related inflammation, the seventh hallmark of cancer: links to genetic instability*. Carcinogenesis, 2009. **30**(7): p. 1073-81.
60. Andersson, U. and K.J. Tracey, *HMGB1 is a therapeutic target for sterile inflammation and infection*. Annu Rev Immunol, 2011. **29**: p. 139-62.
61. Martin, P. and S.J. Leibovich, *Inflammatory cells during wound repair: the good, the bad and the ugly*. Trends Cell Biol, 2005. **15**(11): p. 599-607.
62. Huynh, M.L., V.A. Fadok, and P.M. Henson, *Phosphatidylserine-dependent ingestion of apoptotic cells promotes TGF-beta1 secretion and the resolution of inflammation*. J Clin Invest, 2002. **109**(1): p. 41-50.
63. Mege, J.L., et al., *The two faces of interleukin 10 in human infectious diseases*. Lancet Infect Dis, 2006. **6**(9): p. 557-69.
64. Sindrilaru, A., et al., *An unrestrained proinflammatory M1 macrophage population induced by iron impairs wound healing in humans and mice*. J Clin Invest, 2011. **121**(3): p. 985-97.
65. Laskin, D.L., *Macrophages and inflammatory mediators in chemical toxicity: a battle of forces*. Chem Res Toxicol, 2009. **22**(8): p. 1376-85.
66. Mantovani, A., A. Sica, and M. Locati, *New vistas on macrophage differentiation and activation*. Eur J Immunol, 2007. **37**(1): p. 14-6.
67. Balkwill, F., K.A. Charles, and A. Mantovani, *Smoldering and polarized inflammation in the initiation and promotion of malignant disease*. Cancer Cell, 2005. **7**(3): p. 211-7.
68. Weinberg Robert A., *The biology of Cancer*. 2007, United States of America: Garland science, Taylor & Francis Group, LLC.
69. Solinas, G., et al., *Tumor-associated macrophages (TAM) as major players of the cancer-related inflammation*. J Leukoc Biol, 2009. **86**(5): p. 1065-73.
70. Negus, R.P., et al., *The detection and localization of monocyte chemoattractant protein-1 (MCP-1) in human ovarian cancer*. J Clin Invest, 1995. **95**(5): p. 2391-6.
71. Leek, R.D., et al., *Association of macrophage infiltration with angiogenesis and prognosis in invasive breast carcinoma*. Cancer Res, 1996. **56**(20): p. 4625-9.
72. Lewis, C.E. and J.W. Pollard, *Distinct role of macrophages in different tumor microenvironments*. Cancer Res, 2006. **66**(2): p. 605-12.
73. Katakai, A., et al., *Tumor infiltrating lymphocytes and macrophages have a potential dual role in lung cancer by supporting both host-defense and tumor progression*. J Lab Clin Med, 2002. **140**(5): p. 320-8.

74. Deng, J., et al., *Critical role of CD81 in cognate T-B cell interactions leading to Th2 responses*. Int Immunol, 2002. **14**(5): p. 513-23.
75. Alberts, B., et al., *Molecular biology of the cell*. Fifth ed. Garland Science, Taylor & Francis Group, 2008. 751-755, 784, 791-792,.
76. Biswas, S.K. and C.E. Lewis, *NF-kappaB as a central regulator of macrophage function in tumors*. J Leukoc Biol, 2010. **88**(5): p. 877-84.
77. Vallabhapurapu, S. and M. Karin, *Regulation and function of NF-kappaB transcription factors in the immune system*. Annu Rev Immunol, 2009. **27**: p. 693-733.
78. Bonizzi, G. and M. Karin, *The two NF-kappaB activation pathways and their role in innate and adaptive immunity*. Trends Immunol, 2004. **25**(6): p. 280-8.
79. Sacconi, A., et al., *p50 nuclear factor-kappaB overexpression in tumor-associated macrophages inhibits M1 inflammatory responses and antitumor resistance*. Cancer Res, 2006. **66**(23): p. 11432-40.
80. Thomas, B., et al., *Critical role of C/EBPdelta and C/EBPbeta factors in the stimulation of the cyclooxygenase-2 gene transcription by interleukin-1beta in articular chondrocytes*. Eur J Biochem, 2000. **267**(23): p. 6798-809.
81. Wadleigh, D.J., et al., *Transcriptional activation of the cyclooxygenase-2 gene in endotoxin-treated RAW 264.7 macrophages*. J Biol Chem, 2000. **275**(9): p. 6259-66.
82. Banerjee, A., et al., *Diverse Toll-like receptors utilize Tpl2 to activate extracellular signal-regulated kinase (ERK) in hemopoietic cells*. Proc Natl Acad Sci U S A, 2006. **103**(9): p. 3274-9.
83. Fong, C.H., et al., *An antiinflammatory role for IKKbeta through the inhibition of "classical" macrophage activation*. J Exp Med, 2008. **205**(6): p. 1269-76.
84. Hagemann, T., et al., *"Re-educating" tumor-associated macrophages by targeting NF-kappaB*. J Exp Med, 2008. **205**(6): p. 1261-8.
85. Hagemann, T., et al., *Regulation of macrophage function in tumors: the multifaceted role of NF-kappaB*. Blood, 2009. **113**(14): p. 3139-46.
86. Basseres, D.S. and A.S. Baldwin, *Nuclear factor-kappaB and inhibitor of kappaB kinase pathways in oncogenic initiation and progression*. Oncogene, 2006. **25**(51): p. 6817-30.
87. Bui, J.D. and R.D. Schreiber, *Cancer immunosurveillance, immunoediting and inflammation: independent or interdependent processes?* Curr Opin Immunol, 2007. **19**(2): p. 203-8.
88. Pollard, J.W., *Tumour-educated macrophages promote tumour progression and metastasis*. Nat Rev Cancer, 2004. **4**(1): p. 71-8.
89. Sica, A., P. Allavena, and A. Mantovani, *Cancer related inflammation: the macrophage connection*. Cancer Lett, 2008. **267**(2): p. 204-15.
90. Hanahan, D. and J. Folkman, *Patterns and emerging mechanisms of the angiogenic switch during tumorigenesis*. Cell, 1996. **86**(3): p. 353-64.
91. Egeblad, M. and Z. Werb, *New functions for the matrix metalloproteinases in cancer progression*. Nat Rev Cancer, 2002. **2**(3): p. 161-74.
92. Flavell, R.A., et al., *The polarization of immune cells in the tumour environment by TGFbeta*. Nat Rev Immunol, 2010. **10**(8): p. 554-67.
93. Weber, F., et al., *Transforming growth factor-beta1 immobilises dendritic cells within skin tumours and facilitates tumour escape from the immune system*. Cancer Immunol Immunother, 2005. **54**(9): p. 898-906.
94. Maeda, H. and A. Shiraishi, *TGF-beta contributes to the shift toward Th2-type responses through direct and IL-10-mediated pathways in tumor-bearing mice*. J Immunol, 1996. **156**(1): p. 73-8.
95. Thomas, D.A. and J. Massague, *TGF-beta directly targets cytotoxic T cell functions during tumor evasion of immune surveillance*. Cancer Cell, 2005. **8**(5): p. 369-80.
96. Matsuda, M., et al., *Interleukin 10 pretreatment protects target cells from tumor- and allo-specific cytotoxic T cells and downregulates HLA class I expression*. J Exp Med, 1994. **180**(6): p. 2371-6.

97. Qin, Z., et al., *Interleukin-10 prevents dendritic cell accumulation and vaccination with granulocyte-macrophage colony-stimulating factor gene-modified tumor cells*. J Immunol, 1997. **159**(2): p. 770-6.
98. Beissert, S., et al., *IL-10 inhibits tumor antigen presentation by epidermal antigen-presenting cells*. J Immunol, 1995. **154**(3): p. 1280-6.
99. Hull, M.A., et al., *Cyclooxygenase 2 is up-regulated and localized to macrophages in the intestine of Min mice*. Br J Cancer, 1999. **79**(9-10): p. 1399-405.
100. Bamba, H., et al., *High expression of cyclooxygenase-2 in macrophages of human colonic adenoma*. Int J Cancer, 1999. **83**(4): p. 470-5.
101. Nakanishi, Y., et al., *COX-2 inhibition alters the phenotype of tumor-associated macrophages from M2 to M1 in ApcMin/+ mouse polyyps*. Carcinogenesis, 2011. **32**(9): p. 1333-9.
102. Pontow, S.E., V. Kery, and P.D. Stahl, *Mannose receptor*. Int Rev Cytol, 1992. **137B**: p. 221-44.
103. Magnusson, S. and T. Berg, *Extremely rapid endocytosis mediated by the mannose receptor of sinusoidal endothelial rat liver cells*. Biochem J, 1989. **257**(3): p. 651-6.
104. Malovic, I., et al., *The mannose receptor on murine liver sinusoidal endothelial cells is the main denatured collagen clearance receptor*. Hepatology, 2007. **45**(6): p. 1454-61.
105. Avrameas, A., et al., *Expression of a mannose/fucose membrane lectin on human dendritic cells*. Eur J Immunol, 1996. **26**(2): p. 394-400.
106. Shepherd, V.L., B.I. Tarnowski, and B.J. McLaughlin, *Isolation and characterization of a mannose receptor from human pigment epithelium*. Invest Ophthalmol Vis Sci, 1991. **32**(6): p. 1779-84.
107. Irjala, H., et al., *Mannose receptor is a novel ligand for L-selectin and mediates lymphocyte binding to lymphatic endothelium*. J Exp Med, 2001. **194**(8): p. 1033-42.
108. Qian, H., et al., *Stabilins are expressed in bone marrow sinusoidal endothelial cells and mediate scavenging and cell adhesive functions*. Biochem Biophys Res Commun, 2009. **390**(3): p. 883-6.
109. Martinez-Pomares, L., et al., *Analysis of mannose receptor regulation by IL-4, IL-10, and proteolytic processing using novel monoclonal antibodies*. J Leukoc Biol, 2003. **73**(5): p. 604-13.
110. Schreiber, S., et al., *Regulation of mouse bone marrow macrophage mannose receptor expression and activation by prostaglandin E and IFN-gamma*. J Immunol, 1993. **151**(9): p. 4973-81.
111. Willment, J.A. and G.D. Brown, *C-type lectin receptors in antifungal immunity*. Trends Microbiol, 2008. **16**(1): p. 27-32.
112. Wileman, T.E., M.R. Lennartz, and P.D. Stahl, *Identification of the macrophage mannose receptor as a 175-kDa membrane protein*. Proc Natl Acad Sci U S A, 1986. **83**(8): p. 2501-5.
113. Fiete, D.J., M.C. Beranek, and J.U. Baenziger, *A cysteine-rich domain of the "mannose" receptor mediates GalNAc-4-SO₄ binding*. Proc Natl Acad Sci U S A, 1998. **95**(5): p. 2089-93.
114. East, L. and C.M. Isacke, *The mannose receptor family*. Biochim Biophys Acta, 2002. **1572**(2-3): p. 364-86.
115. Napper, C.E., K. Drickamer, and M.E. Taylor, *Collagen binding by the mannose receptor mediated through the fibronectin type II domain*. Biochem J, 2006. **395**(3): p. 579-86.
116. Mullin, N.P., K.T. Hall, and M.E. Taylor, *Characterization of ligand binding to a carbohydrate-recognition domain of the macrophage mannose receptor*. J Biol Chem, 1994. **269**(45): p. 28405-13.
117. Iobst, S.T. and K. Drickamer, *Binding of sugar ligands to Ca(2+)-dependent animal lectins. II. Generation of high-affinity galactose binding by site-directed mutagenesis*. J Biol Chem, 1994. **269**(22): p. 15512-9.
118. Schweizer, A., P.D. Stahl, and J. Rohrer, *A di-aromatic motif in the cytosolic tail of the mannose receptor mediates endosomal sorting*. J Biol Chem, 2000. **275**(38): p. 29694-700.
119. Llorca, O., *Extended and bent conformations of the mannose receptor family*. Cell Mol Life Sci, 2008. **65**(9): p. 1302-10.

120. Stahl, P.D. and R.A. Ezekowitz, *The mannose receptor is a pattern recognition receptor involved in host defense*. *Curr Opin Immunol*, 1998. **10**(1): p. 50-5.
121. Miller, J.L., et al., *The mannose receptor mediates dengue virus infection of macrophages*. *PLoS Pathog*, 2008. **4**(2): p. e17.
122. Stahl, P.D., *The macrophage mannose receptor: current status*. *Am J Respir Cell Mol Biol*, 1990. **2**(4): p. 317-8.
123. Ezekowitz, R.A., et al., *Molecular characterization of the human macrophage mannose receptor: demonstration of multiple carbohydrate recognition-like domains and phagocytosis of yeasts in Cos-1 cells*. *J Exp Med*, 1990. **172**(6): p. 1785-94.
124. Kahn, S., et al., *Trypanosoma cruzi amastigote adhesion to macrophages is facilitated by the mannose receptor*. *J Exp Med*, 1995. **182**(5): p. 1243-58.
125. Schlesinger, L.S., *Macrophage phagocytosis of virulent but not attenuated strains of Mycobacterium tuberculosis is mediated by mannose receptors in addition to complement receptors*. *J Immunol*, 1993. **150**(7): p. 2920-30.
126. Smedsrod, B., *Receptor-mediated endocytosis of connective tissue macromolecules in liver endothelial cells*. *Scand J Clin Lab Invest Suppl*, 1990. **202**: p. 148-51.
127. Lee, S.J., et al., *Mannose receptor-mediated regulation of serum glycoprotein homeostasis*. *Science*, 2002. **295**(5561): p. 1898-901.
128. Zacks, M.A. and N. Garg, *Recent developments in the molecular, biochemical and functional characterization of GPI8 and the GPI-anchoring mechanism [review]*. *Mol Membr Biol*, 2006. **23**(3): p. 209-25.
129. Dangaj, D., et al., *Mannose receptor (MR) engagement by mesothelin GPI anchor polarizes tumor-associated macrophages and is blocked by anti-MR human recombinant antibody*. *PLoS One*, 2011. **6**(12): p. e28386.
130. Green, E.L., *Handbook on genetically standardized JAX mice*. First ed, ed. J.M. Laboratory. 1968, Bar Harbor Maine: Bar Harbor Times Publishing Company.
131. Wosko, T.J., D.T. Ferrara, and L.S. Sartori, *Histological comparison of the B16 melanoma and its F1 variant*. *Cancer Lett*, 1984. **24**(1): p. 57-63.
132. Gage, G.J., D.R. Kipke, and W. Shain, *Whole animal perfusion fixation for rodents*. *J Vis Exp*, 2012(65).
133. Schneider, C.A., W.S. Rasband, and K.W. Eliceiri, *NIH Image to ImageJ: 25 years of image analysis*. *Nat Methods*, 2012. **9**(7): p. 671-5.
134. Mayhew, T.M., *The new stereological methods for interpreting functional morphology from slices of cells and organs*. *Exp Physiol*, 1991. **76**(5): p. 639-65.
135. Polak J.M and Noorden S.Van, *Introduction to immunocytochemistry*. Third ed. 2003, UK: BIOS Scientific Publishers Ltd.
136. Corporation, I., *Datasheet: HistoMouse™- Plus kit 2013*: p. 4.
137. Roche, *MagNA Lyser Green Beads*. Datasheet.
138. Lau, S.K., P.G. Chu, and L.M. Weiss, *CD163: a specific marker of macrophages in paraffin-embedded tissue samples*. *Am J Clin Pathol*, 2004. **122**(5): p. 794-801.
139. Dan, J.M., et al., *Role of the mannose receptor in a murine model of Cryptococcus neoformans infection*. *Infect Immun*, 2008. **76**(6): p. 2362-7.
140. Lee, S.J., et al., *Normal host defense during systemic candidiasis in mannose receptor-deficient mice*. *Infect Immun*, 2003. **71**(1): p. 437-45.
141. *B6.129P2-Mrc1^{tm1Mnz}/J*. 2014, The Jackson Laboratory, JAX Mice database.
142. Kzhyshkowska, J., et al., *Novel function of alternatively activated macrophages: stabilin-1-mediated clearance of SPARC*. *J Immunol*, 2006. **176**(10): p. 5825-32.
143. Bachmann, I.M., et al., *Tumor necrosis is associated with increased alphavbeta3 integrin expression and poor prognosis in nodular cutaneous melanomas*. *BMC Cancer*, 2008. **8**: p. 362.

144. Siemann, D.W., *The unique characteristics of tumor vasculature and preclinical evidence for its selective disruption by Tumor-Vascular Disrupting Agents*. *Cancer Treat Rev*, 2011. **37**(1): p. 63-74.
145. Prewett, M., et al., *Antivascular endothelial growth factor receptor (fetal liver kinase 1) monoclonal antibody inhibits tumor angiogenesis and growth of several mouse and human tumors*. *Cancer Res*, 1999. **59**(20): p. 5209-18.
146. Meacham, C.E. and S.J. Morrison, *Tumor heterogeneity and cancer cell plasticity*. *Nature* 2013. **501**(7467): p. 328-337.
147. Khazen, W., et al., *Expression of macrophage-selective markers in human and rodent adipocytes*. *FEBS Lett*, 2005. **579**(25): p. 5631-4.
148. Hirsch, S., J.M. Austyn, and S. Gordon, *Expression of the macrophage-specific antigen F4/80 during differentiation of mouse bone marrow cells in culture*. *J Exp Med*, 1981. **154**(3): p. 713-25.
149. Austyn, J.M. and S. Gordon, *F4/80, a monoclonal antibody directed specifically against the mouse macrophage*. *Eur J Immunol*, 1981. **11**(10): p. 805-15.
150. Hussein, M.R., *Tumour-associated macrophages and melanoma tumorigenesis: integrating the complexity*. *Int J Exp Pathol*, 2006. **87**(3): p. 163-76.
151. Morris, S.M., Jr., *Arginine metabolism: boundaries of our knowledge*. *J Nutr*, 2007. **137**(6 Suppl 2): p. 1602S-1609S.
152. Soda, K., *The mechanisms by which polyamines accelerate tumor spread*. *J Exp Clin Cancer Res*, 2011. **30**: p. 95.
153. Pesce, J.T., et al., *Arginase-1-expressing macrophages suppress Th2 cytokine-driven inflammation and fibrosis*. *PLoS Pathog*, 2009. **5**(4): p. e1000371.
154. Mantovani, A. and A. Sica, *Macrophages, innate immunity and cancer: balance, tolerance, and diversity*. *Curr Opin Immunol*, 2010. **22**(2): p. 231-7.

Appendix A

Materials

A.1 Kits

Table A.1: Kits used in the experiments.

Name	Manufacturer	Cat. No
Histomouse-PLUS broad spectrum AEC	Life technologies Invitrogen	859541
DNeasy Blood & Tissue Kit	Qiagen	69504
Allprotect Tissue Reagent	Qiagen	76405
RNeasy Mini Kit	Qiagen	74104
RNeasy Fibrous Tissue Mini Kit	Qiagen	74704
QuantiTect Reverse Transcription Kit	Qiagen	205310
Primer design 6 reference gene kit	Primerdesign.ltd	gePLUS-SY-6
Primer design primer kit	Primerdesign.ltd	SY-mo-600

A.2 Primers

Table A.2: Primers used in genotyping and gene expression analysis by qPCR

Primer name	Forward primer	Reverse primer
Primer used for genotyping		
Mrc1	GACCTTGGACTGAGCAAAGGGG	GACATGATGTCCTCAGGAGGACG
Primers used for gene expression analysis, qPCR		
CD68	TGACACCTACAGCCACAGAA	GCAGGGTTATGAGTGACAGTT
Nos2	CACCTACTTCCTGGACATTACG	TACTCTGAGGGCTGACAA
Arg1	ATTCTCCATGACTGAAGTAGACAA	CGACATCAAAGCTCAGGTGAA

A.3 Antibodies

Table A.3: Primary and secondary antibodies

	Antibody	Manufacturer	Cat. no	Dilution
Primary antibodies	Goat anti-human mannose receptor (CD206)	R&D Systems,	AF2534	1:200
	Rabbit anti- human Arginase I	Santa Cruz <i>Clone H-52</i>	sc-20150	1:100
	Rabbit anti-human Stabilin 1	Millipore	AB6021	1:2000
	Rabbit anti-mouse iNOS	Abcam	ab15323	1:100
	Rat anti- mouse CD68	Abcam <i>Clone FA-11</i>	ab53444	1:100/1:150
	Mouse anti-rat CD163	AbD Serotec	MCA342EL	1:50/1:100

<i>Clone ED2</i>				
	Rat anti-mouse F4/80	AbD Serotec	MCA49RT	1:50/1:100
<i>Clone Cl:A3-1</i>				
	Mouse anti-rat CD11b/c	Cedarlane	CL042B-5	1:150
	Rabbit anti-human CD3	DAKO	A 0452	1:150
	Rabbit anti- human Ki67	Abcam	Ab16667	1:150
Secondary antibodies	Alexa488 donkey anti- goat	Life Technologies	A11055	1:500
	Alexa488 Goat anti- rat	Life Technologies	A11006	1:500
	Alexa488 Goat anti- mouse	Life Technologies	A21042	1:500
	Alexa555 Goat anti- rat	Life Technologies	A21434	1:500
	Alexa488 Goat anti- rabbit	Life Technologies	A21428	1:500

A.4 Chemicals

Agarose	FMC corporation
Boric acid	Merck
Bovine serum albumin	AppliChem
Citric acid monohydrate, reagent grade $\geq 98\%$	Sigma Aldrich
Dako Faramount aqueous mounting medium	Dako
DAPI (4', 6-diamidino-2-phenylindole)	Life Technologies
Draq5	Biostatus
Dulbeccos modified Eagles medium (DMEM)	Sigma Aldrich
Ethanol, 100% and 96%	Sigma Aldrich
Fluorescence mounting medium	Dako
Hydrochloric acid (HCl), 37%	Sigma Aldrich
Hydrogen peroxide (H ₂ O ₂)	Sigma Aldrich
Methanol	Sigma Aldrich
PAP pen	Dako

PBS Tablets
Paraformaldehyde, reagent grade, crystalline
Roswell Park Memorial Institute (RPMI)-1640 medium
Sodium chloride (NaCl)
Sodium citrate
Sodium hydroxide (NaOH)
Sterile filtered fetal calf serum (FCS)
Sucrose (MW 342.3)
Trizma base
Trypsin-EDTA solution 10x
Xylene

Gibco
Sigma Aldrich
Sigma Aldrich
Sigma Aldrich
Sigma Aldrich
Sigma Aldrich
Riedel-deHaen
VWR Prolab
AppliChem
Sigma-Aldrich
Sigma-Aldrich

A.4 Reagents

Alexa fluor® conjugated secondary antibodies
All-protect Tissue Reagent
DAB substrate solution
dNTPs
DyNAzyme™ II DNA polymerase
GelRed Nucleid Acid Gel Stain
PCR buffer x 10
RNAse free water
1000 bp Ladder

Life technologies
Qiagen
Life technologies
Thermoscience
Thermoscience
Biotium
Thermoscience
Thermoscience
Promega

Appendix B

Solutions

Table B.1: 4% paraformaldehyde solution (PFA) in PBS with 0.02M sucrose

Reagent	Amount
Paraformaldehyde	20g
NaOH 1M	2 drops
10x PBS	50 ml
Sucrose (MW 342.3)	34.23g
HCl, 5M	(adjust pH to 7.2)

Procedure:

- All work needs to be done under fume hood.
- 450 ml Milli-Q-water was heated up to 60°C.
- 20g of paraformaldehyde was added, mixed well, and then added 2 drops of 1M NaOH.
- A 10 x PBS solution with 2M sucrose was made by adding 34.23g (MW 342.3) sucrose in 50 ml 10 x PBS. This was then added to the 4 % PFA.
- Solution was cooled to room temperature before pH was adjusted to 7.2 with HCL.
- Solution was filtrated and stored in 50 ml sterile centrifuge tubes. PFA can be stored at -20°C

Table B.2: Sodium citrate buffer , pH 6, for antigen retrieval.

Solution A	Solution B
10.5g Citrate monohydrate	29.4g sodium citrate
500 ml dH ₂ O	1 L dH ₂ O

To make 1 L of buffer, 18 ml of solution A and 82 ml of solution B was mixed , and made up to 1 L with Milli-Q water

Table B.3: Phosphate buffered saline (PBS)

Reagent	Amount
PBS tablets	2 tablets
Milli-Q water	1000 ml

Table B.4: Tris phosphate saline (10x TBS: 0.5 M Tris base, 9 % NaCl, pH 8.4)

Reagent	Amount
Trizma base	61g
NaCl	90g
Milli-Q water	1000 ml
HCl	(adjust pH to 8.4)

TBS with 0.05% Tween 20 (TBS-T), was made by adding 2.5 ml of a 20% solution of Tween 20 to 1 L of 1xTBS, made from 10x stock solution of TBS.

Table B.5: 1% BSA in TBS-T

Reagent	Amount
Bovin serum albumin	0.5g
TBS-T	50 ml

The solution was sterile filtered, and stored at 4 °C.

Table B.6: 5x Tris-borate-EDTA (TBE) buffer

Reagent	Amount
Tris base (FW=121.14)	54g
Boric acid (FW=61.83)	27.5g

dH₂O	900 ml
0.5M EDTA (pH 8.0)	20 ml
dH₂O	(Volume adjusted to 1L)

Procedure:

- Tris base and boric acid was dissolved in 900 ml of dH₂O
- EDTA was added before volume was adjusted to a final volume of 1L

Appendix C

Score sheets

Score sheet C.1: Assessments of human endpoints, mouse experiments:

(Translated from Norwegian)

Evaluation scheme for assessment of humane endpoint, mouse experiments:

Score N = Normal, nothing out of the ordinary

Score 1 = Slightly influenced. Animal must be followed closely.

Score 2 = Significantly affected. Animals should be euthanized.

Examples Score 1:

- Weight loss < 10 %
- Visible tumor, but smaller than the maximum allowed size (diameter < 12-13 mm)
- Visible necrosis in tumor, but without ulceration

Examples Score 2:

- Weight loss \geq 10 %
- Tumor \geq 12-13 mm i diameter
- Ulceration of tumor
- Bristling fur, inactivity

The form has to be filled out for each animal three times per week, in connection with measurements of body weight. If any symptoms are observed between these days by the laboratory of laboratory personnel, the responsible veterinarian and the responsible researcher will be notified.

(Of note, in the present experiments animals were monitored daily by the researchers)

Prosjekt ID (FOTS nr og lokal forsøksnr):	
Mus nummer (bur og øremerke):	
Start kroppsvekt (dag 0 av forsøket):	
Dato og tid for injeksjon av tumorceller:	

Vurdering av dyrets tilstand gjennom forsøket (Score N, 1 eller 2)

Dag av eksperimentet	0	1	2	3	4	5	6	7	8	9	10	11	12	13	14	15	16	17	18	19	20	21	22	23	24	25	26
----------------------	---	---	---	---	---	---	---	---	---	---	----	----	----	----	----	----	----	----	----	----	----	----	----	----	----	----	----

Observasjoner (påfør N, 1 eller 2 etter angitte kriterier)

Uforstyrret aktivitet																												
Oppførsel																												
Kroppsholdning																												
Utseende, pels, egenpleie																												
Kroppsvekt (g)																												
% av utgangsvekt																												
Generell status muskler/fett																												
Bukomfang																												
Tumorstørrelse																												
Tumorutseende																												
INITIALER (Observatør)																												

Kommentarer:

Score sheet C.2: Assessment of IHC staining of B16F1 tumors from mice:

Assessment of IHC staining on B16F1 tumors from mice				Antibody:		Date of labeling:	
Tumor no	No of positive cells (non-tumor cells)			Staining intensity of positive cells			Other observations:
	Score: 0-3			Score: 1-3			
	Tumor central	Tumor peripheral	Extracellular matrix	Tumor central	Tumor peripheral	Extracellular matrix	

Scoring system for assessing the amount of positive cells

- 0. No positive cells
- 1. Few positive cells
- 2. Moderate number of positive cells
- 3. High number of positive cells

Scoring system for assessing staining intensity in positive cells

- 1. Weak staining; 2. Moderate staining; 3: Strong staining

Appendix D

Protocols

Protocol D.1: Fluorescence staining

Reagents:

- Primary antibody (Appendix A, table A.3)
- Secondary antibody (Appendix A, table A.3)
- Washing buffer: TBS, TBS + 0.05% Tween 20 (TBS-T) (pH 8.4)
- Blocking/dilution buffer: 1 % BSA in TBST.
- Citrate buffer (pH 6):
 - Solution A: 10.5g citric acid monohydrate in 500 ml dH₂O (i.e. Milli-Q water)
 - Solution B: 29.4g sodium citrate in 1 L dH₂O
 - 18 ml solution A and 82 ml solution B, make up to 1 L with dH₂O

Negative control:

- 2nd only : 1 slide without primary antibody
- Non-immune IgG at similar concentration as primary antibody
- For mannose receptor staining: Tissue slide from MR-KO liver

Positive control:

- Tissue slide from wild-type mouse liver

Procedure:

1. De-parafinization and rehydration of tissue sections:
 - 3x15 min: Xylene
 - 2x10 min: 100% ethanol
 - 1x5 min: 96% ethanol
 - 1x5 min: 70% ethanol
 - 2x5 min: Milli-Q water
2. Antigen "retrieval", 30 min microwaving in citrate buffer, pH 6:
 - Prewarm buffer to around 95 °C (P10), and place sections in beaker filled with hot buffer.
 - Microwave: 6 x 5 min, 750 W
 - Cool sections for 20 min in buffer at RT. Then wash: dH₂O 3 x 2min.
 - Make a circle with PAP pen
3. Wash
 - TBS-T for 2 min

4. Block in 1% BSA in TBST
 - 30 min, room temperature (RT)

5. Labeling with primary antibody diluted in blocking buffer, overnight 37°C or 1 hour 37°C.
 - 100 µl or enough to cover tissue, per slide.
 - Wash 3x5 min in TBS-T

6. Labeling with secondary Ab (under aluminium foil):
 - Secondary AlexaFluor antibody according to primary antibody, diluted in 1 % BSA in TBST buffer, 1 hour, RT
 - Wash 3x5 min in TBS-T
 - Wash 2x5 min in PBS

7. Contrast staining (under alufoil) and mounting of sections
 - DAPI (1:50.000) in PBS, 5 min, RT
 - Wash in PBS 2x2 min
 - Draq5 in PBS (1:1000), 5 min, RT
 - Wash in PBS 2 min, then 2x2 min in dH₂O
 - Dry section (under aluminium foil)
 - Mount in Dako Fluoromount, and seal

Analyses were done with a Zeiss 510 META Laser Scanning Confocal Microscope (Carl Zeiss Microscopy, Jena, Germany) at the Bioimaging platform, Department of Medical Biology,

Protocol D.2: Enzyme staining methods

AEC method

Reagents:

- Invitrogen HistoMouse™- Plus Kit
Cat.no: 85-9541, broad spectrum, AEC chromogen:
 - Reagents 1A and 1B: BEAT™ blocking solution A and B (ready-to-use)
 - Reagent 1C: Biotinylated secondary antibody (ready-to-use)
 - Reagent 2: Streptavidin-peroxidase conjugate (ready-to-use)
 - Reagent 3: AEC single solution (ready-to-use)
 - Reagent 4: Hematoxylin solution (ready-to-use)
 - Reagent 5: ClearMount™ mounting solution
- Washing buffer: PBS, TBS + 0.05% Tween 20 (TBS-T; 2.5 ml 20% tween in 1L TBS).
- Primary antibody diluted in: 1 % BSA in TBST
- Peroxidase quenching solution:
 - Add 1 part of 30% H₂O₂ to 9 parts of cold absolute methanol. Mix well.
- Citrate buffer (pH 6):
 - Solution A: 10.5g citric acid monohydrate in 500 ml dH₂O
 - Solution B: 29.4g sodium citrate in 1 L dH₂O
 - 18 ml solution A and 82 ml solution B, make up to 1 L with dH₂O

Negative control:

- 2nd only : 1 slide without primary antibody
- Non-immune IgG: One slide with non-immune IgG at similar concentration as primary antibody

Procedure:

1. De-paraffinization and rehydration:
 - 3x15 min: Xylene
 - 2x10 min: 100% ethanol
 - 1x5 min: 96% ethanol
 - 1x5 min: 70% ethanol
 - 2x5 min: dH₂O (Milli-Q water)
2. Antigen “retrieval”, 30 min microwaving in citrate buffer, pH 6:
 - Prewarm buffer to around 95 °C, and place sections in beaker filled with hot buffer.
 - Microwave: 6 x 5 min, 750 W.
 - Cool sections for 20 min in buffer at RT. Then wash: dH₂O, 3 x 2min.
 - Make a circle around the section with PAP pen.

3. Peroxidase quenching solution:
 - 10 min
 - Wash 2x2 min, PBST

4. BEAT™ blocking solutions (reagents 1A and 1B):
 - Add 2 drops or 100 µl of blocking solution 1A to each section, incubate 30 min.
 - Rinse well with dH₂O
 - Add 2 drops of blocking solution 1B, incubate 10 min.
 - Rinse well with dH₂O
 - Wash with PBST 3 x 2 min

5. Primary antibody:
 - Add 100 µl or enough to completely cover tissue
 - Incubate in moist chamber for 60 min at 37°C
 - Wash with TBST 3 x 2 min
 - Wash with PBS 3 x 2 min

6. Biotinylated secondary antibody (reagent 1C):
 - Add 2 drops or enough to cover the tissue,
 - Incubate 30 min
 - Wash with PBST 3 x 2 min

7. Streptavidin-peroxidase conjugate (reagent 2):
 - Add 2 drops
 - Incubate for 20 min
 - Wash with PBST for 3 x 2 min

8. AEC single solution chromogen (reagent 3):

Do not equilibrate AEC to room temperature before use!

 - Add 2 drops of cold AEC. Immediately return AEC to fridge
 - Incubate 15 min
 - Wash with dH₂O

9. Haematoxylin counterstaining (reagent 4):
 - Counterstain with 2 drops
 - Wash in tap water
 - Place slides in PBS until they are blue (app. 30 sec):
 - Rinse with distilled water

10. Mounting:
 - Dako aqueous mounting medium
 - Seal with nail polish

DAB method (used for F4/80 labeling only)

Reagents:

- Washing buffer: PBS
- Primary antibody diluted in: 1 % BSA in PBS
- Secondary antibody: Goat anti-rat HRP from Invitrogen 1:200
- Substrate solution: DAB from Dako
- Citrate buffer (pH 6):
 - Solution A: 10.5g citric acid monohydrate in 500 ml dH₂O
 - Solution B: 29.4g sodium citrate in 1 L dH₂O
 - 18 ml solution A and 82 ml solution B, make up to 1 L with dH₂O

Procedure:

1. De-paraffinization and rehydration
 - 1x20 min: Xylene
 - 1x5 min: 100% ethanol
 - 1x5 min: 96% ethanol
 - 1x5 min: 70% ethanol
 - Incubate in running tap water for 5 min
 - Incubate in PBS 2x5 min
2. Antigen "retrieval", 10 min microwaving in citrate buffer, pH 6:
 - Prewarm buffer to around 95 °C, and place sections in beaker filled with hot buffer.
 - Microwave: 10 min, 750 W
 - Cool sections for 30 min in buffer at RT
 - Make a circle with PAP pen
3. Blocking of unspecific binding:
 - 1% PBSA (PBS with 1% BSA, do NOT shake)
 - Incubate for 30 min in fridge
4. Primary antibody:
 - Primary antibody is diluted with 1% PBSA
 - Add 100 µl or enough to completely cover tissue
 - Incubate overnight in fridge in a humidified box (made wet with PBS)
 - Wash 3x5 min in PBS
5. Secondary antibody:
 - Secondary antibody is diluted in 1% PBSA
 - Add enough to cover the tissue
 - Incubate 45 min at RT
 - Wash with PBS 4 x 5 min

6. Substrate solution DAB (Dako):

- Add substrate solution DAB
- Incubate until you see formation of brown color (may vary from 5 sec to 2 min)

11. Haematoxylin counterstaining (reagent 4 from Histokit™):

- Counterstain with 2 drops
- Wash in tap water
- Place slides in PBS until they are blue (app. 30 sec):
- Rinse with distilled water

7. Dehydrating and mounting:

- Dehydration in:
 - 75% EtOH, 5 min
 - 90% EtOH, 5 min
 - 100% EtOH, 5 min
- Mount with coverslip by using xylene based mounting medium.